Multichannel EEG

Towards applications in clinical neurology

This research was performed at the Department of Neurology, University Medical Center Groningen and at the School of Behavioural and Cognitive Neuroscience (BCN), University of Groningen.

Publication of this thesis was financially supported by:
School of Behavioural and Cognitive Neuroscience (BCN)
University of Groningen (RuG)
Het Remmert Adriaan Laan fonds
ANT B.V.

ISBN 978-90-367-3603-9

Printed by: Gildeprint, Enschede

RIJKSUNIVERSITEIT GRONINGEN

Multichannel EEG
Towards applications in clinical neurology

Proefschrift

ter verkrijging van het doctoraat in de
Medische Wetenschappen
aan de Rijksuniversiteit Groningen
op gezag van de
Rector Magnificus, dr. F. Zwarts,
in het openbaar te verdedigen op
maandag 8 december 2008
om 16.15 uur

door

Wilhelmina Johanna Gerarda van de Wassenberg

geboren op 21 juni 1980
te Sint-Michielsgestel

Promotores:	Prof. dr. ir. N.M. Maurits Prof. dr. K.L. Leenders
Copromotor:	Dr. J.H. van der Hoeven
Beoordelingscommissie:	Prof. dr. R. de Jong Prof. dr. C.J. Stam Prof. dr. ir. D.F. Stegeman

ISBN 978-90-367-3603-9

Contents

1

General introduction

Our body is a very complex machine, in which many chemical, electrical and physical processes take place. Only a small part of these processes is known and understood. The human body is even more complex than the most complex man-made machine. If our machine, the body, is damaged or isn't functioning well, we go to the hospital. There a medical specialist tries to make a diagnosis. To come up with the correct diagnosis, anamnesis, physical examination as well as different medical tests or imaging procedures might be required. These imaging procedures and medical tests are often performed with high-tech medical devices, such as imaging systems that visualize structures and physiological processes in the body and systems that can measure blood flow, electrical activity or the concentration of certain components in the blood.

Finally, if a diagnosis is made the specialist may prescribe a drug, another way of life or plan a surgery. The drug can be packaged in an advanced drug delivery system. The latter administers drugs through controlled delivery in the body so that the optimum amount reaches the desired body location. On the other hand, during surgery again many advanced medical devices can be used, for example to monitor the state of the patient or to better visualize the intervention. In addition, a robot may be used to perform very precise actions or a high-tech prosthesis can be implanted.

Accordingly, many engineers are needed in the field of health care; in the hospital to work with all the high-tech devices and to develop new applications, in business to develop new medical devices and techniques and in fundamental research to learn more about chemical, electrical and physical processes in the body. These fields of research and development have fascinated me since I started to study Biomedical Engineering in Eindhoven. During my studies I did a variety of projects from developing a mechanical and electrical model of the heart to investigating the response of cells to different mechanical loads. After these projects, I found out that one of my fields of interest is biosignal analysis for direct clinical applications. Electroencephalogram (EEG) is an electrical biosignal used for diagnosis of neurological disorders and for monitoring. This thesis aims to investigate new diagnostic applications of multichannel EEG, in particular evoked potentials (EPs) and event-related potentials (ERPs), by developing new analysis techniques.

EEG is a non-invasive technique that measures the electrical activity produced by nerve cells in the brain with electrodes placed on the scalp. EEG activity was first recorded by Hans Berger in 1924. He discovered that different waves or rhythms are present in the normal brain and that alterations of these brain waves occur in neurological disorders like epilepsy. Around 1950, EEG started to be used in hospitals for clinical diagnostic purposes. At that time EEG recordings were analog paper recordings and evaluation was mainly based on visual inspection.
During the 1970s, computers were increasingly used for EEG recording and advanced EEG signal analysis became possible. At that time, EPs were also applied for the first time for clinical diagnosis and ERPs were used for research purposes. EPs and ERPs are electrical brain potentials that are responses to a certain stimulus (visual, auditory, sensory) or action. EPs are exogenous potentials with a short latency that are insensitive to attention and subject performance. On the other hand, ERPs are endogenous long latency potentials elicited by cognitive processes that are influenced by the level of attention and subject performance.
With the development of CT, MRI and PET between 1970 and 1990, it became possible to image the inside of the body noninvasively. These developments had great impact on individual diagnosis, treatment and prognosis in neurology and for a few decades the interest in EEG as a clinical diagnostic tool decreased. However, a major advantage of EEG compared to MRI, CT, SPECT and PET remains its low cost and high temporal resolution; whereas functional MRI and PET have a time resolution in the order of seconds, for EEG this is in the order of milliseconds. Furthermore, EEG can directly measure brain electrical activity, while fMRI, SPECT and PET measure brain electrical activity indirectly by assessing metabolic changes or blood flow. Because of these advantages EEG is still used nowadays as a diagnostic tool for epilepsy and sleep disorders, for monitoring during surgery and for the diagnosis of brain death. Evoked potentials are still used clinically as well, for clinical diagnosis of demyelinating-, visual- or hearing disorders, for the prognosis of comatose patients and for intraoperative monitoring.

A disadvantage of EEG compared to the other imaging techniques is its low spatial resolution. However, with the development of multichannel EEG systems ($>$ 64 electrodes) around 1990 spatial resolution has increased considerably. Initially, multichannel EEG was thought to be infeasible for clinical use, because of its long preparation times. Though, by using electrode caps, clinical application of multichannel EEG, EPs and ERPs has become possible. The question that directly arises from this development is if the extra amount of data obtained with multichannel recordings provides additional benefits compared to conventional techniques that employ fewer electrodes. So far, multichannel EEG has proven to be useful in the study of healthy brain physiology (Huber et al., 2004; Jackson et al., 2004; Massimini et al., 2004; Sabbagh et al., 2004) and has given new

insights in psychiatric diseases (Pae et al., 2003; Ruchsow et al., 2003; Youn et al., 2003). In contrast to what may be expected of a technique that has demonstrated its value in diagnostic neurology when using a few electrodes, only a limited number of studies report clinical neurological applications of multichannel EEG (Elting et al., 2005; Lantz et al., 2003a,b; Michel et al., 2004a). First applications were in pre-operative localization of epileptogenic lesions (Lantz et al., 2003a,b; Michel et al., 2004a). More recently, results from Elting et al. (2005) suggest that multichannel ERP can improve diagnosis and quantification of cognitive disorders after acute brain injury. These clinical applications are based on source localization, a signal analysis technique that can only be applied accurately to multichannel recordings. The hypothesis of the work in this thesis is that the number of clinical applications of multichannel EEG can be further extended partly by using new analysis techniques.
Before a new technique can be used for diagnostic purposes its usefulness must be tested (evidence based diagnostics); 1) the normal range and reproducibility of values must be determined, 2) its sensitivity and specificity for a certain disease must be estimated, 3) the benefits for the patients that undergo the diagnostic test must be evaluated and 4) its feasibility must be tested. Subsequently, one has to decide if the benefits outweigh the (additional) costs and burden for the patient. In this thesis, new analysis techniques are developed and applied to a large group of healthy subjects to determine its normal values and reproducibility. In addition, the techniques are applied to different patient groups to assess their diagnostic value. Furthermore, feasibility in patients is examined for a technique that has already been used for fundamental research in healthy subjects.

1.1 Outline of this thesis

The aim of this thesis is thus to investigate if multichannel EPs and ERPs can improve differential diagnosis of neurological disorders by introducing new analysis techniques.
A standard clinical analysis technique for EPs and ERPs is estimating peak amplitudes and latencies. However, also other analysis techniques can be applied, of which most are currently mainly used for research purposes. **Chapter 2 and chapter 3** give an overview of these analysis techniques, where chapter 3 focuses on the wide range of source localization techniques.
In contrast to latency, E(R)P amplitude is hardly used for diagnostic purposes, because of its large variability among healthy subjects and patients. Only extremely high peaks or absent peaks are defined as abnormal. The variability among healthy subjects might at least partly be due to a combination of anatomical variation and the limited number of electrodes on specific positions used. Therefore, in **chapter 4** we investigate if 128-channel recordings reduce the intersubject variability of

median nerve somatosensory EPs (SEPs), by using topographic mapping and the highest amplitude over all electrodes. In addition, in this chapter normal values are determined and the reproducibility of this approach is investigated.
While intersubject variability is large, the intrasubject variability between left and right hemispheres is relatively small. Therefore, for unilateral neurological disorders, it may be interesting to compare SEP activity in both hemispheres. So far, only peak amplitudes or peak source strengths of left and right SEPs have been compared. However, each subject has a specific SEP waveform and therefore also features other than SEP peaks might be interesting to compare. In **chapter 5** we introduce a new method to quantify SEP symmetry. In this method, we compare left and right median nerve SEP waveforms. Furthermore normal values and reproducibility are determined for this technique.
In **chapter 6** the methods introduced in chapters 4 and 5 are applied to SEPs of patients with different parkinsonian disorders to investigate whether the use of these techniques can improve the differential diagnosis. Previous studies with a limited number of electrodes already found some abnormalities in median nerve SEPs obtained from patients with different parkinsonian disorders. However, so far these abnormalities were too small or present in too few patients to be clinically useful.
Another SEP recording that is often used clinically is the tibial nerve SEP. It is already known that one of the peaks in the tibial nerve SEP differs enormously in position among subjects. Therefore, 128-channel amplitude estimation might be of additional value especially for this peak. In **chapter 7** the amplitude of tibial nerve SEP in healthy subjects is investigated by using 128-channel recordings. Again normal values and reproducibility are estimated.
In contrast to EPs, ERPs have so far mainly been used for research purposes, but they might also be clinically relevant. A disadvantage of ERPs is that they depend on subject performance. In **chapter 8**, we investigate the feasibility for patients with Parkinson's disease of a particular paradigm that is used to assess spatial attention and motor preparation.
Chapter 9 summarizes the results in this thesis and in **chapter 10** future perspectives are given.

2

Signal analysis techniques for evoked and event-related potentials

2.1 Introduction

Event-related potentials (ERPs) and evoked potentials (EPs) have a low amplitude in comparison with the background EEG activity and, as a consequence, they are barely visible in single-trials. The usual way of improving the ratio between the E(R)P signal power and the background EEG power, i.e. the signal to noise ratio (SNR), is by averaging the response of several trials (Chiappa, 1997). Amplitude and latency are usually determined next. However, there are also other techniques to extract relevant information from E(R)Ps. This chapter gives an overview of the analysis techniques most used for evoked and event-related potentials. We will start this chapter with time domain analysis techniques. Subsequently, several techniques will be described for the frequency domain. Source localization, which is also often applied to E(R)P data, will be explained in the next chapter.

2.2 Time domain analysis techniques

2.2.1 Current Source Density / Surface Laplacian

The scalp potential distribution measured with EEG is blurred considerably relative to the potential distribution on the cortex due to the different conductivities of cortex, skull, and scalp (Nunez, 1990). Furthermore, the potential distribution depends strongly upon the location of the reference electrode or electrodes (Nunez et al., 1994; Gevins et al., 1989).
A method that can be used to deblur the EEG signal is to compute the reference-free Surface Laplacian (SL) (Hjorth, 1975; Nunez and Pilgreen, 1991; Yao, 2002b). The SL estimate is thought to be proportional to the current density flowing perpendicular to the skull into the scalp and is also called current source density (CSD) (Nunez et al., 1994) or scalp current density (SCD)(Perrin et al., 1989). It gives a more localized distribution of major components of electric activity as compared

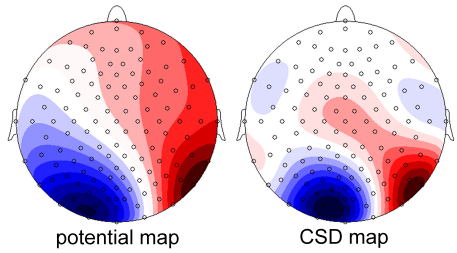

Figure 2.1: Potential map (left) and CSD map (right) of a visual evoked potential (VEP) recording. The CSD map shows more localized activity compared to the potential map.

with the conventional potential mapping (Fig. 2.1) (Hjorth, 1991).

Mathematically, the SL is the sum of the second order spatial derivatives of the scalp potential distribution (Yao, 2002b):

$$\Delta V = \nabla^2 V = \nabla \cdot \nabla V = \frac{\partial^2 V}{\partial x^2} + \frac{\partial^2 V}{\partial y^2} + \frac{\partial^2 V}{\partial z^2} \tag{2.1}$$

The relation between the current source density and SL, when assuming no volumetric current sources in the scalp, is given by the Poisson equation:

$$\nabla \cdot J = -\sigma \nabla^2 V \tag{2.2}$$

where J is the current density, σ the conductivity of the scalp and V the scalp potential. According to this equation CSD is proportional to the divergence of the current density in the scalp (Perrin et al., 1987).

Two different SL estimation procedures have been proposed in literature: a local approach (Hjorth, 1975) and a more global approach (Perrin et al., 1989). The local SL is obtained by computing the difference between the potential at each electrode site and the average potential of its nearest four neighbours provided that the distance and angle between the electrodes are equal (Hjorth, 1975). Mathematically the second order derivative in 1D is then approximated by:

$$\frac{\partial^2 V}{\partial x^2} \cong \frac{V(x_0 + \Delta x) - 2V(x_0) + V(x_0 - \Delta x)}{\Delta x} \tag{2.3}$$

Now consider the surface of the head as a 2-dimensional space. By assuming equal distances between electrodes, assigning these distances unity and when the electrodes are positioned as in figure 2.2, equation 2.1 can be approximated by (Hjorth, 1975):

$$\nabla^2 V = \frac{\partial^2 V}{\partial x^2} + \frac{\partial^2 V}{\partial y^2} \cong (V_1 - V_0) + (V_2 - V_0) + (V_3 - V_0) + (V_4 - V_0) \tag{2.4}$$

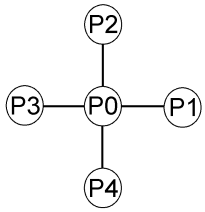

Figure 2.2: Configuration to determine the surface Laplacian according to the local approach introduced by Hjorth (1975).

where V_0 is the electric potential at electrode P_0 that is surrounded by electrodes P_1,P_2, P_3, P_4 with potentials V_1, V_2, V_3, V_4. A disadvantage of the local technique is that the SL cannot be estimated at each electrode, since the computation requires neighbouring electrodes (Hjorth, 1975).
The global approach uses all electrodes to determine the SL instead of only neighbouring electrodes. First a global interpolation function is constructed to represent surface potential distributions and then the SL is calculated for the global interpolation function (Yao, 2002a). Various functions have been used for the global interpolation e.g. 2D thin plate spline functions (Perrin et al., 1989), spherical spline functions (Perrin et al., 1989), and realistic spline Laplacians (Babiloni et al., 2001, 1996). In general, the global approach is a better approximation for the current source density than the local approach (Babiloni et al., 1995).

2.2.2 Principal component analysis and independent component analysis

In general, principal component analysis (PCA) and independent component analysis (ICA) are used for data compression and information extraction. In EEG analysis these techniques are mostly used for artifact rejection. They can easily be used to remove eye, electrocardiogram (ECG), muscle or MRI artifacts (Vigario et al., 2000; Jung et al., 2000; Iriarte et al., 2003; Vigario, 1997). PCA searches for components which are linear combinations of the signals observed, are uncorrelated and have maximum variation in the smallest number of components. The first principal component explains most of the variance, the second principal component explains most of the variance after the first component has been extracted, etc.
Mathematically, PCA relies on an eigenvector decomposition of the covariance matrix of the EEG signals. The covariance matrix contains all the covariances possible between the channels used and for a measured data matrix M it can be defined by:

$$cov(M) = M^T M \tag{2.5}$$

This equation assumes that the columns of M have been mean centered, i.e. the mean is subtracted. The eigenvalues λ of the square matrix $cov(M)$ can be obtained by solving:

$$\det(cov(M) - \lambda I) = 0 \tag{2.6}$$

where I is the identity matrix. Solving equation 2.6 gives n eigenvalues, where n is the size of the covariance matrix. Subsequently, the eigenvectors v_{λ_i} can be calculated by solving the following equation:

$$cov(M)v_{\lambda_i} = \lambda_i v_{\lambda_i} \tag{2.7}$$

The eigenvectors represent the directions of the principal components in n-dimensional space and the eigenvalues represent a measure for the variance in that direction. Consequently, the eigenvector with the highest eigenvalue is the direction of the principal component that accounts for most of the variance, i.e. the eigenvector that corresponds to the strongest correlation in the dataset.
To reduce the data, the eigenvectors with a small eigenvalue can be ignored. For data extraction one can ignore other unwanted data such as eigenvectors that represent eye movements. By multiplying the chosen eigenvectors with the original data, the principal components are obtained:

$$Y = A_s M \tag{2.8}$$

where A_s is the orthogonal matrix containing the selected eigenvectors of the covariance matrix as the row vectors, and Y contains the principal components. To return to the original dimensions, the transpose of matrix A must be multiplied by Y:

$$M_s = A_s^T Y \tag{2.9}$$

where M_s is the compressed data.
An assumption made by PCA is that the data has a Gaussian distribution. If the data is not Gaussian, independent component analysis (ICA) can be used instead of PCA (Vigario et al., 2000). ICA searches for the most independent components instead of uncorrelated components. Statistically, uncorrelated is defined as:

$$E\{y_i y_j\} - E\{y_i\}E\{y_j\} = 0, for\ i \neq j \tag{2.10}$$

and independent is defined as:

$$E\{g_1(y_i)g_2(y_j)\} - E\{g_1(y_i)\}E\{g_2(y_j)\} = 0, for\ i \neq j \tag{2.11}$$

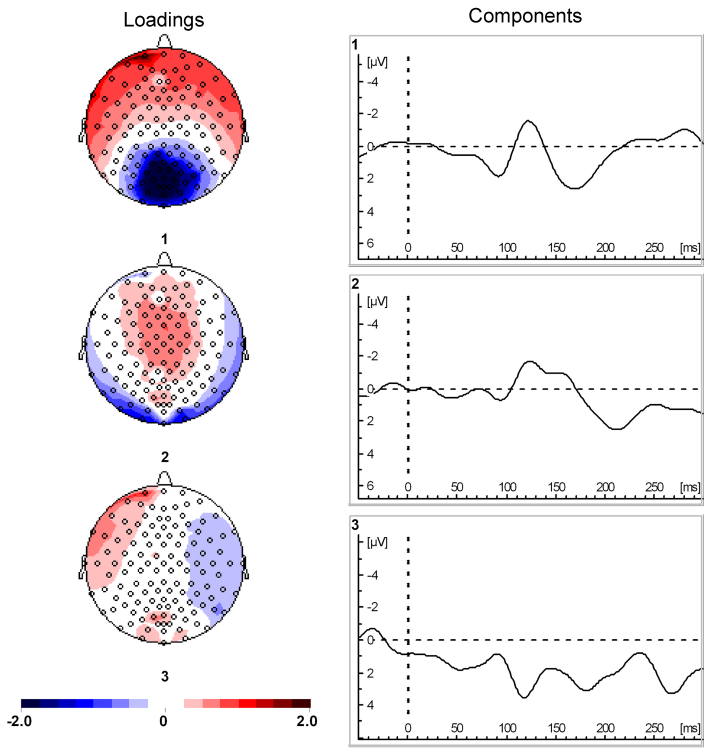

Figure 2.3: PCA of a visual evoked potential (VEP) recording. Loadings (left) of each channel and the corresponding largest principal components (right). The loadings are defined by the eigenvectors.

where g_1 and g_2 can be any function and E is the expected value. Independent variables are always uncorrelated, while uncorrelated does not always mean independent (Calhoun et al., 2001). Thus independence is a much stronger requirement than uncorrelatedness. Both requirements are equivalent concepts only in the case of Gaussian distributed signals (Vigario et al., 2000).
There are some assumptions that underlie ICA decomposition of EEG time series: 1) there must be at least as many channels as the number of independent sources, 2) sources are non-Gaussian 3) sources must be temporally independent (Vigario et al., 2000; Brown et al., 2001). ICA tries to find a matrix W such that:

$$C = WM \tag{2.12}$$

where the components of C are as independent as possible and M is the original data matrix. Before using an ICA algorithm, some preprocessing must be performed on the data. As in PCA the data must be mean centered first. Secondly,

the observed data must be whitened, i.e. the data is linearly transformed to obtain uncorrelated components with variance that equals unity (Hyvarinen and Oja, 2000). This transformation can be performed by using PCA:

$$\tilde{X} = D^{-\frac{1}{2}} A_s M \tag{2.13}$$

where $\tilde{X}$ is the transformed data and D is the diagonal matrix of the eigenvalues of the covariance matrix. The estimation of the matrix W is accomplished by minimizing or maximizing a cost function that represents dependence or independence: maximum non-Gaussianity estimation (kurtosis, negentropy), maximum likelihood estimation or minimum mutual information (Hyvarinen and Oja, 2000). To find the optimum of the cost function different iteration methods can be used depending on the choice of cost function, such as gradient and Newton-like methods.
For example, Infomax is an ICA procedure that is often used and that was introduced by Bell and Sejnowski (1995). This method calculates the matrix W by maximizing the entropy U, which is a measure for mutual information:

$$U = g(WM) \tag{2.14}$$

where g is defined by:

$$g(WM) = (1 + e^{-WM})^{-1} \tag{2.15}$$

2.2.3 Cross-correlation

In statistics cross-correlation is a measure for the linear relationship between two variables. It is mostly used to examine the relation between two completely different parameters, for example arm length and median nerve somatosensory evoked potential (SEP) latency. In statistics the cross-correlation coefficient between two variables X and Y is defined by:

$$\rho_{xy} = \frac{E[(X - \mu_X)(Y - \mu_Y)]}{\sigma_X \sigma_Y} \tag{2.16}$$

where μ_X is the mean and σ_X is the standard deviation of variable X. They are defined by:

$$\mu_X = E(X) \tag{2.17}$$

$$\sigma_X = \sqrt{E(X^2) - E^2(X)} \tag{2.18}$$

In the same way mean and standard deviation for variable Y can be calculated. The cross-correlation can have a value between -1 and 1. A value of -1 suggests a complete linear inverse correlation, a value of 1 complete linear direct correlation

and a value of 0 a lack of linear relationship. If there is a positive relation the cross-correlation coefficient is also positive, while if there is a negative relation the cross-correlation coefficient is negative. In digital signal processing the cross-correlation is a measure of similarity of two signals as a function of the relative time τ between the signals:

$$\rho_{xy}(\tau) = \frac{\sum_{t=1}^{T-\tau}[(X(t) - \mu_x][Y(t+\tau) - \mu_y]}{\sqrt{\sum_{t=1}^{T-\tau}[X(t) - \mu_x]^2 \sum_{t=1}^{T-\tau}[Y(t+\tau) - \mu_y]^2}} \tag{2.19}$$

where T is the total number of discrete time samples. The denominator of equation 2.19 is called the cross-covariance of variables X and Y. Assuming that coordinated brain processing is reflected by a similar potential wave shape among the regions involved, covariance is sometimes used to investigate functional relationships between different brain areas (Gevins et al., 1987, 1989). For each electrode pair cross-covariance between their waveform segments is calculated. This gives a cross correlation function for each electrode pair. Next, the maximum as a funtion of τ of each function is determined and used as a measure for the functional relationship between the areas. Furthermore, cross-covariance and cross-correlation are both used in single trial analysis as described later in this chapter. Autocorrelation is the cross-correlation of a signal with itself. It is useful for finding repeating patterns in a signal.

2.2.4 Symmetry measures

A method to quantify symmetry of E(R)Ps is the laterality index. The laterality index is the amplitude difference between left and right hemisphere after stimulation or action of respectively right and left body side, divided by the sum of these amplitudes (Jung et al., 2003). This method is, for example, used for estimating the similarity of SEP peak amplitudes after stimulation of left and right median nerve. However, this method could also be used within a task recording bilateral activity.
A technique to investigate lateralized activity is by calculating event-related lateralizations (ERLs). The main goal of this technique is to enhance the detectability of lateralized activity by suppressing symmetric activity and all activity which is present in recordings of both sides. It computes the difference potentials between homologues electrodes contra and ipsilateral to the side of stimulus or action. As an example, the ERL for homologues electrode pair C3-C4 is defined as (Oostenveld et al., 2001):

$$ERL = \frac{1}{2}[(C4 - C3)_L + (C3 - C4)_R)] \tag{2.20}$$

where L and R represent the measurements from the left and right task. Thus, for estimation of this difference potential left and right side need to be stimulated or moved one side at a time. Furthermore, it is assumed that activity in the contralateral hemisphere is similar for the left and right task. The same assumption is made for the ipsilateral hemisphere.

2.2.5 Single-trial analysis

When averaging single-trials for improving the SNR, one usually assumes that the E(R)P waveform is fixed and that its peak latency is constantly time-locked to the stimulus (Chiappa, 1997). However, information concerning individual trials and the variation in E(R)Ps is lost using this technique. Therefore, alternative techniques have been developed to determine single-trial latency, amplitude and/or other parameters.
The simplest single-trial analysis method used is "peak picking" (Smulders et al., 1994). This method takes the latency of the maximum amplitude in a specific window as latency of the peak of interest that normally occurs in this window. However, this technique often does not work, because the SNR is too low.
Rodionov et al. (2002) developed a more complex version of this technique, in which the number and amplitude of positive and negative deflections of the EEG is used to determine the variability of latency and amplitude of single-trials. This technique requires a lower SNR. A disadvantage of this technique is that the temporal resolution of the latency is very low due to summation of every five successive samples in the EEG signal.
Another single-trial analysis method calculates the cross-correlation or cross-covariance between the single-trials and a template. Next the maximum cross-correlation or cross-covariance is used as peak latency. In literature different templates are used:

1. half sine wave (Smulders et al., 1994; Pfefferbaum and Ford, 1988)
2. stimulus locked average ERP (Michalewski et al., 1986; Wastell and Kleinman, 1980; Thomas et al., 1989)
3. peak locked average ERP (Suwazono et al., 1994)
4. first two principal components of the average ERP (Kisley and Gerstein, 1999)

The stimulus locked average ERP may not be a perfect template for single-trial analysis, since the averaged peaks might be broadened in time and decreased in amplitude due to latency variation of the single-trial responses.
Another group of single-trial analysis methods models the ERP as a linear combination of multiple components (e.g. wavelets) whose component parameters (e.g.

latency and amplitude) are calculated for each single-trial (Lange et al., 1997; Quian and Garcia, 2003; Truccolo et al., 2003; Heinrich et al., 1999) by using for example a least squares method (Lange et al., 1997). The components and initial parameters are often extracted from the average ERP (Lange et al., 1997; Quian and Garcia, 2003; Heinrich et al., 1999).
The quality of the results obtained by the described techniques depends mainly on the SNR of the signal. By filtering the signal before using it for single-trial analysis, the noise can be reduced and the SNR may be improved.
Single-trial analyses have been mainly used for ERP analyses, since ERP responses are sensitive to the subject's performance, state of mind (Nishida et al., 1997), habituation, and have often a sufficient SNR (more than EPs).

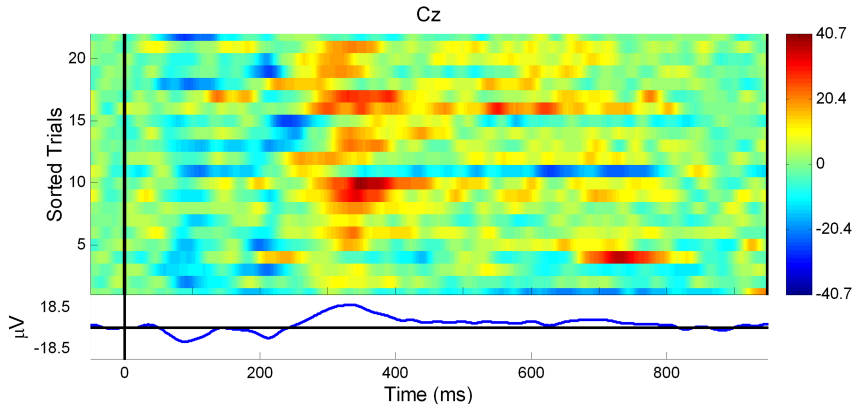

Figure 2.4: Single-trial plot of a standard oddball paradigm, whereby a target auditory stimulus is presented amongst more frequent standard auditory stimuli. Raw data is filtered (low pass 30 Hz, high pass 0.16 Hz) and segments with eye blinks have been removed. This plot only shows the target segments. Notice that the P300 peak is observable in most single-trials.

2.3 Frequency domain analysis techniques

2.3.1 Fourier transform

The Fourier transform (FT) converts signals from the time domain to the frequency domain. It can be used to study frequencies in the signal or for filtering.
Because EEG signals are digitally recorded nowadays, the discrete Fourier transform (DFT) is used to calculate the FT. The fast Fourier transform (FFT) is an efficient algorithm to compute the DFT. The (D)FT decomposes the original signal $s(t)$ in cosines and sines with a certain frequency, amplitude and phase. The frequencies of these cosines and sines are determined by the segment time T_0 and

the sample frequency f_s.
Mathematically the DFT for a signal $s(n)$ with N sample points is given by (Roerdink, 1993):

$$S(k) = \sum_{n=0}^{N-1} s(n) e^{\frac{-i2\pi kn}{N}}, \; k = 0, .., N-1 \tag{2.21}$$

where, according to Euler's formula:

$$e^{\frac{-i2\pi kn}{N}} = \cos\left(\frac{-2\pi kn}{N}\right) + i \sin\left(\frac{-2\pi kn}{N}\right) \tag{2.22}$$

In 2.21 $s(n)$ is the original signal at sample point n, i is the imaginary number ($i^2 = -1$) and $S(k)$ is the k^{th} spectral coefficient. The index k uniquely determines the frequency associated with the spectral component $S(k)$. Index k can be transformed to a frequency f by:

$$f = \frac{k}{T_0} \tag{2.23}$$

where T_0 is the segment time.
The resolution Δf and the minimum frequency $f_{\min}$ in the frequency domain are also determined by the segment time T_0:

$$f_{\min} = \Delta f = \frac{1}{T_0} \tag{2.24}$$

The Nyquist frequency f_N, which is the maximum frequency that can be correctly represented in the sampled signal, depends on the sample frequency f_s:

$$f_N = \frac{f_s}{2} \tag{2.25}$$

Discrete Fourier transform algorithms assume that the data contain only frequencies that are an integer multiple of the minimum frequency. However, this is not the case with EEG data and this leads to spectral leakage; loss of power of a given frequency to other frequencies (Fig. 2.5).
The effect of spectral leakage can be diminished by multiplying the original signal by a window function before calculating the DFT. The Hanning window and Hamming window are often used (Fig. 2.6). They are defined by:
Hanning:

$$w(n) = 0.5\left(1 - \cos\frac{2\pi n}{N-1}\right), \; n = 0, ..., N-1 \tag{2.26}$$

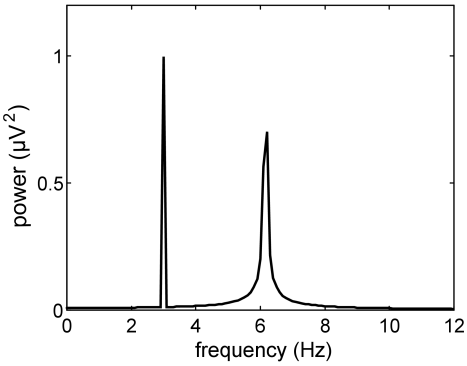

Figure 2.5: Frequency spectrum of a signal consisting of a sinusoid with a frequency (3 Hz) that is an integer multiple of the minimum frequency (0.1 Hz) and a sinusoid of which the frequency is not an integer multiple of the minimum frequency (6.05 Hz). The latter causes spectral leakage.

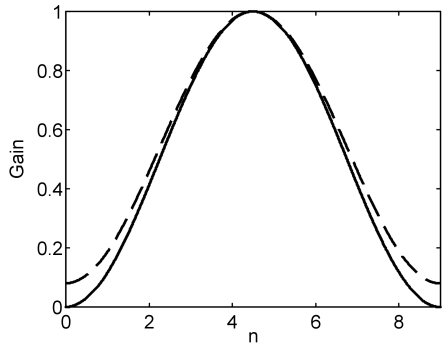

Figure 2.6: Hanning Window (solid line) and Hamming window (dashed line) with N=10.

Hamming:

$$w(n) = 0.54 - 0.46 \cos \frac{2\pi n}{N-1}, \; n = 0, ..., N-1 \tag{2.27}$$

When using the FT for filtering, unwanted frequencies are removed by using high-pass, low-pass, band-pass or band-stop filters. A filter commonly used for EEG is the Butterworth filter. It is designed to have a frequency response that is mathematically as flat as possible in the pass band and goes to zero in the stopband. The transfer function, which describes the amplification of the frequency amplitude by the filter, of the low-pass Butterworth filter is defined by:

$$H(\omega) = \frac{1}{\sqrt{1 + \left({}^{\omega}/_{\omega_c}\right)^{2p}}} \tag{2.28}$$

where ω_c is the cut-off angular frequency, ω is the angular frequency of the signal in radians per second ($\omega = 2\pi f$) and p is the order of the filter. A steeper slope of the filter, indicating sharper cut-off, is obtained by increasing the order of the filter (Fig. 2.7). Equation 2.28 shows that when $|\omega| < \omega_c$ the response is about unity, while if $|\omega| > \omega_c$ the response drops rapidly to zero. The transfer function can be easily modified into a high-pass filter or a band-pass filter.
If the DFT is used for spectral analysis of E(R)Ps, the DFT is estimated for each segment and subsequently the DFTs of the segments are averaged. In this way the random noise is reduced.

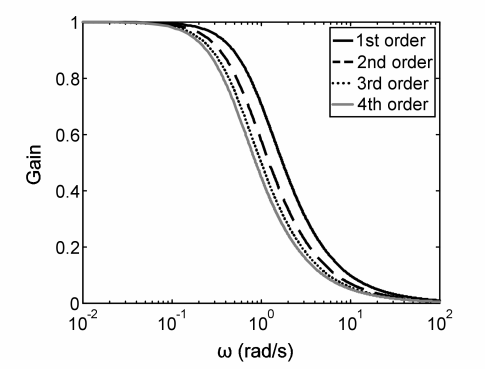

Figure 2.7: Frequency responses of a first, second, third and fourth order Butterworth filter. $\omega_0 = 1$.

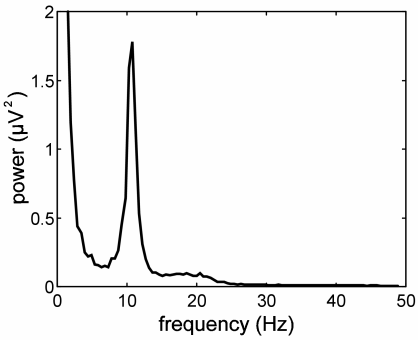

Figure 2.8: Frequency-amplitude spectrum of a P300 recording with alpha activity (8-12 Hz).

2.3.2 Coherence

Coherence analysis has been applied to EEG data for many years as a tool for studying the phase consistency or synchrony between two signals recorded from different scalp regions. High coherence between scalp areas has been interpreted as evidence for anatomical connections (Fein et al., 1988) and functional coupling (Thatcher et al., 1986) between the cortical structures underlying these areas. To study dynamic coupling between different brain areas in relation to specific motor, sensory or cognitive events, event-related coherence can be used (Andrew, 1996). Mathematically, coherence is analogous to a cross-correlation coefficient in the frequency domain. To calculate (event-related) coherence, the Fourier transform is calculated for each segment of the two channels. Secondly, the auto-spectra of channel X ($\hat{G}_{xx}$) and channel Y ($\hat{G}_{yy}$) and the cross-spectra of both channels ($\hat{G}_{xy}$) are determined as follows (Andrew, 1996):

$$\hat{G}_{xx}(k) = \frac{1}{N}\sum_{n=1}^{N}|X_n(k)|^2 \tag{2.29}$$

$$\hat{G}_{yy}(k) = \frac{1}{N}\sum_{n=1}^{N}|Y_n(k)|^2 \tag{2.30}$$

$$\hat{G}_{xy}(k) = \frac{1}{N}\sum_{n=1}^{N}X_n(k)Y_n(k) \tag{2.31}$$

where N is the number of trials. $X_n(k)$ is the frequency amplitude of trial n measured at channel X for index k. Equation 2.23 describes the relation between index k and the corresponding frequency. Next the coherence can be calculated as

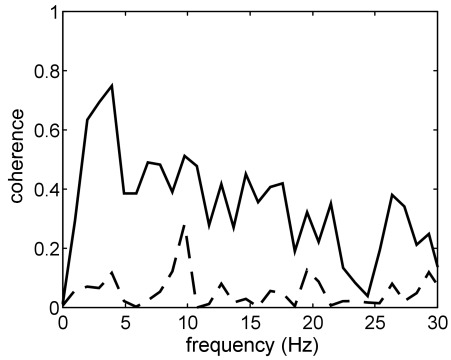

Figure 2.9: Coherence between channel Pz and P4 (solid line) and between Pz and F4 (dashed line) of an oddball task recording. The coherence between Pz and P4 is considerably higher due to volume conduction effects: channel P4 lies much closer to Pz than F4.

the normalization of the cross-spectrum by the two auto-spectra:

$$C_{xy}^2(k) = \frac{\left|\hat{G}_{xy}(k)\right|^2}{\hat{G}_{xx}(k)\hat{G}_{yy}(k)} \tag{2.32}$$

Or alternatively, a band-averaged coherence can be calculated according to (Andrew, 1996):

$$C_{xy}^2(\bar{k}) = \frac{\left|\sum_{k=k_1}^{k_2} \hat{G}_{xy}(k)\right|^2}{\sum_{k=k_1}^{k_2} \hat{G}_{xx}(k) \sum_{k=k_1}^{k_2} \hat{G}_{yy}(k)} \tag{2.33}$$

with the limits of summation (k_1, k_2) related to the frequency band of interest (f_1, f_2) and the segment time by equation 2.23 and $\bar{k}$ the average of all indices k. Additionally, it is possible to obtain a time course of coherence by shifting the segments over small periods from the start to the end of the trial (Pfurtscheller and Andrew, 1999). The latter technique can only be applied if the used segment length is much smaller than the trial length.

In coherence analysis the choice of reference is very important. Data with similar reference electrodes can increase the coherence compared to reference independent methods (Andrew, 1996). Reference methods that improve the coherence estimations are the closely spaced bipolar reference, the linked ear reference, the average reference, and the more complex surface Laplacian (see section 2.2.1) and cortical imaging (Nunez, 1997).

Alternative methods for coherence analysis are covariance analysis (see section

2.2.3), phase locking statistics (Lachaux et al., 1999) and a method introduced by Nikolaev et.al. (2001). The latter method first calculates the wavelet transform of averaged EPs and then computes the correlation coefficient between the wavelet transform curves of pairs of channels. Furthermore, Gross et. al. (2001) designed a technique called DICS (Dynamic Imaging of Coherent Sources). DICS uses a spatial filter, which allows computation of coherence with respect to a reference point at any given location in the brain.

2.3.3 Wavelet transform

Similar to the FT, the wavelet transform (WT) is a method to analyze the frequency content of a signal. In addition, wavelet transforms can be used for filtering (Quian et al., 2001).
The main difference with FT is that wavelets are localized in both time and frequency, whereas the base function of the FT is only localized in frequency. Therefore, WT is used in EP and ERP studies to investigate changes in frequency bands due to stimulation. Başar et al. (1979b; 1979a) suggested that E(R)Ps appear as a reorganization of the spontaneous brain oscillations in response to a stimulus.
Instead of sine and cosine functions, the wavelet transform uses wavelet functions to decompose the signal. In the continuous wavelet transform (CWT) method these "wavelets" are obtained from a mother wavelet by scaling:

$$\varphi_{a,b}(x) = \frac{1}{\sqrt{|a|}}\varphi\left(\frac{x-b}{a}\right) \tag{2.34}$$

where a is the dilation parameter, which governs the frequency of the wavelet and b is the position parameter, which governs the time displacement. However, the shape of the wavelets is always the same as that of the original mother wavelet φ. For φ different wavelets may be chosen. Examples of mother wavelets are the Morlet wavelet and the Mexican hat wavelet (Fig. 2.10). The Morlet wavelet is defined by:

$$\varphi = e^{i\omega_0 x}e^{-\frac{1}{2}x^2} \tag{2.35}$$

The Mexican hat wavelet is defined by:

$$\varphi = (1-x^2)e^{-\frac{1}{2}x^2} \tag{2.36}$$

The wavelet transform calculates the correlation between the wavelet and the original signal, i.e.:

$$W_\varphi X(a,b) = \frac{1}{\sqrt{|a|}}\int_{-\infty}^{\infty} X(t)\varphi^*\left(\frac{t-b}{a}\right)dt \tag{2.37}$$

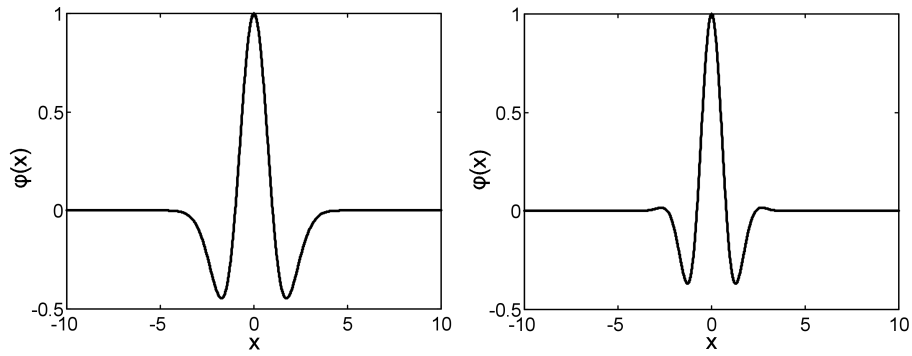

Figure 2.10: Mexican hat wavelet (left) and real part of Morlet wavelet (right).

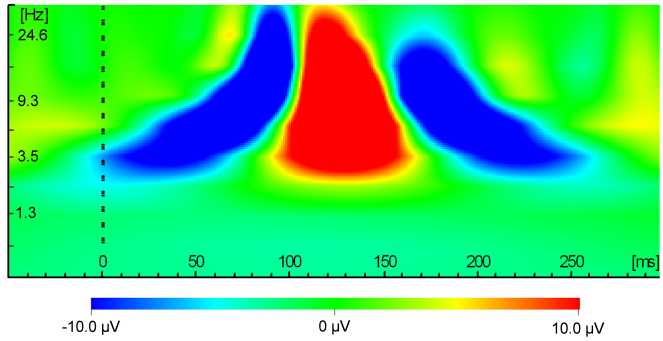

Figure 2.11: Time-frequency chart obtained with the continuous wavelet transform of a VEP recording at channel Oz. After 100 ms the frequency components of the P100 can be observed.

where φ^* is de complex conjugate of the mother wavelet. As a result, the correlation coefficient is obtained as a function of frequency and time.
For discrete signals the discrete wavelet transform (DWT) can be used and like for the discrete Fourier transform, a fast operation, the fast wavelet transform (FWT) has been developed to compute the DWT. In case of the DWT, time frequency information is obtained by digital filtering techniques (Quian et al., 2001). The DWT is computed by low pass and high pass filtering of the discrete time domain signal. This results in two signals; the high pass signal contains frequencies between half the Nyquist frequency and the Nyquist frequency, the low pass signal consists of all frequencies lower than the Nyquist frequency. Next, the resulting high-pass and low-pass signals are downsampled by 2. This procedure is then repeated many times for the lowpass filter signal to further increase the frequency resolution. The signals that are high pass filtered are the outcome of the DWT.

2.3.4 ERD/ERS

When averaging single trials, one assumes that the evoked activity or signal of interest has a fixed time-delay to the stimulus, while the ongoing EEG activity behaves as additive noise. However, due to the stimulus, the ongoing EEG signal may change. The power in a specific frequency band can either decrease or increase. A decrease is called event-related desynchronization (ERD) (Pfurtscheller, 1977), since it is caused by a decrease in synchrony of the underlying neuronal populations. An increase is called event-related synchronization (ERS) (Pfurtscheller, 1992), since it is assumed to be caused by an increase in synchronization.
These changes are time-locked, but not phase-locked, i.e. the power of some frequency bands of the ongoing EEG changes at a fixed time delay, but the phase of the ongoing EEG at that fixed time delay varies over the different trials. When single trials are averaged, this change in the ongoing EEG is no longer detectable. A prerequisite of calculating ERD or ERS is that the interval between two consecutive events should last at least 10 seconds, because event-related changes in ongoing EEG need time to develop and to recover (Pfurtscheller and Andrew, 1999).
ERD and ERS can be calculated using the following steps (see also Fig. 2.12):

1. band pass filtering of all event-related trials
2. calculating the power by squaring the amplitude
3. averaging the power across all trials
4. averaging of time samples to smooth the data and reduce the variability
5. calculating the power relative to a reference period. The reference period is a period of a few seconds before the event occurs.

A disadvantage of this technique is that phase locked (e.g. evoked potentials) cannot be distinguished from non-phase locked EEG, when both types of activity are in the same frequency band. To calculate only the non-phase locked power, the second step can be replaced by squaring the intertrial variance, which is the difference between the single trial and the averaged signal over all trials (Kalcher and Pfurtscheller, 1995). A limitation of this technique is that it does not account for latency and amplitude variability of the stimulus locked component within individual trials. As a result, this technique might remove too little or too much signal. Therefore McFarland et al. (2004) introduced the regression subtraction procedure. In this procedure the average that is subtracted was first corrected for latency and amplitude using the covariance between the averaged signal and the single trials.
Since the introduction of ERD and ERS, various alternative methods have been reported. For example, Makeig (1993) introduced a method called event-related spectral perturbation (ERSP). The advantage of this method is that it calculates

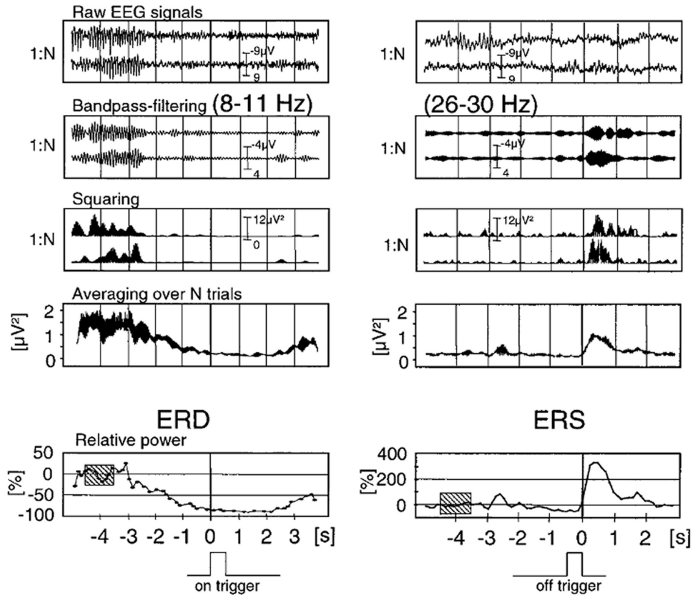

Figure 2.12: Principle of ERD (left) and ERS (right) processing (from Pfurtscheller, 1999).

the amplitude change for the full frequency spectrum. This technique divides all trials in small overlapping windows. The amplitude spectrum is calculated for each window. Next a moving average of these windows is created and the spectra are related to a pre-stimulus period. Finally the trials are averaged.
Other comparable techniques are amplitude modulation (Clochon et al., 1996), task related power (Gerloff et al., 1998), complex demodulation (Nogawa et al., 1976) and temporal spectral evolution analysis (Salmelin and Hari, 1994). This results in negative percentages for ERD and positive percentages for ERS (Pfurtscheller and Lopes da Silva, 1999).

2.4 Conclusion

As shown in this chapter many different analysis techniques can be applied to E(R)P data. However, for clinical applications only a few techniques are applied routinely. Possibly, future studies can extend the clinical applications of E(R)Ps by applying these techniques or variants of these techniques to multichannel recordings.

3

Source localization techniques

3.1 Introduction

Source localization is an inverse method to determine the location and strength of the sources that cause the potentials measured at the scalp. This technique is especially suitable for E(R)Ps, because they have a high SNR. Furthermore, brain activity of E(R)Ps is related to a specific event and therefore the brain activity is often more focused. A problem with the inverse method is that its solution is not unique (Helmholtz, 1853). In other words, different combinations of sources can cause similar potential fields on the head. On the other hand, the forward problem does have a unique solution. The forward problem calculates the potential field at the scalp from known source locations, source strengths and conductivity in the head and can be used to solve the inverse problem.

3.2 Forward problem

The sources of brain activity cause electrical fields according to Maxwell's and Ohm's law. Due to the high propagation velocity of the electromagnetic waves, the currents caused by the sources in the brain behave in a stationary way. This means that no charge is accumulated at any time in the brain. Therefore, it can be stated that for any current density J:

$$\nabla \cdot J = 0 \tag{3.1}$$

In the case of a stationary current, the electric field E is related to the electric potential V by the following expression:

$$E = -\nabla V \tag{3.2}$$

The minus sign indicates that the electric field is orientated from an area with a high potential to an area with a low potential. The current density in the head associated with neural activation is the sum of the primary current J_p, related to

the original neural activity and a passive current flow σE:

$$J = J_p + \sigma E \tag{3.3}$$

where σ is the conductivity of the head tissues. The primary currents are of interest when solving the inverse problems because they represent neuronal activation. However, the effects of volume currents must still be considered when solving the forward problem because they contribute to the scalp potentials. Taking the divergence of both sides of equation 3.3 gives:

$$\nabla \cdot J_p = -\nabla \cdot E\sigma \tag{3.4}$$

Substituting equation 3.2 in equation 3.4 gives the Poisson equation for the potential field:

$$\nabla \cdot J_p = \nabla \cdot (\nabla V \sigma) \tag{3.5}$$

When the medium is assumed to be infinite, isotropic and homogeneous, it can be proven that the solution of the Poisson equation is:

$$V(r_0) = -\frac{1}{4\pi\sigma} \iiint_{volume} \frac{\nabla \cdot J_p}{|r - r_0|} \tag{3.6}$$

which gives the value of the potential at a point r_0 in the volume conductor resulting from a current density J_p. Unfortunately, the human head is not isotropic and homogeneous and it has an irregular shape. To solve the Poisson equation for realistic head shapes, numerical solution methods are required, like the finite element method (FEM) and boundary element method (BEM), and further assumptions need to be made. It depends on the application, which method is sufficient. When FEM and BEM are used to solve the Poisson equation the head is usually divided into three sublayers: the brain, the skull and the scalp, with each a different conductivity. These conductivities are typically standard values that have been measured in vitro using postmortem tissue (Geddes and Baker, 1967). BEM assumes homogeneous conductivity for each layer. In this method the differential equations for the potentials on the surfaces can be transformed into an integral equation over the interfaces of the different conductivity compartments. By discretising these boundaries, the integrals are turned into sums, and the solution of the problem is found by solving a set of linear equations. The surfaces are discretised by triangle meshes and the total number of nodes in all meshes defines the complexity of the linear system. The numerical accuracy depends on the size of the elements relative to the distance of the source to the nearest boundary, so finer elements are required when sources are close to the boundaries.

The finite element model has the advantage that it can determine potentials for non-homogenous conductivity. This model discretises the complete head in volume

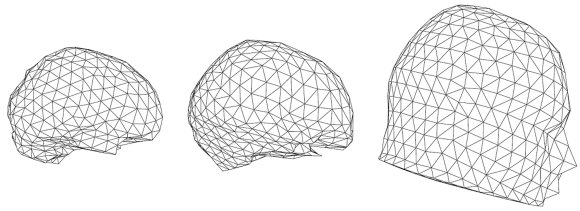

Figure 3.1: Example meshes of the human head used in BEM. Triangulated surfaces of the brain (left), skull (middle) and scalp (right).

elements and can therefore prescribe conductivity for each particular element. The discretisation for FEM also leads to a linear system of equations.
The accuracy of both FEM and BEM models depends on the knowledge of the true conductivities and on the numerical details of the FEM and BEM implementation, in particular the resolution of the mesh on which the solution is computed.

3.3 Inverse problem

First a few key definitions and linear algebraic models will be provided that will clarify the different approaches taken in the inverse methods described in the next section. The general forward model can be presented as:

$$M = AS^T + N \tag{3.7}$$

where M is the matrix with the measured data, N is the vector representing the error or noise in the measurements, A is the gain matrix or lead field matrix and S^T is the matrix containing the dipole amplitudes over time (time series). Each column of matrix A describes the relation between a source and the electrodes. The issue in the inverse problem is, given a set of recordings M, knowing the lead field matrix A, and making a certain assumptions about N, to determine S^T.
The inverse problem can be solved using different methods dependent on the assumptions made. One can assume that the current density distribution can be represented by a small number of equivalent current dipoles (ECD). In this method the locations and time series of each of the ECDs are estimated. The second approach models brain activity by a large number of sources that represent a continuous distribution of neural current generators. Because these generators are believed to lie in the cerebral cortex, the sources are usually constrained to lie on the cortical surface, with the orientation normal to the surface. The inverse solution is then reduced to estimating the set of unknown time series for each elemental source. Here, the latter method is referred to as distributed source localization. In the next paragraphs an overview will be given of the existing source localization methods. This

overview is based on a review by Michel et al. (2004b).

3.3.1 Equivalent dipole source localization

ECD source localization models it sources as electromagnetic dipoles located somewhere in the brain and uses a fixed number of sources. The number of sources can be estimated with singular value decomposition, ICA or PCA, based on physiological knowledge or based on other functional imaging data such as fMRI or PET. However these methods are not without errors.
The number of unknown sources has to be less than or equal to the number of electrodes. The best source locations are found by computing the surface electric potential map generated by these dipoles using a forward model and comparing it with the actual measured map. This comparison is usually based on calculating the squared error X between these two maps:

$$X = \left\| M - AS^T \right\|_F^2 \text{ with } \|B\|_F^2 = \sum\sum B_{ij}^2 \tag{3.8}$$

The solution with minimal squared error is then accepted as best explaining the measured electric activity. Since scanning through the whole solution space with any possible location and orientation of the sources is very demanding and nearly impossible if more than one dipole is assumed, non-linear optimization methods based on directed search algorithms are usually used (Uutela et al., 1998). A general risk of these methods is that they can get trapped in undesirable local minima, resulting in the algorithm accepting a certain location because moving in any direction increases the error of the fit (de Peralta Menendez and Andino, 1994). The number of local minima increases with the number of dipoles. Therefore, the initial position of the dipoles is important, which can be based on imaging studies or physiological knowledge.

3.3.2 Scanning methods

Another approach to overcome the problem of local minima, is the use of a scanning method. These methods use a discrete grid to search for optimal dipole positions throughout the source volume. Source locations are then determined as those for which a metric computed at that location exceeds a given threshold. While these approaches do not lead to a true least squares solution, they can be used to initialize a local least squares search (Darvas et al., 2004). The most common scanning methods are the linearly constrained minimum variance (LCMV) beamformer and multiple signal classification (MUSIC) methods and their variants.
LCMV is a beamformer, which means that it performs spatial filtering on data to discriminate between signals arriving from a location of interest and those originating elsewhere. This is accomplished by simply multiplying the measurement matrix with a weighting matrix. The weighting matrix should pass signals coming

from the location of interest, while attenuating signals from elsewhere. The difference between beamformers is the constraint for estimating the weighting matrix. LCMV determines the weighting matrix by minimizing the output power of a filter under the constraint that its gain is unity at the location of interest. The limitation of this approach is that signal cancellation may occur, when different sources are correlated (Baillet et al., 2001). Another beamformer often used is Synthetic Aperture Magnetometry (SAM) (Vrba and Robinson, 2001).
MUSIC is a widely known signal processing technique that was first applied to EEG data by Mosher et al. (1992). The primary assumptions for this method are that the dipolar time series are linearly independent among each other, the number of time samples is greater than the number of sensors and the number of sources is smaller than the number of sensors. MUSIC is based on a singular value decomposition (SVD) of the measured data, which results in orthogonal basis vectors and singular values. Any true source localization will have a lead field vector in A (equation 3.7) that also lies in the signal subspace computed with the SVD. MUSIC searches throughout the brain volume for source locations that satisfy this condition. The lead field vector at every candidate dipole location is systematically projected on the signal subspace. The dipole source locations with the largest projections on the signal subspace are the active sources (Mosher et al., 1992, 1999).
However, MUSIC suffers from some problems. First, when the noise present in the data is correlated across channels, MUSIC can produce larger errors in the dipole localization than would have been observed with uncorrelated noise of the same power. Another problem is the detection of multiple MUSIC peaks in a 3D volume of the head, each of which may correspond to a different ECD. A related problem is to determine which peaks are truly indicative of a dipolar source rather than a local minimum in the error function (Mosher et al., 1999).
The latter problem is solved in the extended version of MUSIC, recursively applied and projected (RAP)-MUSIC, by recursive estimation of multiple sources (Mosher and Leahy, 1999). In other words, one first estimates the dipole location with the largest projection on to the signal subspace. Then the gain vector and subspace are adapted to find the second dipole location.
Recently, an alternative method was developed called FINES (Xu et al., 2004). This method is able to localize closely spaced correlated sources.

3.3.3 Distributed source localization

Distributed source localization estimates the amplitudes of a dense set of dipoles distributed at fixed locations within the head volume. These methods are based on reconstruction of the brain electric activity in each point of a 3D grid of solution points, the number of points being much larger than the number of electrodes on the scalp. Each solution point is considered as a possible location of a current source, thus there is no a priori assumption on the number of dipoles in the brain.

In these methods again a lead field matrix A is used to relate the activity of the sources to the measured electrode potentials:

$$M = AI \tag{3.9}$$

where M is the vector containing the measured potentials at a certain time point and I is the matrix containing the actual source amplitudes. The task to solve is to find a unique configuration of activity at these solution points that explains the surface measurements. The linear solution for I can be written as:

$$I = TM \tag{3.10}$$

where T is some generalized inverse of the lead field matrix A. Unfortunately, an infinite number of distributions of current sources can lead to exactly the same scalp potential. In other words, there exist an infinite number of different generalized inverse matrices T, all producing a current density vector I that satisfies the original measurements M.
This leads to the application of different assumptions in order to identify the 'optimal' or 'most likely' solution. The methods described in literature differ in their choice and implementation of these assumptions. The constraints can be based on mathematics, on biophysical or physiological knowledge or on findings using other imaging modalities. The validity of these methods is defined by the validity of the assumptions. In the next sections methods most often described in literature are explained in more detail.

Minimum Norm

The general estimate for a 3D brain source distribution in the absence of any a priori information is the Minimum Norm solution (Hämäläinen and Ilmoniemi, 1994). It only assumes that the 3D current distribution should have minimum overall intensity. Stated mathematically:

$$J = \|I\|_2 = \sqrt{\sum_{i=1}^{n} (J_i)^2} \tag{3.11}$$

should be minimized under the constraint given by equation (3.10). This gives a solution for the matrix T. This method leads to only one solution. However, the restriction that the overall intensity should be minimal is not necessarily physiologically valid. This minimum norm algorithm favors superficial sources, because less activity is required in superficial solution locations to give a certain surface voltage distribution. Therefore, deeper sources are incorrectly projected on the surface, which can lead to erroneous interpretations (Pascual-Marqui, 1999; Michel et al., 2004a).

Weighted Minimum Norm

To overcome the problem that the Minimum Norm method prefers superficial source locations, different weighting strategies have been proposed. In these approaches, the function minimized instead is:

$$J = \|WI\|_2 \tag{3.12}$$

where W is a weighting matrix with dimensions equal to the number of rows in I. Each element in W is chosen to downweight the grid points in the head model that are closer to the surface. In this way the error toward large current densities near the surface is reduced. Results of these methods show that sources can be localized, but that the three dimensional current density predicted inside the head is very blurred, which makes accurate source localization difficult (Koles, 1998). Therefore, an alternative method has been developed named FOCUSS (FOCal Underdetermined System Solution) (Gorodnitsky et al., 1995). This method changes iteratively the weight according to the solutions estimated in previous steps. A disadvantage of this method is that the weightings are based on purely mathematical operations without any physiological basis that would justify the choice of weights (Michel et al., 2004a) and might get stuck in local minima (Saeid Sanei, 2007).

Low resolution tomography (LORETA)

Another method to find a unique solution for the 3D distribution among the infinite set of different possible solutions is low resolution brain electromagnetic tomography (LORETA). This method assumes that neighbouring neurons are simultaneously and synchronously activated. This basic assumption rests on evidence from single cell recordings in the brain that demonstrate strong synchronization and correlation of adjacent neurons (Pascual-Marqui et al., 1994). In mathematical terms, the task is to find the smoothest of all possible solutions. While this assumption is basically correct, it has been criticized that the distance between solution points and the limited spatial resolution of EEG recordings lead to a spatial scale where such correlations can no longer be reasonably expected (Hämäläinen, 1995). Because of the assumption of correlation over relatively large distances, LORETA generally provides blurred (over-smoothed) solutions.

Standardized low resolution tomography (sLORETA)

In 2002 Pasqual-Marqui introduced an alternative method called standardized low resolution brain electromagnetic tomography (sLORETA). This method does not use measures of spatial smoothness such as LORETA in order to obtain a smooth solution. sLORETA employs the current density estimate given by the minimum norm solution, followed by a standardization. The current density estimates are

standardized by using the variance of the estimated current density. From simulations it is concluded that the sLORETA method is fast and localizes well, as compared to other distributed solutions, like MN and LORETA (Wagner et al., 2004; Pascual-Marqui, 2002). However, simultaneously active sources can only be separated if their fields are distinct enough and of similar strength. In the context of a strong or superficial source, weak or deep sources remain invisible, and nearby sources of similar orientation tend not to be separated but interpreted as one source located roughly in between (Wagner et al., 2004).

Local autoregressive average (LAURA)

This distributed inverse solution incorporates biophysical laws as constraints in the minimum norm algorithm (Grave de Peralta et al., 2001). The strength of the potentials or fields at a certain brain location depends upon the strength of the current creating the field and upon the distance between the site where the field is created and the place of detection. LAURA expresses the relation between brain activity at one point and its neighbours in terms of a local autoregressive estimator with coefficients depending on the distances between these points. The activity at one point now depends upon two contributions: one fixed by the biophysical laws and another free to be determined from the data.
Simulations showed that LAURA performed better than MN, WMN and LORETA (Grave de Peralta et al., 2001). A comparison with sLORETA has not been made.

EPIFOCUS

EPIFOCUS (Grave de Peralta et al., 2001) has mainly been developed for the analysis of focal epileptic activity where a single, dominant source with a certain spatial extent can be assumed. This method assumes a single focal source but differs from the equivalent dipole location in that it allows this source to have a spatial extent beyond a single point. It is a linear inverse method that scans the solution space and calculates the current density vector by projecting the scalp potential data on each solution point. The results of this estimate can be interpreted as the probability of finding a single source at each specific point. In contrast to the MUSIC method, EPIFOCUS does not require a certain time period of EEG analysis but can rather be applied to instantaneous potential maps. Simulations and analyses of real data have demonstrated a remarkable robustness of EPIFOCUS against noise (Grave de Peralta et al., 2001).

3.3.4 Other models

Bayesian method

The Bayesian approach is a statistical method to incorporate a priori information into the estimation of the sources. The types of a priori information that have been

incorporated in this approach include information on the neural current (Schmidt et al., 1999), the focal nature of the sources, combined spatial and temporal constraints (Baillet and Garnero, 1997), as well as strategies to penalize ghost sources (Trujillo-Barreto et al., 2004).

ELECTRA

ELECTRA is a source model in which the generators of the scalp maps are the intracranial potentials instead of a dipole at each solution. This is based on the findings that EEG measures only the volume currents (passive current caused by passive conductance) and not the active current (induced by ionic flow around the active neuron) (de Peralta Menendez et al., 2000). An advantage of this method is that the number of unknowns is reduced. This increases the spatial resolution for the same amount of data. However this method does still not provide a unique solution, which makes the use of regularization strategies, like MN, WMN and LORETA necessary (Grave de Peralta Menendez et al., 2004).

3.4 Conclusion

To localize the sources that generate the E(R)Ps, the so-called inverse problem must be solved. However, the inverse problem has no unique solution and can only be solved by introducing assumptions regarding source and head models. In the last decades, different assumptions, based on mathematical, biophysical, statistical or physiological theories, have been formulated and implemented in inverse solution algorithms. The reliability of the solution depends on the validity of these assumptions.
One possible future application of source localization may be the separation of E(R)P components that overlap in time and space. A study by Elting et al. (Elting et al., 2003) already showed that source localization can be used to separate the P3a and P3b components.

4

Multichannel recording of median nerve somatosensory evoked potentials

This chapter is published as:
Multichannel recording of median nerve somatosensory evoked potentials. W.J.G. van de Wassenberg, J.H. van der Hoeven, K.L. Leenders, N.M. Maurits. Neurophysiologie Clinique 2008; 38(1):9-21.

Abstract

Objectives. Clinical applications of multichannel (> 64 electrodes) EEG have been limited so far. Amplitude variability of evoked potentials in healthy subjects is large, which limits their diagnostic applicability. This amplitude variability may be partially due to spatial undersampling of anatomical variations in cortical generators. In the present study we therefore investigated if 128-channel recordings of somatosensory evoked potentials (SEPs) can reduce this amplitude variability in healthy subjects. Additionally, we explored the relation between amplitude and age.
Methods. We recorded median nerve SEPs using a 128-channel EEG system in 50 healthy subjects (20-70 years) and compared N20, P27 and P45 amplitude as obtained with a 128-channel analysis method - based on butterfly plots and spatial topographies - and as obtained using a conventional one cortical channel configuration and analysis. Scalp and earlobe references were compared.
Results. Although amplitude variability itself was not reduced, a reduced coefficient of variation was obtained with the 128-channel method due to higher SEP amplitudes compared to the conventional one-channel method, independent of reference.
Conclusion. These results suggest that, at the cost of some additional preparation time, the 128-channel method can measure SEP amplitude more accurately and might therefore be more sensitive to physiological and pathological changes. For optimal amplitude estimation, we recommend to increase the number of centroparietal electrodes or, preferably, to perform at least a 64-channel recording.

4.1 Introduction

Electroencephalography (EEG) is an important diagnostic tool in clinical neurophysiology. A disadvantage of this technique is its low spatial resolution compared to imaging techniques such as MRI, CT, PET and SPECT. However, the temporal resolution of EEG is superior and its costs are much lower. With the development of multichannel systems (> 64 electrodes) since the 1990s the spatial resolution of EEG has increased considerably. Whether the data obtained with this more time-consuming multichannel technique provides additional benefits compared to conventional techniques that employ fewer electrodes, is still under investigation.
So far, multichannel EEG has proven to be useful in the study of healthy brain physiology (Huber et al., 2004; Jackson et al., 2004; Massimini et al., 2004; Sabbagh et al., 2004) and has given new insights in psychiatric diseases (Pae et al., 2003; Ruchsow et al., 2003; Youn et al., 2003). Yet, in contrast to what may be expected of a technique that has proven its value in diagnostic neurology when using a few electrodes, only a limited number of studies report clinical neurological applications of multichannel EEG (Elting et al., 2005; Lantz et al., 2003a,b; Michel et al., 2004a). First applications were in pre-operative localization of epileptogenic lesions using source localization (Lantz et al., 2003a,b; Michel et al., 2004a). More recently, results from Elting et al. (2005) suggest that multichannel event-related potentials can improve diagnosis and quantification of cognitive disorders after acute brain injury.
As far as we know, there have been no studies investigating the added clinical value of multichannel recordings for evoked potentials (EPs). Visual, somatosensory and brainstem auditory EPs are widely applied clinically, typically using only a few (< 10) electrodes. Specifically, EP latencies are used to assess nerve conduction velocities in peripheral and central sensory pathways (Chiappa, 1997). Here, we investigate the added value of multichannel recordings for somatosensory EPs (SEPs), because of their well-known and superficially positioned generators, and their interest for a diverse range of neurological disorders (movement disorders, neuropathies, MS, plastic cortical changes after stroke or related to pain, coma) (Chiappa, 1997).
Each SEP component is characterized both by its latency and its amplitude. Nonetheless, since intersubject SEP amplitude variability is large in healthy subjects (Chiappa, 1997; Ferri et al., 1996; Gardill and Hielscher, 2001), this parameter seems to be less useful for clinical purposes. Several authors that investigated SEP amplitude in healthy subjects and in neurological patients support this thought (Bostantjopoulou et al., 2000; Ferri et al., 1996; Gardill and Hielscher, 2001; Kofler, 2000). However, these studies used a limited number of electrodes (< 16 electrodes), which means that the interelectrode distance was 7 cm or higher. Because of large intersubject variation in size, shape and topography of the somatosensory cortical areas (Geyer et al., 1999; Uylings et al., 2005), the position of the maximum amp-

litude varies between subjects (Buchner et al., 1992; Legatt et al., 1987; Legatt and Kader, 2000). According to Spitzer et al. (1989), who investigated the minimum interelectrode distance necessary for optimal amplitude estimation by using the Nyquist criteria for the spatial frequencies of SEP components, an interelectrode distance of at most 3 cm is required. Thus, the large intersubject variability and low sensitivity and specificity found for SEP amplitude might, at least partly, be due to inaccurate amplitude estimation.
We hypothesize that using 128-channel SEP recordings for amplitude estimation, will reduce intersubject variability and thereby improve the diagnostic sensitivity and specificity of SEP amplitude for neurological disorders.
A prerequisite for the diagnostic use of 128-channel SEP amplitude is the availability of normal values. For this purpose it is important to know if SEP amplitude is related to age. If so, then normal values must be defined for different age groups. Previous studies, using a maximum of 16 electrodes, found different results for the age-amplitude relation (Desmedt and Cheron, 1981; Ferri et al., 1996; Kakigi and Shibasaki, 1991; Kazis et al., 1983; Strenge, 1986). If 128-channel recordings reduce the intersubject amplitude variability, this method will probably also better quantify the effect of age on the amplitude. Besides, Strenge (1986) suggested that a reorganization of primary cortical areas may occur with aging, which may further modify the topography and the position of maximum amplitude. When using 128-channel recordings for SEP amplitude estimation this alteration can be taken into account as well. The aim of the current study is to investigate if a 128-channel recording decreases the intersubject amplitude variability of SEP components. We compared SEP amplitudes obtained using the electrode configuration proposed by Mauguière et al. (1999) with one cortical channel to SEP amplitudes obtained by 128-channel recordings in healthy subjects. Furthermore, we compared scalp and earlobe references. In addition, we investigated the effect of age on 128-channel SEP recordings and defined normal values, which can be used for future patient studies. We conclude with some recommendations for clinical practice.

4.2 Materials and methods

4.2.1 Subjects

Median nerve SEPs were recorded from 50 right-handed healthy volunteers. For each decade between 20 and 70 years five males and five females were included, except for the highest decade, where four males and six females were included. None of the subjects had a history of head injury or other neurological conditions. All subjects gave their informed consent. The protocol was approved by the medical-ethical board of the University Medical Center Groningen.

4.2.2 SEP recording

The subjects were sitting in a chair in a warm and quiet room and were instructed to relax and keep their eyes open. We stimulated the median nerve at both wrists 500 times, one side at a time, and repeated each recording once. The stimuli were square wave impulses of 0.2 ms, which were delivered at a frequency of 2.1 Hz. The stimulus intensity was slightly above motor threshold, producing a small thumb switch. We placed Ag/AgCl-disc electrodes over Erb's point with the reference electrode at the sternum and recorded EEG from the scalp using a 128-electrode cap, which was connected to a 128-channel headbox (Twente Medical Systems BV, Enschede, Netherlands). To place the cap we measured the distance between nasion and inion, positioned Fpz at 10% of the nasion-inion distance above the nasion and checked if the Cz electrode was positioned at the centre of the nasion-inion distance and between both pre-auricular points. Impedance values were kept below 10 kΩ. We used Onyx software (Silicon Biomedical Instruments BV, Westervoort, The Netherlands) to record the data at a sampling frequency of 1000 Hz.
Data at Erb's point were recorded, segmented, amplified and averaged with the Medelec Synergy N-EP system (Oxford Instruments Medical, Concord, USA) to verify peripheral propagation parameters against normal data from our laboratory.
The raw EEG data was processed off-line using Brain Vision Analyzer 1.05 (Brain Products GmbH, München, Germany). We high-pass filtered the data at 3 Hz (12 dB/octave, zero-phase shift Butterworth filter). With this filter all components, including the later ones, are preserved. A clinically more often applied 20 Hz high-pass filter, although preserving the N20 component, would have suppressed the amplitude of later components. Next, the data was segmented into epochs of 100 ms including a 10 ms pre-stimulus interval. Artifact rejection was set at 100 μV and a baseline correction procedure was performed using the pre-stimulus interval. Channels with muscle artifacts that obscured the SEP were excluded for further analysis.
On each stimulation side, we used the recording with the highest signal-to-noise ratio for further analysis. The signal-to-noise ratio was calculated by dividing the N20 peak amplitude by the mean baseline amplitude.
We repeated the complete protocol in 5 subjects, one from each decade, within 6 months to assess long-term intrasubject reproducibility.

4.2.3 SEP analysis

Conventional SEP analysis

We considered both CP4-Fz/CP3-Fz (conventional scalp reference) and CP4-A1/CP3-A2 (conventional earlobe reference) for estimation of N20, P27 and P45 latency and amplitude for left/right side stimulation. The largest early negative peak was identified as the N20. The main prominent positive peak succeeding

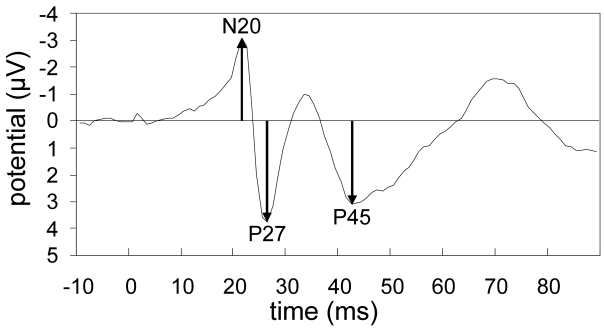

Figure 4.1: Conventional analysis technique for scalp and earlobe reference analyses. Peak to baseline amplitude of CP3-Fz/CP3-A2 (right side stimulation) or CP4-Fz/CP4-A1 (left side stimulation) is used as amplitude.

the N20 was recognized as the P27 and the P45 was the main prominent positive peak following the P27 (Fig. 4.1). All amplitudes were defined as peak-to-baseline amplitudes.

128-channel SEP analysis

For further analysis, the averaged data were exported to ASA 2.21 (ANT software BV, Enschede, The Netherlands) using either an average (dataset 1) or earlobe reference (dataset 2). The results of the subsequent analysis on dataset 1 were compared to the conventional scalp reference results. The results of the analysis on dataset 2 were compared to the conventional earlobe reference results.
For both 128-channel analyses we searched for negative (N20) and positive peaks (P27 and P45) in the butterfly plot between 15 and 65 ms and checked if the corresponding map met the criteria we defined for N20, P27 and P45. These criteria were a frontal positive field together with a parietal negative field for the N20 map, a parietal positive field in combination with a negative frontal field for the P27 map and a positive parietal/central field for the P45 map, all contralateral to the stimulation side. In both analyses we used the topographic map with average reference, which is the reference of choice for these maps (Pascual-Marqui and Lehmann, 1993b).
If the map matched, we used the difference between maximum and minimum amplitude at the time of the peak as (total) amplitude in the analysis of dataset 1. In the analysis of dataset 2 we used the peak to baseline amplitude as (total) amplitude at the time of the peak (Fig. 4.2). The latency of the 128-channel method was defined as the time between stimulus onset and the time of the peak.

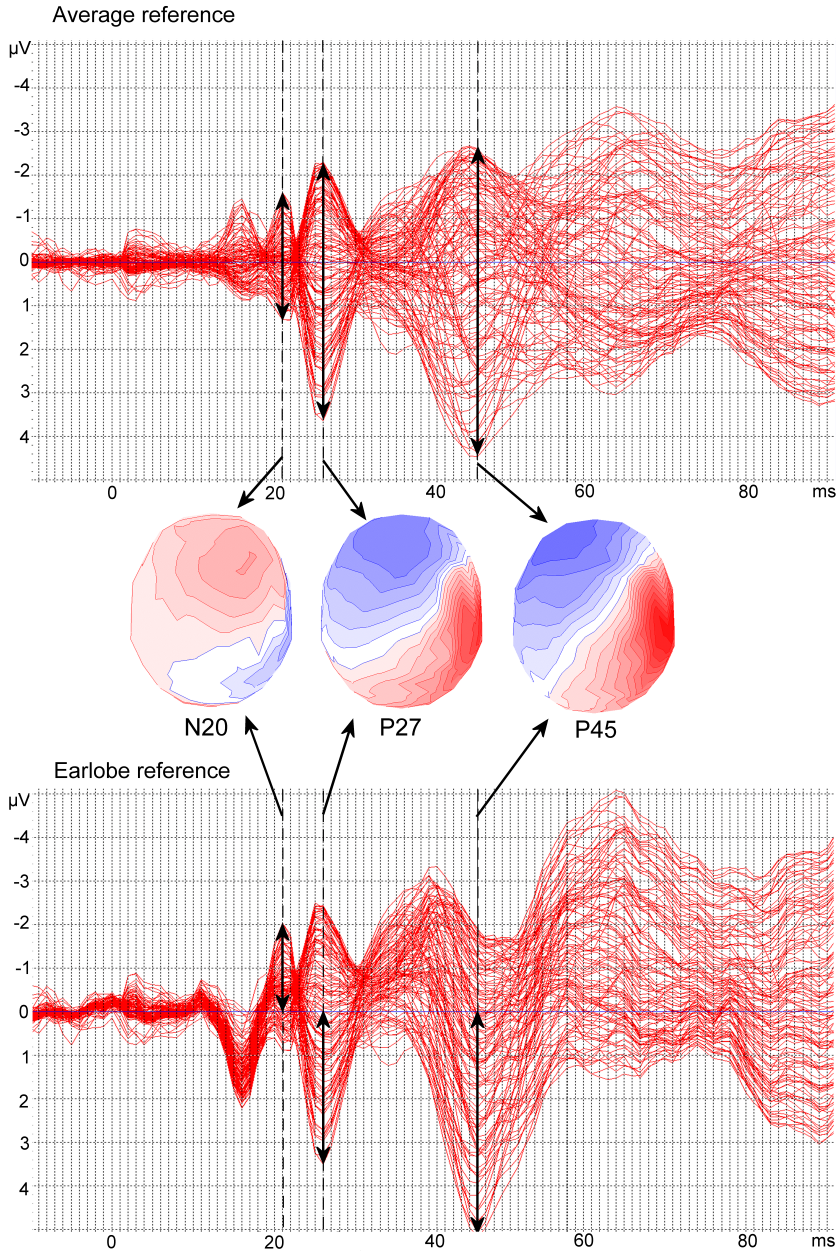

Figure 4.2: 128-channel analysis technique for scalp and earlobe reference analyses. Topographic maps that correspond with peaks in the butterfly plot are compared with a reference map. For the scalp reference the difference between maximum and minimum amplitude at the time of the peak is used as (total) amplitude (top butterfly plot). For the earlobe reference the maximum amplitude to baseline is used as (total) amplitude (bottom butterfly plot).

Table 4.1: Subject characteristics

Age group	Number	Age
20-30	10	26.4 ± 2.8
30-40	10	33.9 ± 3.0
40-50	10	44.9 ± 2.6
50-60	8	54.3 ± 2.8
60-70	10	62.7 ± 2.6

Age is given in years as mean ± sd.

Statistics

We used the intraclass correlation coefficient (ICC) to test the intrasubject amplitude variability of two successive recordings on the same day for scalp reference analyses. The ICC is a measure of agreement between data and was calculated according to Rousson et al. (2002). If peak amplitudes of two successive recordings are equal, the ICC is 1, if they have no agreement at all the ICC is 0.
For the statistical analysis of both scalp and earlobe reference analyses we divided the subjects in different age groups. To include at least 10 persons in each age group and because we mainly expected age effects from 30 years onwards we divided the subjects in the following age groups: 1) 20-30 years, 2) 30-50 years and 3) 50-70 years.
Since not all parameters were normally distributed and a group of 10 subjects is rather small for parametric testing, we used Wilcoxon signed ranks test for comparison of latencies and amplitudes between methods. Additionally, we compared the amplitude and latencies of the different age groups using the Kruskal-Wallis test. Post hoc testing was performed using the Kolmogorov-Smirnov Z test with subsequent Bonferroni correction. All parameters were described in terms of medians and interquartile ranges. Furthermore, regression analysis was performed to examine the effect of age on amplitude and latency.
Furthermore, interquartile range divided by the median was used as alternative coefficient of variation (aCOV). We compared aCOV of the 128-channel analyses to the conventional analyses for both scalp and earlobe references, since a lower aCOV is indicative for a better sensitivity/specificity when evaluating patients.

4.3 Results

We excluded two of the 50 subjects (males; 50 and 56 years old), because they experienced the stimuli as too painful. None of the subjects had an abnormal latency at Erb's point. A few subjects had no reproducible Erb response. However, the cortical responses of these subjects were normal and for that reason these subjects were included in the analysis. Subject characteristics are given in table 4.1. We analyzed the SEP data of the remaining 48 subjects according to the conventional

Table 4.2: Number of observed components per SEP peak in 48 healthy subjects for both scalp and earlobe reference analyses.

		N20		P27		P45	
Method		L	R	L	R	L	R
Scalp	Con	47	47	33	36	44	39
	128	43	46	25	27	48	48
Earlobe	Con	42	43	34	31	40	42
	128	44	43	31	29	47	46

Con: conventional method; 128: 128-channel method.
L: left side stimulation; R: right side stimulation.

and 128-channel analysis methods, using both scalp and earlobe references. N20, P27 and P45 could not be identified in all subjects. Table 4.2 shows the number of detected components. P45 was identified in more subjects with the 128-channel method, while P27 was identified more often with the conventional method. There was no relationship between age and the absence of components. Since at most one component was missing per stimulation side in all subjects, none of the subjects was excluded for this reason.

4.3.1 Reproducibility

We tested amplitude reproducibility when using the scalp reference by calculating the ICC of the same components identified in two successive recordings on the same day. Values ranged from 0.81 to 0.92 for the 128-channel method and from 0.86 to 0.95 for the conventional method. According to the criteria proposed by Lee et al. (1989) these ICC values represent a good reliability. In figure 4.3 the Bland-Altman plots (Bland and Altman, 1986) are displayed for peak amplitudes of two successive recordings at the same day and for two recordings obtained with a time interval of 2-6 months. Differences between recordings at separate days were in the same range as differences between two successive recordings on the same day. The amplitude difference between two successive recordings was in most cases less than 1.0 μV, but there were outliers with maximum values up to 2.94 μV.

4.3.2 Comparison between conventional and 128-channel analyses

In tables 4.3 and 4.4 amplitudes and latencies for both scalp and earlobe reference analyses are displayed. Median amplitudes as obtained with 128-channel analyses were significantly higher than amplitudes determined with conventional analyses, while interquartile ranges of conventional and 128-channel methods were typically similar. Consequently, in general aCOV was lower for the 128-channel method compared to the conventional method (Table 4.5).

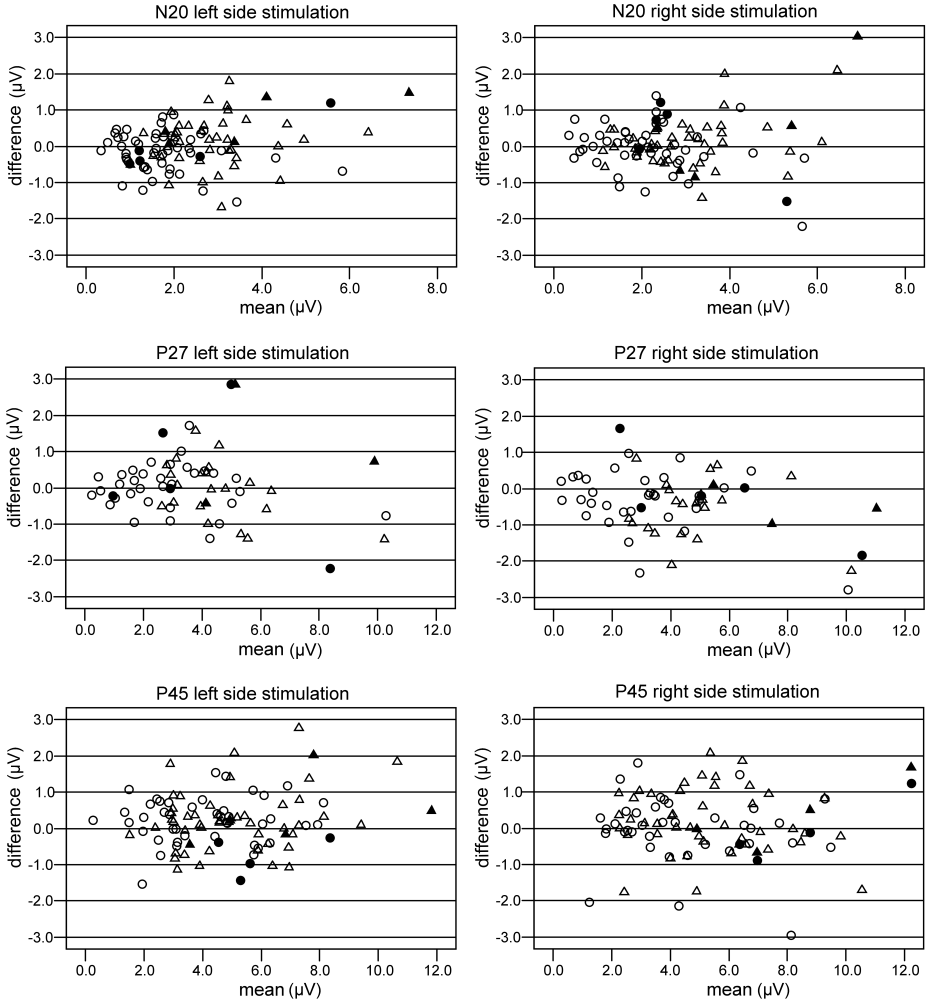

Figure 4.3: Difference against mean of two successive recordings at the same day and two recordings with a time interval of 2-6 months for the scalp reference analyses. Open circle: conventional (same day); closed circle: conventional (2-6 months interval); open triangle: 128-channel (same day); closed triangle: 128-channel (2-6 months interval). Differences between 2 recordings with a time interval of 2-6 months lie in the range of the differences between 2 successive recordings.

Table 4.3: Median and interquartile range (IQR) for peak amplitudes in μV (A) and latencies in ms (B) per age group and for the entire group of subjects obtained with scalp reference analyses.

Amplitude		20-30				30-50				50-70				Total			
		Median		IQR		Median		IQR		Median		IQR		Median		IQR	
Peak	Method	L	R	L	R	L	R	L	R	L	R	L	R	L	R	L	R
N20	Con	1.91	1.86	1.12	1.01	1.65	2.46	1.24	1.90	1.79	2.18	1.47	2.26	1.69	2.13	1.26	1.76
	128	2.71	2.16	1.42	1.16	2.84	3.18	1.54	2.13	2.73	3.40	1.53	2.04	2.76	2.71	1.27	1.86
P27	Con	2.81	3.41	2.49	2.36	1.96	2.35	1.98	3.64	3.35	3.11	2.78	2.77	2.62	3.17	2.38	3.01
	128	3.73	4.04	3.45	2.09	3.70	4.04	1.58	2.09	5.17	4.43	2.63	2.40	4.18	4.17	2.05	1.69
P45	Con	2.02	3.22	3.23	3.20	4.68	4.96	2.84	4.91	3.31	4.07	3.20	4.42	3.82	4.07	3.30	4.08
	128	3.55	3.69	2.71	4.41	5.14	5.22	3.37	3.61	4.82	5.65	3.48	3.65	4.70	5.03	3.25	3.61

A

Latency		20-30				30-50				50-70				Total			
		Median		IQR		Median		IQR		Median		IQR		Median		IQR	
Peak	Method	L	R	L	R	L	R	L	R	L	R	L	R	L	R	L	R
N20	Con	21	20	2	1	21	21	2.75	2	22	22[1]	1.5	2	21	21	2	2
	128	21	20	1	1	21	21	3	3	22	22[1]	1.5	2	21	21	2	3
P27	Con	26	26	4.25	4	26	29.5	6	6.5	28.5	30	3.75	2	27	29.5	6	5.75
	128	27	28.5	6	6.5	30.5	31	3	4.75	27	30	3	3	29	30	4.5	4
P45	Con	42	43	7.5	10.5	45	43	10.5	6	45	46	7.5	8	45	43	7.75	7
	128	43.5	44.5	7.25	5	46.5	47	7.75	7.75	45.5	48.5	7.25	10.5	46	46.5	6	8

B

Con: conventional method; 128: 128-channel method.
L: left side stimulation; R: right side stimulation.
Amplitudes are all significantly higher for the 128-channel method than for the conventional method except for P45 right side (age group 20-30).
Latencies are only significantly different between both methods for N20 left side (age group 30-50) and for N20 right side (total group).
[1] significant difference with age group 20-30 ($p < 0.05$).

Table 4.4: Median and interquartile range (IQR) for peak amplitudes in μV (A) and latencies in ms (B) per age group and for the entire group of subjects obtained with earlobe reference analyses.

Amplitude		20-30				30-50				50-70				Total			
		Median		IQR		Median		IQR		Median		IQR		Median		IQR	
Peak	Method	L	R	L	R	L	R	L	R	L	R	L	R	L	R	L	R
N20	Con	1.41	1.53	1.32	0.67	1.39	1.89	0.58	1.31	1.70	1.75	0.95	1.54	1.45	1.75	0.85	1.17
	128	2.13	1.86	0.69	0.65	1.94	2.03	0.97	1.58	2.34	2.54	1.32	1.76	2.12	1.93	0.84	1.34
P27	Con	1.70	2.33	1.04	1.75	1.51	2.08	1.64	2.21	1.91	1.50	1.91	1.84	1.58	2.06	1.31	1.63
	128	2.07	2.28	1.24	1.01	2.10	2.18	1.76	1.85	3.07	3.10	1.15	2.28	2.60	2.47	1.67	1.40
P45	Con	3.02	2.67	2.15	3.11	2.41	3.19	2.19	3.46	3.62	3.63	2.58	2.33	3.05	3.14	2.11	2.87
	128	3.73	3.12	1.88	2.70	3.05	4.06	2.52	2.49	4.00	4.62	2.57	2.64	3.39	4.18	2.15	2.56

A

Latency		20-30				30-50				50-70				Total			
		Median		IQR		Median		IQR		Median		IQR		Median		IQR	
Peak	Method	L	R	L	R	L	R	L	R	L	R	L	R	L	R	L	R
N20	Con	20	20	2.5	1	21	21	2.5	2.5	21	22	1.75	2	21	21	2	2
	128	20	20	2	1	21	21.5	2	3	21	22	1.75	2	21	21	2	2
P27	Con	25	24.5	5	3.75	27	26	5	5.5	27.5	28.5	2.75	3	27	27	4.25	5
	128	27	26.5	8.25	4.5	31	30	3.75	4	28	30[1]	3	3.5	29	30	5	5.5
P45	Con	43	42	6.5	7.75	45	46.5	8	5.25	45	47.5	7.25	8.75	44.5	46	6.75	5.50
	128	43	44	6	4.75	46	46	7	7	47	48	5.25	9.5	46	46	6	5.25

B

Con: conventional method; 128: 128-channel method.
L: left side stimulation; R: right side stimulation.
Amplitudes are all significantly higher for the 128-channel method than for the conventional method except for P27 right side age group 20-30. Latencies are only significantly different between both methods for P27 left side in the middle age group and the total group and for N20 right side in the total group.
[1] significant difference with age group 20-30 ($p < 0.05$).

Table 4.5: Alternative coefficient of variation (aCOV) of amplitude for each SEP peak for all analyses

		Scalp		Earlobe	
Peak	Method	L	R	L	R
N20	Con	0.74	0.83	0.59	0.67
	128	0.46	0.69	0.39	0.69
P27	Con	0.91	0.95	0.83	0.79
	128	0.49	0.41	0.64	0.57
P45	Con	0.86	1.00	0.69	0.92
	128	0.70	0.72	0.63	0.61

Con: conventional method; 128: 128-channel method.
L: left side stimulation; R: right side stimulation.

Latencies were not significantly different between conventional and 128-channel analyses, for neither scalp nor earlobe reference.
Fig. 4.4 shows the difference in amplitude between conventional and 128-channel analyses against the amplitude as determined by the 128-channel methods for both references. N20 amplitude was always larger for the 128-channel method compared to the conventional method. In a few subjects P27 and P45 amplitude was however lower for the 128-channel method. No systematic difference as a function of 128-channel amplitude was observed.
Since the difference in amplitude between conventional and 128-channel methods can be rather large, we further investigated the position of the maximum amplitude. Figure 4.5 illustrates the results for the scalp reference analysis; results for the earlobe reference analysis are similar. These results show that the maximum amplitude of all SEP components can be found in a widespread area, including central, temporal and parietal positions on the scalp.

4.3.3 Age effect

When evaluating the age effect, we observed no significant differences in amplitude between age groups. Regression analysis resulted in a few significant positive age-effects (Table 4.6 and 4.7). However, these age effects were not consistent between analyses techniques. Furthermore, the regression parameters and age-amplitude scatterplots, showed that these effects were very small.

4.4 Discussion

In this study we examined the added value of 128-channel recordings for somatosensory EPs. We compared amplitude and amplitude variability of 128-channel SEP analyses, combining butterfly plots and potential maps to find the location at which the SEP peak amplitude is maximal, with conventional analyses. We hypothesized that a 128-channel recording would decrease the intersubject variability

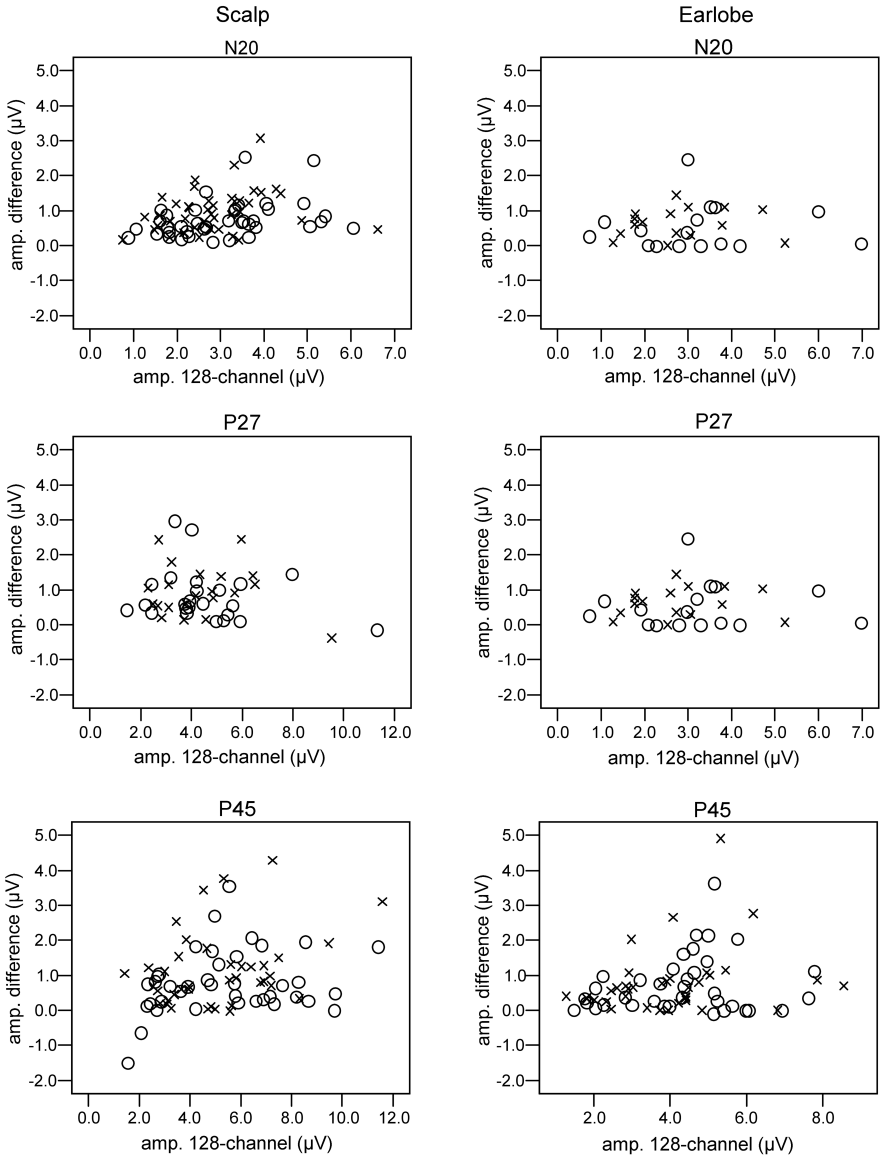

Figure 4.4: N20, P27 and P45 amplitude difference between 128-channel method and conventional method plotted against the amplitude obtained with 128-channel method for both scalp (left) and earlobe reference analyses (right). Cross: left side stimulation; open circle: right side stimulation. In most cases amplitude is higher when determined with 128-channel method compared to the conventional method.

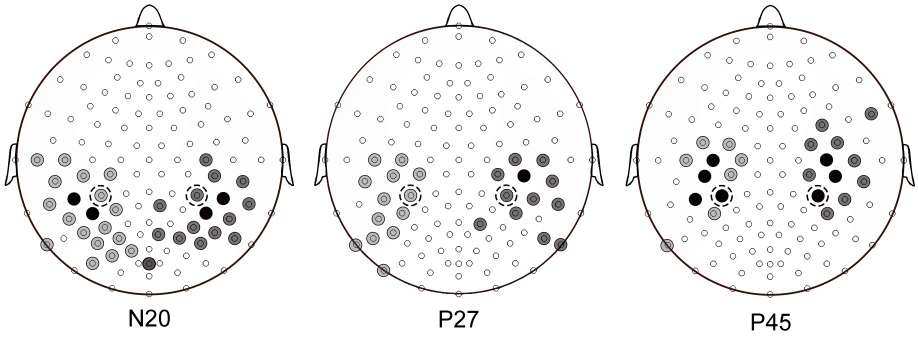

Figure 4.5: Positions of maximum amplitude for the different SEP components for the 128-channel scalp reference analysis. Light grey circles: positions with maximum amplitude for right side stimulation. Dark grey circles: positions of maximum amplitude for left side stimulation. Black circles: positions where maximum amplitude was found in more than 5 subjects. The electrodes used in the conventional method (CP3/CP4) are indicated with a dashed circle.

Table 4.6: Slope in μV/year and R^2 for the amplitude-age en latency-age regression analysis for each SEP peak as estimated by scalp reference analyses.

			Slope		R^2	
	Peak	Method	L	R	L	R
amplitude	N20	Con	0.017	0.024	0.046	0.072
		128	0.014	0.036	0.032	0.146*
	P27	Con	0.022	0.012	0.026	0.006
		128	0.040	0.008	0.123	0.004
	P45	Con	0.043	0.028	0.081	0.026
		128	0.051	0.052	0.108*	0.093*
latency	N20	Con	0.044	0.050	0.138*	0.189*
		128	0.035	0.051	0.105*	0.202*
	P27	Con	0.042	0.077	0.036	0.093
		128	-0.053	0.008	0.041	0.001
	P45	Con	0.089	0.075	0.050	0.050
		128	0.023	0.053	0.004	0.021

Con: conventional method; 128: 128-channel method.
L: left side stimulation; R: right side stimulation.
* significant correlation ($p < 0.05$).

Table 4.7: Slope in μV/year and R^2 for the amplitude-age en latency-age regression analysis for each SEP peak as estimated by earlobe reference analyses.

			Slope		R^2	
	Peak	Method	L	R	L	R
amplitude	N20	Con	0.013	0.008	0.056	0.017
		128	0.018	0.021	0.101*	0.098*
	P27	Con	0.022	-0.005	0.076	0.002
		128	0.038	0.017	0.263*	0.032
	P45	Con	0.044	0.025	0.138*	0.038
		128	0.034	0.031	0.079	0.067
latency	N20	Con	0.026	0.029	0.060	0.069
		128	0.029	0.043	0.078	0.149*
	P27	Con	0.059	0.075	0.103	0.149*
		128	-0.014	0.032	0.003	0.015
	P45	Con	0.096	0.137	0.070	0.142*
		128	0.040	0.116	0.014	0.121*

Con: conventional method; 128: 128-channel method.
L: left side stimulation; R: right side stimulation.
* significant correlation ($p < 0.05$).

in amplitude, since it potentially overcomes the discrepancy caused by intersubject variation in position and orientation of cortical SEP generators with respect to the fixed, conventional recording position. In contrast to our expectations, we found similar intersubject amplitude variability for conventional and 128-channel methods. Nevertheless, amplitudes obtained with 128-channel method were considerably higher compared to the conventional method (Tables 4.3 and 4.4 and Fig. 4.4), because the electrode position where the SEP component was maximal was typically not the same as the electrode position used in the conventional method. Consequently, the higher amplitude caused a lower aCOV when using the 128-channel method. Therefore, the 128-channel method is likely to be more sensitive to pathological changes than a conventional recording and analysis.

As expected, no significant differences in latency were observed between conventional and 128-channel methods, except for N20 left side stimulation in the middle age group for scalp reference analyses, right side stimulation in the entire group of subjects for both scalp and earlobe reference analyses and P27 right side stimulation for earlobe reference analyses. In a few subjects we found a smaller P27 or P45 amplitude with the 128-channel method, which can be explained by a latency difference between methods. Apparently, the potential map that corresponds to P27 or P45 latency in the conventional method does not always match the reference map used in the 128-channel method.

We also investigated the effect of age on amplitude. Previous SEP studies showed an increase of N20, P27 and P45 amplitude with age (Desmedt and Cheron, 1981; Kakigi and Shibasaki, 1991; Kazis et al., 1983; Strenge, 1986) although others reported no significant age effect on N20, N30 and P45 amplitude (Ferri et al., 1996). In our study, a comparison of amplitude between age groups did not result in signi-

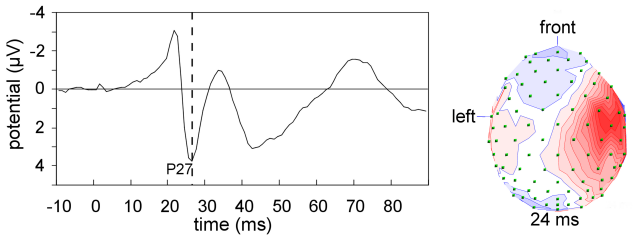

Figure 4.6: Results of scalp reference analyses. Left: Peak in the conventional derivation at 24 ms identified as a P27. Right: Topographic map that corresponds to the peak detected at 24 ms. Topographic map does not correspond to the reference map and this peak is therefore not identified as a P27 with the 128-channel method.

ficant differences. Some of the SEP studies mentioned above included subjects with a maximum age of approximately 90 years (Desmedt and Cheron, 1980; Kakigi and Shibasaki, 1991), whereas in our study we included subjects between 20-70 years old only. As age effects are likely to be more prominent in older age, this may explain the absence of a significant difference between age groups. Furthermore, we used the less powerful non-parametric Kruskal-Wallis test instead of a t-test or ANOVA used in the other studies, since we took the non-normality of distributions into account (Chiappa, 1997). Previous studies that used the t-test or ANOVA did not report the results of normality tests.

We found positive correlations between age and amplitude for different SEP components after left and right side stimulation, but these correlations were small ($<$ 20% explained variance) and not consistent between scalp and earlobe reference analyses.

In the present study amplitude reproducibility of the 128-channel method was comparable with the conventional method for scalp reference analyses (Fig. 4.3). Differences in amplitude between two recordings at separate days were in the same range as the differences between two successive recordings. Consequently, we may conclude that the variation between two 128-channel recordings at different days is caused by physiological variability only.

The 128-channel method identified a P45 peak more often and a P27 peak less often than the conventional method. Again, this may be explained by a mismatch between the potential map at the latency of the conventional method and the 128-channel reference map. In some cases a central positive field is found at the P27 latency (Fig. 4.6) as obtained with the conventional method, which might correspond to a central P22 field. Secondly, it might be that P27 amplitude is below noise level, making the P27 invisible in the butterfly plot. Since P27 could ultimately only be identified in half of the subjects with the 128-channel method independent of reference, this peak may be less useful for clinical applications compared to the N20 and P45 peaks. The absence of P27 has been reported in some previous studies

(Desmedt and Cheron, 1980; Gardill and Hielscher, 2001; Strenge, 1989).
Additionally, Desmedt and Bourguet (1985) reported an absent P45 in half of a group of young subjects (21-34 years) in a 16-channel SEP study, while P45 was found more regularly in older subjects. However, they used the contralateral earlobe electrode as reference, which may be contaminated with SEP activity (Tomberg et al., 1991). This may have caused lower amplitudes, especially for the more central P45 field, leading to a smaller number of detected P45 peaks.
The P27 may have different morphologies and amplitudes in scalp and non-cephalic montages. However, the number of identified P27 components did not differ notably between scalp and earlobe references in the present study.
In our study, we used the maximum sample frequency of our system (1 kHz) feasible for 128-channels. In conventional clinical SEP measurements a sample frequency around 10 kHz is generally applied, which is especially important for adequate sampling of fast and sharp EP components. Therefore, we believe that a higher sample frequency will not have a large effect on the slower and less sharp N20, P27 and P45.
The reference for SEP recordings has often been the matter of debate (Desmedt and Tomberg, 1990; Tomberg et al., 1991, 1990). For the conventional method Fz or earlobe electrodes are recommended as reference (Mauguière et al., 1999), whereas potential maps can better be studied using an average reference (Pascual-Marqui and Lehmann, 1993b,a). However, in our recordings, the earlobe electrodes presented SEP activity and were contaminated with artifacts. For that reason, we first chose Fz as reference electrode, realizing that in this way it is not possible to study parietal and frontal SEP components separately. Average reference was used for the 128-channel method, allowing the use of topographic maps in the analysis (Pascual-Marqui and Lehmann, 1993b,a). By defining amplitude as the difference between highest and lowest amplitude in the butterfly plot, we ensured that the choice of reference did not influence this parameter and that 128-channel and conventional results could be compared. To judge the influence of reference on the identification of separate components and to allow comparison with existing literature, we also included earlobe reference analyses.
Our results show that conventional scalp derivations may not be optimal (CP3-Fz/CP4-Fz and CP3-A2/CP4-A1): the position of maximum amplitude obtained from 128-channel recordings is found more posterior and lateral for the N20, more lateral for the P27 and more anterior and lateral for the P45 component compared to CP3/CP4 (Fig. 4.5). We therefore recommend to increase the number of electrodes for optimal SEP component amplitude estimation compared to conventional recordings. This could be achieved by recording from a larger cluster of centroparietal electrodes or by using a multichannel recording as described in this paper. Multichannel recordings with 64 electrodes are theoretically sufficient, since according to Spitzer et al. (1989) a spatial distance of at most 3 cm is required for optimal amplitude estimation of SEP components.

A drawback of using multichannel EEG recordings for clinical purposes may be the extra preparation time (Desmedt et al., 1987), but when electrode caps are used by skilled technicians or experimenters, our experience is that the preparation of 128-channels takes only an additional 20 minutes. If 64 electrodes are sufficient the additional preparation time can thus even be reduced to 10 minutes.
In conclusion, this study shows that the alternative coefficient of variation for amplitude is lower for 128-channel recordings compared to the conventional one-channel method, independent of reference. These results suggest that, at the cost of some additional preparation time, the 128-channel method can measure SEP amplitude more accurately and might therefore be more sensitive to pathological changes. With this study, employing a rather straightforward analysis technique, we have shown that multichannel SEP recordings show promise for clinical applications.

5

Quantifying interhemispheric symmetry of somatosensory evoked potentials with the intraclass correlation coefficient

This chapter is published as:
Quantifying interhemispheric symmetry of somatosensory evoked potentials with the intraclass correlation coefficient. W.J.G. van de Wassenberg, J.H. van der Hoeven, K.L. Leenders, N.M. Maurits. Journal of Clinical Neurophysiology. 2008; 25(3):139-146.

Abstract

Objectives. Although large intersubject variability is reported for cortical somatosensory evoked potentials (SEPs), variability between hemispheres within one subject is thought to be small. Therefore, interhemispheric comparison of SEP waveforms might be clinically useful to detect unilateral abnormalities in cortical sensory processing. We developed and evaluated a new technique to quantify interhemispheric SEP symmetry that uses a time interval including multiple SEP components, measures similarity of SEP waveforms between both hemispheres and results in high symmetry values even in the presence of small interhemispheric anatomical differences.
Methods. Median nerve SEPs were recorded in 50 healthy subjects (20-70 years) using 128-channel EEG. Symmetry was quantified by the intraclass correlation coefficient (ICC) and correlation coefficient (CC) between global field power (GFP) of left and right median nerve SEPs.
Results. In 74% of subjects left-right ICC was higher than 0.60, implying high SEP hemispheric symmetry in terms of shape and amplitude. Left-right ICCs lower than 0.60 were due to either differences in amplitude, unilateral absence of peaks or shape differences.
Conclusion. We quantified SEP waveform interhemispheric symmetry and found it to be high in most healthy subjects. This technique may therefore be useful for detection of unilateral abnormalities in cortical sensory processing.

5.1 Introduction

Somatosensory evoked potentials (SEPs) are mostly used clinically to evaluate conduction in somatosensory pathways. For this purpose, analyses of (inter)peak latencies are sufficient. Other SEP parameters, for example amplitude and shape of the SEP waveforms, have a high intersubject variability (Ferri et al., 1996; Chiappa, 1997; Gardill and Hielscher, 2001) which makes them less useful for clinical application.
However, several magnetoencephalography (MEG) studies have shown high intrasubject interhemispheric symmetry of somatosensory evoked field (SEF) wave morphology (Rossini, 1994; Tecchio et al., 2000; Theuvenet et al., 2005) when comparing left and right median nerve stimulation in healthy subjects, whereas in stroke patients interhemispheric asymmetry of SEFs was found (Tecchio et al., 2000; Rossini et al., 2001; Rossini, 2004). These results suggest that comparing SEF waveforms of left and right side stimulation might provide useful information to detect unilateral abnormalities in the sensory cortical activation patterns as a consequence of cerebral lesions (Tecchio et al., 2000) or other unilateral cortical pathology.
An advantage of MEG compared to EEG is that magnetic fields are not influenced by the presence of the skull. However, MEG is less sensitive to deep and radial sources (Huizenga et al., 2001), is expensive and is only available in a limited number of hospitals. Therefore, we here investigate the interhemispheric symmetry of SEPs, i.e. the electrical equivalent of SEFs.
So far, only a small number of studies investigated interhemispheric median and tibial nerve SEP (a)symmetry in healthy subjects. Kanovsky et al. (1997) compared peak-to-peak left and right median nerve SEP amplitude of the precentral P22/N30 complex at electrodes F3(F4) and 2 cm posterior to C3(C4) in healthy subjects. However, even healthy subjects can have small interhemispheric anatomical differences (Steinmetz et al., 1991; Penhune et al., 1996; Amunts et al., 2000). These interhemispheric variations can cause asymmetry in position and orientation of SEP sources, which will result in asymmetric SEP topography and differences in location of peak maxima, even in the absence of pathological abnormalities. Recording SEP amplitude with a standard derivation, like in the study of Kanovsky et al. (1997), may then result in large differences in SEP amplitude, whereas source strength and source activation are actually similar.
Therefore, Buchner et al. (1995) used maximum N20, P22, P25 and N30 peak amplitude instead of a standard derivation for estimating interhemispheric amplitude asymmetry in healthy subjects. According to this study, SEP amplitude differences obtained from standard derivations between left and right side stimulation are partly due to differences in SEP topography.
Elaborating on these findings, Jung et al. (2003) used dipole source analyses to investigate the P14, N20 and P22 amplitude asymmetry in sixteen healthy young

subjects. They found significantly higher source strength and deeper located N20 sources in the left hemisphere.
However, all previous studies investigating interhemispheric SEP symmetry only used maximum peak amplitudes for estimation of interhemispheric symmetry except the studies of Kresch et al. (1998) and Jung et al. (2003). The latter used the time interval from onset to peak to estimate the location of the source for each SEP component and compared source location and maximum source strength, but not source activity waveform. We hypothesize that besides peak amplitude and source location other aspects of the SEP, such as waveform and potential field, might also provide useful information for clinical purposes, similar to the SEF studies (Tecchio et al., 2000; Rossini et al., 2001). So far, only Kresch et al. (1998) investigated the symmetry of SEP waveform morphology. In that study, Pearson's correlation coefficient (CC) between left and right tibial nerve SEP measured at an electrode 2 cm posterior to Cz was used as measure for waveform symmetry. A disadvantage of the CC is that it only measures the linear relation between two variables or signals and does not further quantify their similarity. A second disadvantage of the method used by Kresch et al. is that only one electrode position was used.
In this study, we introduce a new method to estimate interhemispheric SEP symmetry. This method is designed such that it measures SEP waveform similarity between both hemispheres instead of linear correlation only, includes potentials of multiple electrode positions and is not influenced by small interhemispheric anatomical differences.
We evaluate the new symmetry estimate in a healthy population and compare it with CC. Furthermore, Strenge (1986) suggested that a reorganization of primary cortical areas may occur with age, which may influence the interhemispheric SEP waveform symmetry. Therefore, we also investigated the effect of age on our symmetry estimate.

5.2 Materials and methods

5.2.1 Subjects

Median nerve SEPs were recorded from 50 right-handed healthy volunteers. For each decade between 20 and 70 years, five males and five females were included, except for the highest decade, where four males and six females were included. None of the subjects had a history of head injury or other neurological conditions. All subjects gave their informed consent. The protocol was approved by the medical-ethical board of the University Medical Center Groningen.

5.2.2 SEP recording

The subjects were sitting in a chair in a warm and quiet room and were instructed to relax and keep their eyes open. During the recording we continuously monitored the ongoing EEG for signs of drowsiness (increased alpha activity) and gave subjects verbal feedback whenever we noticed that they were closing their eyes. In this manner we ensured that subjects kept their eyes open during the entire recording period and thereby, that their level of consciousness did not change over recordings. We stimulated the median nerve at the wrist 500 times, one side at a time, and repeated each recording once. The stimuli were square wave impulses of 0.2 ms, which were delivered at a frequency of 2.1 Hz. The stimulus intensity was slightly above motor threshold, producing a small thumb switch. We placed Ag/AgCl-disk electrodes over Erb's point with the reference electrode at the sternum and recorded EEG from the scalp using a 128-electrode cap, which was connected to a 128-channel headbox (Twente Medical Systems BV, Enschede, The Netherlands). To place the cap we measured the distance between nasion and inion, positioned Fpz at 10% of the nasion-inion distance above the nasion and checked if electrode Cz was positioned at the centre of the nasion-inion distance and between both pre-auricular points. Impedance values were kept below 10 kΩ. We used Onyx software (Silicon Biomedical Instruments BV, Arnhem, The Netherlands) to record the EEG data at a sampling frequency of 1000 Hz.
Data at Erb's point were recorded, segmented, amplified and averaged with the Medelec Synergy N-EP system (Oxford Instruments Medical, Concord, USA) to verify peripheral conductivity data against normal data from our laboratory. If the data at Erb's point were not reproducible, we checked the N20 latency. If both the N10 at Erb's point and the N20 were absent, the subject was excluded in further analyses.
The raw EEG data was processed off-line using Brain Vision Analyzer 1.05 (Brain Products GmbH, München, Germany). We filtered the data with a high pass filter of 3 Hz and segmented it into epochs of 100 ms including a 10 ms pre-stimulus interval. Artifact rejection was set at $\pm$ 100 μV and a baseline correction procedure was performed using the pre-stimulus interval.
We repeated the complete protocol in 5 subjects, one from each decade, within 6 months to assess long-term intrasubject variability.

5.2.3 SEP interhemispheric symmetry measure

We developed a new method to estimate interhemispheric SEP symmetry. This method compares left and right median nerve SEP by using the global field power (GFP) instead of one standard deviation or a derivation with maximum amplitude as used in previous SEP studies (Kresch et al., 1998; Tecchio et al., 2000). GFP is a quantity for the total amount of activity over all electrodes at each timepoint

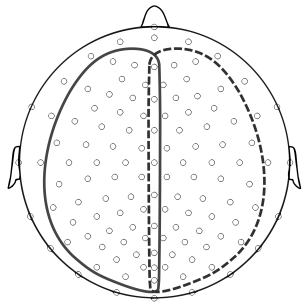

Figure 5.1: Electrodes used for GFP calculation. Solid lin: encloses all electrodes for GFP calculation of right side stimulation. Dashed line: encloses all electrodes for GFP calculation of left side stimulation.

(Lehmann and Skrandies, 1984). By using the GFP, brain potentials over a large area of the head are included in the symmetry estimate. In this way, small interhemispheric differences in position and orientation of SEP sources due to underlying anatomical differences will not decrease the symmetry estimate (Steinmetz et al., 1991; Penhune et al., 1996; Amunts et al., 2000). In addition, by using the GFP, we include more SEP components as well as more information on each component. The GFP was calculated in Brain Vision Analyzer 1.05 using all contralateral electrodes and the electrodes at the midline excluding the electrodes at the outer layer of the cap (Fig. 5.1). We only included the contralateral electrodes, because cortical SEP components are generated by sources in the contralateral hemisphere and contribute mostly to the potential field at the contralateral side. Furthermore, we excluded the outer layer, because these electrodes are prone to containing muscle artifact. The GFP is defined as the root mean square of the individual channels at every timepoint;

$$GFP(t) = \sqrt{\frac{1}{N}\sum_{n=1}^{N}[V_n(t)]^2} \tag{5.1}$$

In this equation N is the number of electrodes and $V_n(t)$ is the potential recorded at electrode n and timepoint t.

To calculate the similarity of the GFP waveforms of left and right median nerve SEPs, we calculated both the CC and ICC. The distinction between ICC and CC is that CC is a linearity index; it measures the degree to which one variable y can be equated to another variable x by a linear transformation ($y = ax + b$). ICC on the other hand is an additivity index; it measures the degree to which one variable y can be equated to another variable x ($y = x$ or $y = x + b$, depending on the ICC form) (Mcgraw and Wong, 1996). This means that in the context of SEP waveform comparisons the CC is a measure for shape similarity, while the ICC is a measure

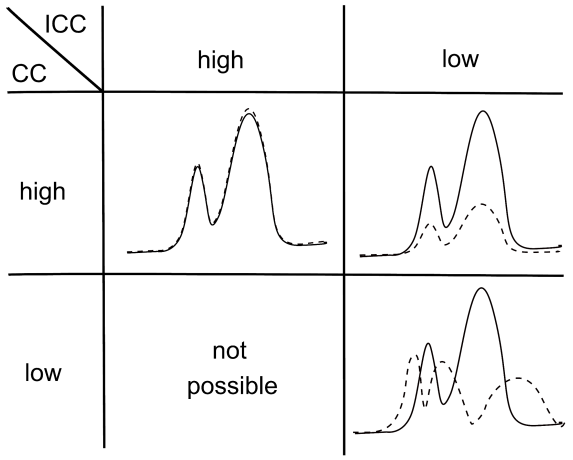

Figure 5.2: Examples of curves with high and low ICC and CC.

for shape and amplitude similarity (Fig. 5.2).
There are several forms of the ICC. In this study we used ICC(A,1) as defined in McGraw and Wong (1996), where A stands for absolute agreement. ICC(A,1) is a measure of the variance due to - in this case - time, divided by the total variance (see appendix for the exact estimation of ICC(A,1)). The ICC ranges from 0 to 1. An ICC of 1 means that the GFPs are equal; the lower the ICC the less similar i.e., symmetric the GFPs are (Fig. 5.2 and 5.3).
The ICC and CC were calculated in SPSS 14.0 (SPSS Inc., Chicago, USA) using the GFP between 16 and 35 ms. In this interval SEP components are likely not dependent on subjective attention, which may otherwise influence symmetry measures (Mauguière et al., 1997). Before we calculated left-right ICC and CC from the GFPs of left and right SEPs, we used the same ICC and CC calculation to determine the within-session repeatability of left side stimulation (left-left) and right side stimulation (right-right) respectively. In addition, we determined Pearson's correlation coefficient between age and ICC and Spearman's correlation coefficient between signal-to-noise ratio (SNR) and ICC. The latter correlation was considered, because two recordings with a SNR below a certain threshold are expected to always have a low ICC. The SNR was calculated by taking the mean GFP of the interval from 16 to 35 ms divided by the mean GFP of the interval from -10 to 0 ms.
Two SEP recordings were performed for each side, which means that in total 4 left-right ICCs could be calculated. The maximum left-right ICC and CC were used for further analyses. To estimate the intersession repeatability, five subjects came back within 6 months for a second session. We compared the maximum left-right ICCs and CCs of both sessions.

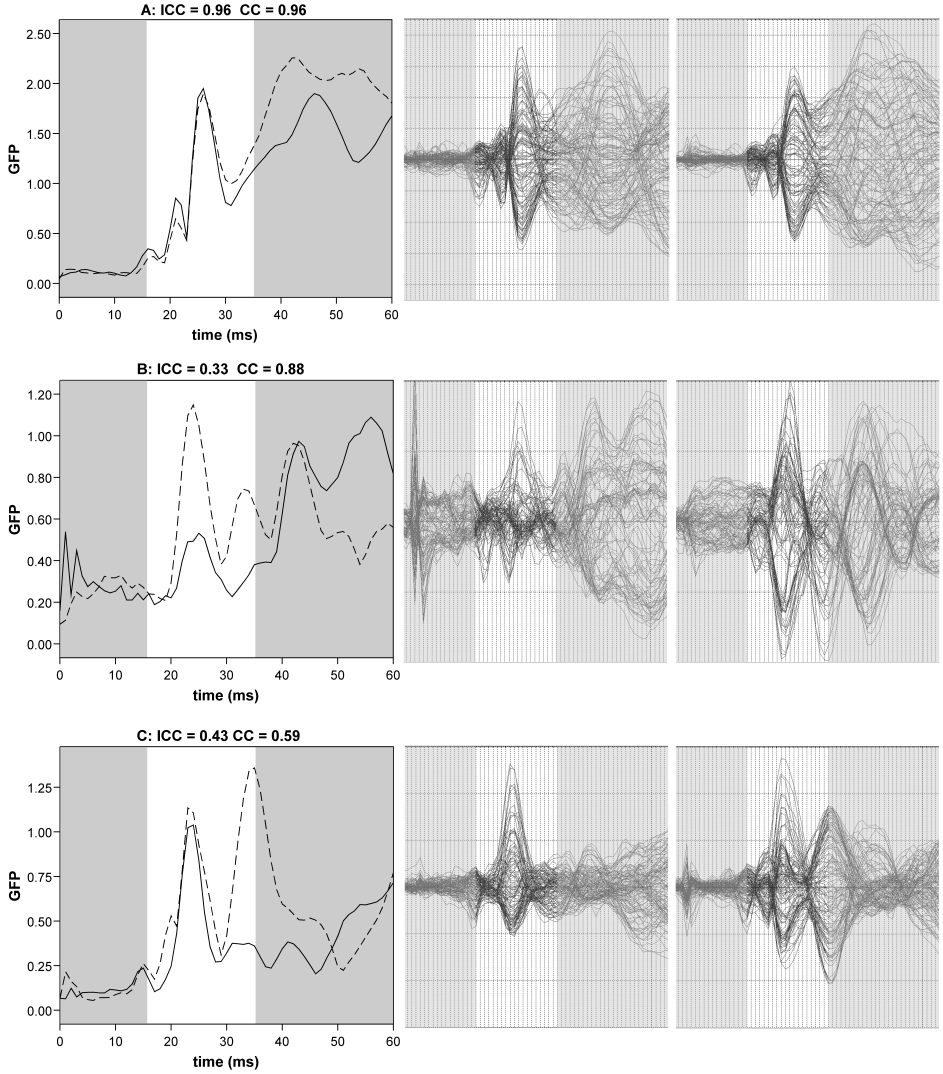

Figure 5.3: GFPs and butterfly plots of left and right median nerve SEP of subjects with; A) high ICC (> 0.6), B) low ICC (< 0.6) and high CC (> 0.6) and C) low ICC and CC (< 0.6). Left plots show GFPs of left side stimulation (solid line) and right side stimulation (dashed line). The letters A, B and C correspond to the areas A, B and C in figure 5.5. Middle and right plots show the butterflyplots of left and right median nerve SEP, respectively. Analysis interval (16-35 ms) is indicated in all figures.

5.3 Results

We excluded five of the 50 subjects (males; 36, 50, 56, 63 and 64 years old). Two of these subjects experienced the stimuli as too painful. One subject had no reproducible Erb response in combination with an absent N20 potential at CP3-Fz after right side stimulation. Two other subjects were excluded, because in each subject one of the right cortical median nerve SEPs contained too many artifacts to give reproducible peaks. In four subjects no reproducible Erb response was found at one stimulation side. However, the N20 potentials of these subjects were normal and for that reason these subjects were included in the analysis.
Subject characteristics are given in table 5.1.

Table 5.1: Subject characteristics

Age group	Number	Age
20-30	10	26.4 ± 2.8
30-40	9	33.7 ± 3.1
40-50	10	44.9 ± 2.6
50-60	8	54.3 ± 2.8
60-70	8	62.5 ± 2.9

Age is given in years as mean ± sd.

5.3.1 Within session reproducibility

We estimated the within-session reproducibility of left and right SEPs by calculating the left-left and right-right ICC and CC of the GFPs. The averages of the left-left and right-right ICC and CCs are given in table 5.2. In this table the SEPs are classified in four different groups based on their ICC and CC value. The different groups correspond to the different areas in the right graph of figure 5.4.
SEPs with an ICC value higher than 0.60 are considered to have a similar shape and amplitude. This threshold and following thresholds are chosen by visual judgement of GFP overlay plots and based on the distribution shown in figures 5.4 and 5.6, in which the majority of the subjects should have an ICC and CC above the threshold. Six subjects had a left-left ICC lower than 0.60, whereas eleven subjects had a right-right ICC lower than 0.60.
In this study, we used the CC as a measure of shape similarity. SEPs with a CC higher than 0.60 and an ICC lower than 0.60 are considered to have only a shape similarity. In seven subjects either left-left and/or right-right ICC was lower than 0.60 with a concurrent CC higher than 0.60.
The SEPs with a left-left or right-right CC ranging between 0.40 and 0.60 had an amplitude difference during one peak or an amplitude difference that was not consistent during the entire interval.
Three subjects with a left-left and/or right-right CC lower than 0.4 were excluded

for further analysis, since peaks were not consistent between GFPs partly due to a low SNR (<3.2).
Additionally, we investigated the relation between SNR and left-left ICC/CC and right-right ICC/CC (Fig. 5.5) and found significant correlations between SNR and both ICCs (left: r = 0.518, p<0.001, right: r = 0.504, p<0.001 (two-tailed)) and between SNR and both CCs (left: r = 0.483, p=0.003, right: r=0.435, p = 0.003(two-tailed)). In the present study, recordings with low SNR (<0.10) had high ICCs/CCs (>0.60) as well as low ICCs/CCs (<0.60), while recordings with high SNR (>0.10) had only high ICCS/CCs (>0.60).
We also tested the relation between age and left-left ICC/CC and right-right ICC/CC (Fig. 5.4). There was neither a significant correlation between age and ICC (left r = 0.009, p = 0.956, right: r = -0.213, p = 0.159) nor between age and CC (left r = -0.029, p = 0.848, right: r = -0.206, p = 0.174).

Table 5.2: Group values of left-left and right-right ICC and CC

				Left-left			Right-right	
Area	ICC	CC	N	ICC	CC	N	ICC	CC
A	> 0.60	> 0.60	39	0.83 ± 0.12	0.89 ± 0.11	34	0.84 ± 0.11	0.91 ± 0.09
B	< 0.60	> 0.60	4	0.26-0.54	0.74-0.95	4	0.31-0.55	0.75-0.99
C	< 0.60	> 0.40 < 0.60	1	0.48	0.55	4	0.32-0.53	0.47-0.57
D	< 0.40	< 0.40	1	0	-0.39	3	0.00-0.19	-0.24-0.29

N: number of subjects in each group.
The letters of the areas correspond with the areas in figure 5.4
For the group with ICC > 0.6 mean ± sd is given.
For the other two groups the range of ICC and CC is given.

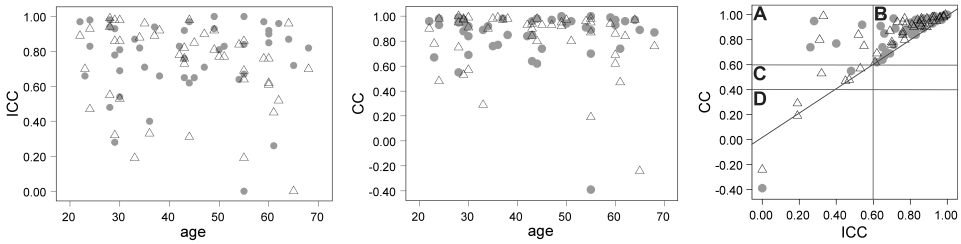

Figure 5.4: Scatterplot of left-left and right-right ICC (left) and CC (middle) versus age and scatterplot of CC versus ICC (right). Closed circles: left-left ICC/CC. Open triangles: right-right ICC/CC.

5.3.2 Interhemispheric symmetry

The interhemispheric symmetry of SEP waveforms was calculated using the ICC and CC of the GFPs of SEPs resulting from left and right median nerve stimulation. The averages of the left-right ICC and CCs are given in table 5.3. Similar to

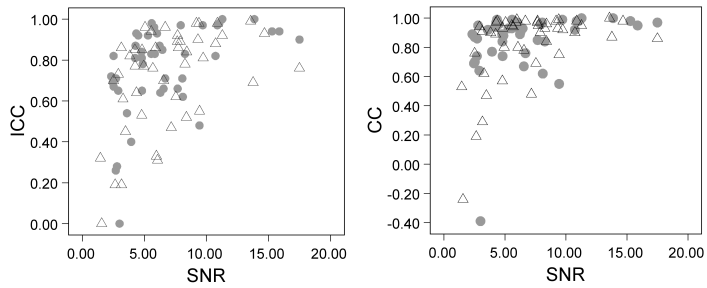

Figure 5.5: Left-left ICC (closed circles) and right-right ICC (open triangles) versus minimum SNR of both GFPs (left). Left-left CC (closed circles) and right-right CC (open triangles) versus minimum SNR of both GFPs (right).

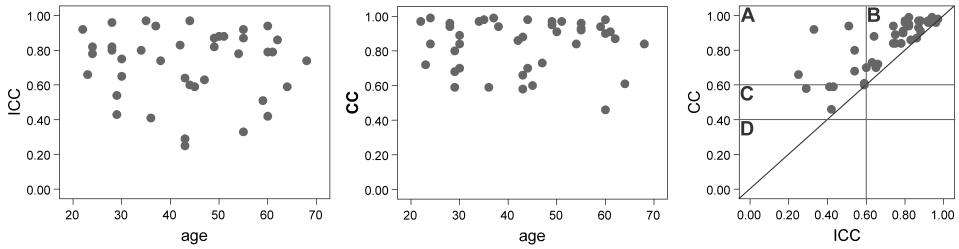

Figure 5.6: Scatterplots of left-right ICC (left) and CC (middle) versus age and scatterplot of CC versus ICC (right).

table 5.2 the SEPs are classified in four different groups based on their ICC and CC value. The different groups correspond to the different areas in the right plot of figure 5.6.

SEP recordings with a left-right ICC higher than 0.60 had similar shape and amplitude and were thus highly symmetric. Eleven out of 42 subjects had a left-right ICC lower than 0.60, from which seven had a left-right CC higher than 0.60. These recordings concern SEPs that were only shape symmetric.

The subjects with both ICC and CC lower than 0.60 had shape differences (3 subjects) or a peak was missing (1 subject). Figure 5.6 shows the individual left-right ICC and CC values as a function of age. No significant correlation was found, neither between age and left-right ICC ($r = -0.033$, $p = 0.837$) nor between age and left-right CC ($r = -0.021$, $p = 0.893$).

In five subjects we performed a second recording session within six months. The maximum left-right ICCs and CCs of both sessions are given in table 5.4. One subject shows a remarkable difference in ICC between session 1 and 2. This difference is due to an amplitude shift that starts after 15 ms and continuous at least till 90 ms after stimulation.

Table 5.3: Group values of left-right ICC and CC

				Left-Right	
Area	ICC	CC	N	ICC	CC
A	> 0.60	> 0.60	31	0.81 ± 0.10	0.90 ± 0.09
B	< 0.60,	> 0.60	7	0.33-0.59	0.60-0.94
C	< 0.60	> 0.40 ,< 0.60	4	0.29-0.43	0.46-0.59
D	< 0.40	< 0.40	0	-	-

N: number of subjects in each group
The letters of the areas correspond with the areas in figure 5.6.
For the group with ICC > 0.6 mean $\pm$ sd is given.
For the other two groups the range of ICC and CC is given.

Table 5.4: Left-right ICC and CC at first and second session.

	Left-Right ICC		Left-Right CC	
Subject	Session 1	Session 2	Session 1	Session 2
1	0.74	0.97	0.94	0.98
2	0.82	0.76	0.99	0.98
3	0.82	0.85	0.95	0.91
4	0.94	0.96	0.98	0.98
5	0.39	0.87	0.92	0.95

5.4 Discussion

We introduced a new method to quantify interhemispheric median nerve SEP symmetry, which takes both shape and amplitude into account. This method compares GFP waveforms from left and right side stimulation by using the ICC, such that 1) the similarity of median nerve SEP activity patterns instead of only the linear correlation is quantified, 2) small interhemispheric differences in position and orientation of SEP sources have no consequences for the symmetry measure and 3) multiple successive SEP components are included. We showed that the ICC can be an appropriate measure for quantifying interhemispheric symmetry. We found high symmetry between GFP waveforms of left and right side median nerve stimulation in healthy subjects, which is in agreement with MEG studies investigating interhemispheric symmetry of SEF waveforms (Tecchio et al., 2000; Theuvenet et al., 2005).

The low left-right ICCs of eleven subjects were to a large extent caused by differences in amplitude (7 subjects), unilateral absence of peaks (1 subject) or shape differences (3 subjects). The left and right SEP recordings with low ICC due to amplitude differences, had a high left-right CC (>0.60), indicating that the SEP waveforms were only symmetric regarding to shape. The differences in amplitude might be related to the handedness of the subject. Several previous studies report higher amplitudes after stimulation of the dominant side (Buchner et al., 1995; Soros et al., 1999; Jung et al., 2003; Theuvenet et al., 2005), while other studies

report no difference (Kakigi and Shibasaki, 1991; Kanovsky et al., 1997). However, in our study only three out of seven subjects with a low left-right ICC due to amplitude differences had higher peak amplitudes for stimulation of the dominant hand.

Another cause for amplitude differences between GFPs of left and right stimulation as well as between GFPs of repeated measures might be stimulus-locked alpha activity. Previous studies showed that alpha activity is sometimes time-locked to a stimulus and can alter potential amplitudes up to 30% (Başar et al., 1997; Palva et al., 2005).

Three subjects were excluded for symmetry analysis, because their SEPs were less reproducible partly caused by a low SNR. Additionally, we investigated the influence of SNR on the ICC. We found a significant correlation between SNR and left-left and right-right ICC. In this study, high ICCs/CCs (>0.60) were found for recordings with low as well as high SNR, while low ICCs/CCs (<0.60) were only found in recordings with a SNR lower than 10. According to these findings, we could not assign a minimum required SNR for estimation of the ICC. However, SEP recordings of patients often contain more noise than healthy subjects. Therefore, it is important to check the SNR of recordings that have low ICCs/CCs.

In our study, eleven subjects out of 43 had a left-right ICC lower than 0.60. However, considering the findings of Rossini et al. (2004) and Tecchio (2000), who investigated the SEF waveform in patients with a history of stroke, we expect even lower left-right ICC values in these patients, since the butterflyplots of stroke patients in the studies by Rossini and Tecchio and coworkers show larger interhemispheric asymmetry than the butterflyplots (Fig. 5.3) of our healthy subjects even if they have a relatively low ICC. Future studies including patients with unilateral cortical pathology, will demonstrate if the left-right ICC of these patients is indeed lower than the left-right ICC in our healthy subject group.

Strenge (1986) suggested that a reorganization of primary cortical areas may occur with age, which may decrease the interhemispheric SEP waveform symmetry. In our study, no correlation was found between age and left-right ICC in our group of healthy subjects between 20 and 70 years. Possibly, this reorganization causes only small differences in position or orientation of the SEP sources which will not lead to differences in source activity pattern and GFP and therefore not to differences in our symmetry measure.

Furthermore, we found no significant correlation between age and ICC or CC. Thus the reproducibility of SEPs does not decrease with age.

As expected the ICC is lower compared to CC when left and right GFP differ in amplitude. Accordingly, ICC is a better method to estimate SEP symmetry when amplitude needs to be taken into account. However, if one is only interested in shape similarity, CC might be appropriate.

In this study, we recorded two left and two right median nerve SEPs. Therefore, a total of 4 left-right ICCs could be determined, of which the maximum left-right

ICC was used for further comparison in this study. An alternative would be to use the average left-right ICC. However, if one of the 4 recordings has for example a low SNR, this could have a large effect on the average left-right ICC, while this would not influence the maximum left-right ICC.
In conclusion, we introduced a new method to quantify interhemispheric SEP symmetry that compares SEP waveforms. This method calculates the ICC between the GFPs of left and right median nerve SEPs and results in high symmetry in a group of healthy subjects. From our analyses we advise to verify the SNR for recordings with low ICC, before ascribing the low value to interhemispheric asymmetry of the SEP waveform.
Future studies with patients, will demonstrate how interhemispheric comparison of SEP waveforms can be used in clinical applications.

5.5 Appendix: ICC estimation

The variance model used for ICC(A,1) is (Mcgraw and Wong, 1996):

$$GFP_{ts} = \mu + r_t + c_s + e_{ts} \tag{5.2}$$

According to this equation, each GFP at time point t and stimulation side s (GFP_{ts}) can be modelled by the mean GFP over both stimulation sides (μ) plus r_t, which depends on the timepoint, plus c_s, which depends on the stimulation side, plus a residue, e_{ts}. With this model ICC is defined as the ratio of the variance due to time effect and the total variance:

$$\rho = \frac{\sigma_r^2}{\sigma_r^2 + \sigma_c^2 + \sigma_e^2} \tag{5.3}$$

In this equation σ_r^2, σ_c^2 and σ_e^2 are the variances corresponding to r_t, c_s and e_{ts}. According to this equation ICC becomes smaller, when the variance between both recordings, σ_c^2, and the residual variance, σ_e^2, increase. The variances in equation 5.3 can be estimated by using the mean squares of analysis of variance for repeated measures;

$$\begin{aligned} \hat{\sigma}_r^2 &= \tfrac{MS_r - MS_e}{2} \\ \hat{\sigma}_c^2 &= \tfrac{MS_c - MS_e}{k} \\ \hat{\sigma}_e^2 &= MS_e \end{aligned} \tag{5.4}$$

where k is the number of points in time, MS_r the mean variation between timepoints, MS_c the mean variation between the stimulation sides and MS_e is the mean variation that cannot be explained by the effect of time or stimulation side. If $\hat{\sigma}_r^2$, $\hat{\sigma}_c^2$ or $\hat{\sigma}_e^2$ was negative, it was set to zero in further calculations. The

mean squares are defined by:

$$\begin{aligned} MS_r &= \tfrac{2}{(k-1)} \textstyle\sum_{t=1}^{k} (\overline{GFP}_{t.} - \overline{GFP}_{..})^2 \\ MS_c &= k \textstyle\sum_{s=1}^{2} (\overline{GFP}_{.s} - \overline{GFP}_{..})^2 \\ MS_e &= \tfrac{1}{(k-1)} \textstyle\sum_{t=1}^{k} \sum_{s=1}^{2} (GFP_{ts} - \overline{GFP}_{t.} - \overline{GFP}_{.s} + \overline{GFP}_{..})^2 \end{aligned} \tag{5.5}$$

where

$$\begin{aligned} \overline{GFP}_{t.} &= \textstyle\sum_{s=1}^{2} GFP_{ts}/2 \\ \overline{GFP}_{.s} &= \textstyle\sum_{t=1}^{k} GFP_{ts}/k \\ \overline{GFP}_{..} &= \textstyle\sum_{t=1}^{k} \sum_{s=1}^{2} GFP_{ts}/(2k) \end{aligned} \tag{5.6}$$

Combining equation 5.2 with equation 5.3 gives:

$$ICC(A,I) = \frac{MS_r - MS_e}{MS_r + MS_e + \frac{2}{k}(MS_c - MS_e)} \tag{5.7}$$

6

128-channel median nerve somatosensory evoked potentials in the differential diagnosis of parkinsonian disorders

This chapter is submitted for publication as:
128-channel median nerve somatosensory evoked potentials in the differential diagnosis of parkinsonian disorders. W.J.G. van de Wassenberg, J.H. van der Hoeven, K.L. Leenders, N.M. Maurits.

Abstract

Objectives. Clinical practice shows that the differential diagnosis of parkinsonian disorders can be very difficult, especially in an early stage. In this study, we investigated whether SEP amplitude can be used as diagnostic tool for parkinsonian disorders by using 128-channel recordings, and in particular whether SEP symmetry can differentiate corticobasal ganglionic degeneration (CBGD) from other parkinsonian disorders.
Methods. We recorded SEPs in 47 patients with parkinsonism who were suspected to have CBGD or progressive supranuclear palsy (PSP) or who had a definite diagnosis of Parkinson's disease (PD). We compared SEP symmetry and parietal peak amplitudes of the patients by grouping them based on the clinical diagnosis after 1-5 years of follow-up. In nine subjects the diagnosis remained unclear.
Results. Three out of 13 patients with CBGD had an abnormal SEP asymmetry. However, similar abnormalities were also found in patients with possible PSP, Parkinson's disease and multiple system atrophy (MSA). Furthermore, we found extremely high N20 amplitudes in three other patients with CBGD.
Conclusion. Cortical median nerve SEP symmetry and parietal amplitude have a low sensitivity and specificity for differentiating CBGD from other parkinsonian disorders in an early stage of the disease. A possible reason for this may be that the hand area of the primary somatosensory cortex is not affected in most patients with CBGD in an early stage of their disease.

6.1 Introduction

Parkinsonism is a clinical syndrome characterized by resting tremor, bradykinesia, rigidity and postural instability. These clinical features not only occur in patients with Parkinson's disease (PD), but also in patients with progressive supranuclear palsy (PSP), corticobasal ganglionic degeneration (CBGD) and multiple system atrophy (MSA). The differential diagnosis of parkinsonian disorders based on clinical criteria can therefore be very difficult, especially in an early stage of the disease (Litvan et al., 1998, 1999; Hughes et al., 2002). A definite diagnosis can only be made in combination with post-mortem neuropathological examination (Cornford et al., 1995; Mitra et al., 2003; Mahapatra et al., 2004). In the past, different methods have been assessed to improve the accuracy of the differential diagnosis in patients with parkinsonism in an early stage of the disease. An imaging technique that can improve differential diagnosis of parkinsonian disorders is [18F]-fluorodeoxyglucose (FDG) PET (Eckert et al., 2005). However, also this technique cannot always help in an early stage. Therefore, there is an ongoing search for alternative methods that may contribute to the differential diagnosis of parkinsonian disorders. A number of studies report somatosensory evoked potential (SEP) abnormalities in parkinsonian disorders.
In patients with CBGD a reduced N20, N20-P27 and N30 amplitude after stimulation of the most affected as well as the less affected side, increased N20 latency and absence of the N30 after stimulation of the most affected side have been found unilaterally (Brunt, 1995; Carella et al., 1997; Okuda et al., 1998; Monza, 2003; Klodowska-Duda et al., 2006). Bilaterally, an increased N13-N20 latency, abnormally increased N30 latency and enlarged N20 and N20-P27 amplitude have been reported (Thompson et al., 1994; Takeda et al., 1998; Monza, 2003). Besides differences between studies, differences in abnormalities within studies have been reported as well. Based on what is known about the pathology of CBGD, asymmetric abnormalities in N20 and P27 may be expected, since CBGD is characterized by asymmetric frontoparietal cortical atrophy, particularly in the pre- and post-central regions where the primary somatosensory cortex is positioned and the N20 and P27 are thought to be generated (Dickson et al., 2002; van de Berg et al., 2007).
Other studies have investigated SEPs in patients with PSP and PD and found abnormal as well as normal results. In patients with PSP increased frontal and parietal SEP amplitudes and reduced frontal SEP amplitudes were found compared to healthy controls and patients with PD (Abbruzzese et al., 1991; Kofler, 2000; Miwa and Mizuno, 2002), whereas decreased as well as normal frontal SEP amplitudes were reported in patients with PD compared to healthy controls (Mauguière et al., 1993; Rossini et al., 1995; Garcia et al., 1995; Bostantjopoulou et al., 2000). The reduced frontal N30 SEP amplitude in patients with PD might be due to basal ganglia dysfunction, since the N30 is assumed to be generated in the supplementary motor cortex (SMA) (Rossini et al., 1989, 1996) that receives major input from

the basal ganglia. In patients with PSP the abnormal N30 amplitude might be related to frontal lobe atrophy (Dickson, 1999; van de Berg et al., 2007) or to basal ganglia dysfunction as well.
According to these findings, SEP might contribute to the differential diagnosis of parkinsonian disorders, since for each parkinsonian disorder different abnormalities were found. On the other hand, results so far are diverse and none of these studies included more than two parkinsonian disorders or investigated the diagnostic value of SEPs by including patients in an early stage when the diagnosis is still unclear. In this study, we included patients who are suspected to have CBGD or PSP, patients with PD and age-matched healthy controls and recorded 128-channel median nerve SEPs. We investigated whether CBGD could be differentiated from the other parkinsonian disorders at an early stage of the disease. First we compared SEP symmetry, calculated with a technique introduced in our previous paper (van de Wassenberg et al., 2008c), between the parkinsonian disorders. We hypothesized that SEPs are most asymmetric in patients with CBGD.
In addition, we investigated SEP amplitudes, since previous studies also reported bilateral amplitude abnormalities in CBGD as well as in other parkinsonian disorders. SEP amplitudes were estimated with a conventional derivation used in previous studies, as well as with a 128-channel method as described in our earlier paper (van de Wassenberg et al., 2008b). The 128-channel method was proven to be more accurate for amplitude estimation than the conventional method that uses a limited number of electrodes. We hypothesize that amplitude differences are estimated more accurately with the 128-channel method. Therefore, we expect to find more homogeneous results within patient groups, which were not found in previous studies, and clearer differences between the various parkinsonian disorders.

6.2 Materials and methods

6.2.1 Patients

Patients were recruited from the Movement Disorders Clinic of the University Medical Center Groningen. From 2005 till 2007 we included prospectively all patients with parkinsonism who were suspected to have CBGD or PSP or with definite PD (Hughes et al., 1992) and who wanted to take part in the study according to a preset protocol. Patients who additionally suffered from other neurological disorders were excluded. In addition, we studied 15 patients retrospectively who were referred for a 128-channel SEP recording for clinical work-up between 2001 and 2005 and were suspected to have CBGD. In total we included 47 patients.
For all patients except the patients diagnosed with PD, an FDG PET scan was performed. Diagnoses of the parkinsonian disorders were made based on clinical criteria and on the FDG PET scan for PSP and CBGD. PD diagnoses were based on the United Kingdom Parkinson's Disease Society Brain Bank (UK-PDSBB) cri-

Table 6.1: Characteristics of the patients with PD

Pt	Sex	Age[1]	Duration[2]	Hoehn and[3] Yahr stage	L-dopa[4]	Stim[5] freq
1	m	70	2	2	-	2.1
2	m	63	2	2	+	2.1
3	m	77	2	2	+	2.1
4	m	62	1	1	-	2.1
5	m	78	8	3	+	2.1
6	m	66	8	2	+	2.1
7	f	68	4	1	+	2.1
8	f	70	3	3	+	2.1
9	m	62	3	2	-	2.1
10	m	52	3	1	-	2.1
11	m	67	6	3	+	2.1
12	f	57	10	3	+	2.1
13	f	53	5	2	+	2.1
14	m	64	4	2	+	2.1
15	f	62	2	3	+	2.1
Mean		64.7	4.2	2.1		
SD		7.5	2.7	0.8		

Pt = patient number; f = female; m = male.
[1] Age at the time of SEP recording in years.
[2] Disease duration at the time of SEP recording in years.
[3] Hoehn and Yahr stage (Hoehn and Yahr, 1967) at the time of SEP recording.
[4] Use of L-dopa medication at the time of SEP recording.
[5] Stimulus frequency used for SEP recording in Hz.

teria (Hughes et al., 1992). Clinical diagnosis of PSP was made according to the NINDS-SPSP inclusion criteria (Litvan et al., 1996) with the addition that patients with probable PSP also had to have an FDG PET scan with hypometabolism of the medial frontal cortex or brainstem and no features of MSA or CBGD (Eckert et al., 2005). The diagnosis of possible CBGD was based on the criteria proposed by Mahapatra et al. (2004), while the diagnosis of probable CBGD had the addition that the FDG PET scan had to show cortical hypometabolism or basal ganglia hypometabolism both contralateral to the most affected side (Eckert et al., 2005). All patients were followed for 1-5 years. In January 2008 we checked all patient files to obtain the latest diagnosis. This diagnosis was used for the analyses performed in this study. Patient characteristics are given in tables 6.1-6.4.
Ten, elderly subjects (5 male: age 62.7 $\pm$ 2.6 years) without a history of head injury or other neurological conditions who participated in an earlier study were used as healthy controls (van de Wassenberg et al., 2008b).
The protocol was approved by the medical-ethical board of the University Medical Center Groningen. All subjects gave their informed consent, when the SEP was not made to assist in the clinical diagnosis.

Table 6.2: Characteristics of the patients with CBGD

Pt	Sex	Probable/possible[1]	Age[2]	Duration[3]	Side[4]	FDG PET[5]	L-dopa[6]	Stim. freq.[7]
1	f	possible	75	3	L	R: co + th + st	-	2.9
2	f	probable	71	3	L	R: put + th	-	2.9
3	f	probable	74	3	R	L: co + st + put	-	2.9
4	m	probable	64	6	R	L: co + th +st R: cb	-	2.9
5	m	probable	70	1	R	L: co + th R: cb	-	2.9
6	m	probable	69	2	L	R: co + st+ th L: cb	-	2.9
7	m	probable	63	2	R	L: co+st + th R: cb	-	2.1
8	f	probable	73	1	R	L: co + th + st R: cb	+	2.1
9	m	probable	72	3	R	L: co + st + th R: cb	+	2.1
10	f	probable	73	2	L	R: co	-	2.1
11	f	probable	57	1	L	R: co +th + st	+	2.1
12	f	possible	80	2	R	co + th + st	+	2.1
13	f	probable	64	2	L	R: co + th + st + nc	-	2.9
Mean			69.6	2.4				
SD			6.1	1.4				

Pt = patient number; f = female; m = male.
[1] Most recent diagnosis.
[2] Age at the time of SEP recording in years.
[3] Disease duration at the time of SEP recording in years.
[4] Most affected side based on neurological examination. L = left; R = right.
[5] Structures with glucose hypometabolism according to the FDG PET scan: R = right hemisphere; L = left hemisphere; cb = cerebellum; co = cortex; nc = nucleus caudatus; put = putamen; st = striatum; th = thalamus.
[6] Use of L-dopa medication at the time of SEP recording.
[7] Stimulus frequency used for SEP recording in Hz.

Table 6.3: Characteristics of the patients with PSP

Pt	Sex	Probable/possible[1]	Age[2]	Duration[3]	Side[4]	FDG PET[5]	L-dopa[6]	Stim. freq.[7]
1	f	possible	73	4	L=R	mf	+	2.9
2	m	probable	57	4	L=R	mf	-	2.1
3	f	possible	74	3	L<R	-	-	2.1
4	m	probable	58	1	L=R	mf	-	2.1
5	m	probable	61	1	L=R	mf	-	2.1
6	f	possible	66	1	L=R	mf	-	2.1
7	f	probable	68	1	L=R	mf +nc	+	2.1
8	f	possible	59	3	L>R	mf + cb	-	2.1
Mean			63.9	2.3				
SD			5.9	1.4				

Pt = patient number; f = female; m = male.
[1] Most recent diagnosis.
[2] Age at the time of SEP recording in years.
[3] Disease duration at the time of SEP recording in years.
[4] Affected side based on neurological examination. L=R = left and right side equally affected; L<R = left less than right side affected; L>R = left more than right side affected.
[5] Structures with glucose hypometabolism according to the FDG PET scan: cb = cerebellum; mf = mediofrontal area; nc = nucleus caudatus.
[6] Use of L-dopa medication at the time of SEP recording.
[7] Stimulus frequency in Hz used for SEP recording in Hz.

Table 6.4: Characteristics of patients with a different diagnosis or unclear diagnosis

Pt	Sex	Diagnosis[1]	Age[2]	Duration[3]	Side[4]	FDG PET[5]	L-dopa[6]	Stim. freq.[7]
1 †	f	probable MSA	64	3	L>R	cb +st	+	2.9
2	f	probable MSA	65	3	L>R	put +par	-	2.1
3	f	other	69	5	L<R	no scan	-	2.9
4	m	unclear	57	3	L>R	cb	-	2.9
5 †	f	unclear	60	1	L=R	par +f	-	2.1
6 †	f	unclear	64	2.5	L>R	R: par	+	2.1
7	f	unclear	59	2	L<R	-	-	2.9
8 †	f	unclear	73	2.5	L<R	-	-	2.9
9	f	CBGD/PSP	74	3	L<R	mf	+	2.9
10 †	m	CBGD/PSP	75	6	L=R	mf R: co	-	2.1
11	m	CBGD/PSP	66	5	L=R	mf R: temp	-	2.1

† Patient has passed away. Autopsy was not performed and thus definite diagnosis remains unclear.
Pt = patient number; f = female; m = male.
[1] Most recent diagnosis. CBGD/PSP = most likely CBGD or PSP.
[2] Age at the time of SEP recording in years.
[3] Disease duration at the time of SEP recording in years.
[4] Affected side based on neurological examination. L=R = left and right side equally affected; L<R = left less than right side affected; L>R = left more than right side affected.
[5] Structures with glucose hypometabolism according to the FDG PET scan: R = right hemisphere; L = left hemisphere; cb = cerebellum; co =cortex; f = frontal lobe; mf = mediofrontaal; par = parietal lobe; put = putamen; st = striatum; temp = temporal lobe.
[6] Use of L-dopa medication at the time of SEP recording.
[7] Stimulus frequency used for SEP recording in Hz.

6.2.2 SEP recording

The subjects were sitting in a chair in a warm and quiet room and were instructed to relax and keep their eyes open. We stimulated the median nerve at the wrist 500 times, one side at a time, and repeated each recording once. In the subjects recorded between 2001 and 2005 we used square wave impulses of 0.2 ms, which were delivered at a frequency of 2.9 Hz with the Viking IV system (Nicolet Instrument, Madison, Wisconsin, USA). In the other subjects we used the same stimuli, but at a stimulus frequency of 2.1 Hz, that were delivered with the Medelec Synergy N-EP system (Oxford Instruments Medical, Concord, USA). These systems were also used for recording of potentials at Erb's point. Since previous studies only found amplitude differences when stimulus frequencies differed more than 2.4 Hz (Delberghe et al., 1990; Fujii et al., 1994) and according to Delberghe et al. (1990) and Mauguiere et al. (1999) amplitude differences will only appear if the stimulus rate exceeds 3.1 Hz, we expect no differences in amplitude due to the stimulus rate difference.
The stimulus intensity was slightly above motor threshold, producing a small thumb switch. We placed Ag/AgCl-disk electrodes over Erb's point with the reference electrode at the sternum and recorded EEG from the scalp using a 128-electrode cap, which was connected to a 128-channel headbox (Twente Medical Systems BV, Enschede, The Netherlands). To place the cap we measured the distance between nasion and inion, positioned Fpz at 10% of the nasion-inion distance above the nasion and checked whether electrode Cz was positioned at the centre of the nasion-inion distance and between both pre-auricular points. Impedance values were kept below 10 kΩ. We used Onyx software (Silicon Biomedical Instruments BV, Arnhem, The Netherlands) to record the EEG data at a sampling frequency of 1000 Hz.
The data at Erb's point were segmented, amplified and averaged. Subsequently, amplitude and latency were determined at Erb's point to verify peripheral conductivity data against normal data from our laboratory. If the data at Erb's point was not reproducible and no reproducible cortical SEPs could be recognized either, the subject was excluded for further analysis. This was the case in one patient with CBGD, one patient with PD and three subjects with an unclear diagnosis.
The raw EEG data was processed off-line using Brain Vision Analyzer 1.05 (Brain Products GmbH, München, Germany). We filtered the data with a high pass filter of 3 Hz and segmented it into epochs of 100 ms including a 10 ms pre-stimulus interval. Artifact rejection was set at $\pm$ 100 μV and a baseline correction procedure was performed using the pre-stimulus interval.

6.2.3 SEP analysis

In this study, we used a sampling rate of 1000 Hz for SEP recording. The sampling rate recommended for SEP recordings is 20 kHz (Mauguière et al., 1999). However, simultaneous recording of 128 channels decreases the maximum possible sample

rate to 1000 Hz. Due to this low sample frequency, latency could not be compared accurately between groups.

Conventional SEP amplitude

We used CP4-A1/CP3-A2 for estimation of N20, P27 and P45 amplitude for left/right side stimulation, since this derivation allows us to compare our results with other studies (Brunt, 1995; Miwa and Mizuno, 2002). The largest negative peak around 20 ms was identified as the N20. The main prominent positive peak succeeding the N20 was recognized as the P27 and the P45 was the main prominent positive peak following the P27. All amplitudes were defined as peak-to-baseline amplitudes. Amplitudes were compared between groups and compared to upper and lower normal limits. The lower and upper normal limits are based on a previous study and are defined as 5th and 95th percentile of amplitude estimates in a group of 47 healthy subjects (van de Wassenberg et al., 2008b). The age of this group ranged from 20 to 68 years and in this group no age effect was found. The upper limits are 2.92 μV, 4.80 μV and 6.92 μV for N20, P27 and P45 amplitude respectively. The lower limits are 0.30 μV, 0.43 μV and 0.99 μV for N20, P27 and P45 amplitude respectively.

128-channel SEP amplitude

Amplitude estimation with the 128-channel method is described in detail in our earlier study (van de Wassenberg et al., 2008b) and will be briefly outlined here. For analysis, the averaged data were exported to ASA 2.21 (ANT software BV, Enschede, The Netherlands) using an average reference. Subsequently, we searched for negative (N20) and positive peaks (P27 and P45) in the butterfly plot between 15 and 65 ms and checked whether the corresponding scalp topography met the criteria we defined for N20, P27 and P45. These criteria were a frontal positive field together with a parietal negative field for the N20 topography, a parietal positive field in combination with a negative frontal field for the P27 topography and a positive parietal/central field for the P45 topography, all contralateral to the stimulation side. If the topography matched, we used the difference between maximum and minimum amplitude at the time of the peak as (total) amplitude. Again the peak amplitudes were compared between groups and compared to normal limits. The lower and upper limits were defined in the same way as the conventional amplitude limits. The upper limits are 5.21 μV, 8.50 μV and 9.49 μV for N20, P27 and P45 amplitude respectively. The lower limits are 1.31 μV, 2.23 μV and 2.27 μV for N20, P27 and P45 amplitude respectively.

SEP interhemispheric symmetry

First of all we determined the absolute laterality index (LI) of each peak (Jung et al., 2003). The LI is defined as the absolute difference between left and right amplitude divided by the sum of both amplitudes.
Furthermore we used the method that we described in more detail in Van de Wassenberg et al. (van de Wassenberg et al., 2008b) as a measure of interhemispheric symmetry. This method has the advantage that it takes both SEP shape and amplitude into account and includes multiple successive SEP components. Furthermore, small interhemispheric differences in position or orientation of the SEP source do not influence the symmetry measure. The method compares left and right median nerve SEP by using the global field power (GFP). GFP is a measure for the total amount of activity over all electrodes at each timepoint (Lehmann and Skrandies, 1984). By using the GFP, brain potentials over a large area of the head are included in the symmetry estimate. The GFP was calculated in Brain Vision Analyzer 1.05 using all contralateral electrodes and the electrodes at the midline excluding the electrodes at the outer layer of the cap.
Finally, to estimate interhemispheric symmetry, we calculated the similarity of the GFP waveforms of left and right median nerve SEPs, by means of the intraclass correlation (ICC) of both recordings. The ICC ranges from 0 to 1. An ICC of 1 means that the GFPs are equal; the lower the ICC the less similar the GFPs and thus the less symmetric the SEPs. The ICC was calculated in SPSS 14.0 (SPSS Inc., Chicago, USA) based on the GFP between 16 and 35 ms. For the subjects with low ICC we additionally calculated the signal to noise ratio (SNR) to investigate whether a low SNR could be the cause of the low ICC.

6.3 Results

6.3.1 Amplitude

The N20, P27 and P45 peaks could not be detected in all subjects. Table 6.5 shows the missing peaks for each patient group and for both the conventional and 128-channel method. No clear differences in the absence of peaks could be observed between groups.
We compared N20, P27 and P45 amplitudes between groups as determined with the 128-channel method as well as with the conventional method (Fig. 6.1). N20 amplitude was extremely high (128-channel >10 μV, conventional > 5 μV) compared to the other patients and subjects in one patient with CBGD after both left and right side stimulation and in two patients with CBGD after stimulation of the most affected side (right side) only. However, when comparing the amplitude to the upper normal limits for N20 amplitude, we see that in each patient group one

Table 6.5: Missing peaks per patient group

		128-channel			conventional		
Pt	N	N20	P27	P45	N20	P27	P45
group		left/right	left/right	left/right	left/right	left/right	left/right
PSP	8	1/1	2/4	1/1	0/0	0/0	0/1
CBGD	13	0/0	4/1	0/0	1/1	4/1	1/2
PD	15	0/0	1/2	0/0	1/0	2/2	1/1
Other	3	0/0	3/2	0/0	1/0	2/2	1/0
unclear	8	0/0	1/2	0/1	1/1	1/3	0/2
healthy	10	1/1	4/2	0/0	1/3	3/3	1/2

Pt group = patient group; N = number of subjects in group

or more patients exceeded the upper normal limit. Only 3 patients in different groups exceeded the normal lower limit when the amplitude was obtained with the 128-channel method as well as with the conventional method.
The P27 was extremely high (128-channel >12 μV, conventional >7 μV) compared to other subjects in one patient with CBGD after both left and right side stimulation. Again also other patients exceeded the upper normal limit. Only a small number of patients of different groups exceeded the lower normal limit.
The P45 estimated with the 128-channel method was extremely high (>14 μV) compared to other subjects in one patient with CBGD after stimulation of the most affected side and in one patient with PSP after right hand stimulation. Using the conventional method, P45 amplitude of one patient with PSP and one patient with PD was extremely high (>10 μV) unilaterally. In addition, in more patients P45 amplitude exceeded the upper normal limit. Only one patient with an unclear diagnosis had a P45 amplitude that exceeded the lower normal limit.
In general, SEP amplitudes of our patient groups were overlapping. Four out of 13 patients with CBGD had extremely high amplitude of one or more SEP components in the 128-channel method. When SEP amplitude was obtained with the conventional method three out of 13 subjects had an extremely high amplitude. However, with the 128-channel method also one patient with PSP had extremely high amplitude of one of the components and for the conventional method this was the case for one patient with PSP and for one patient with PD.

6.3.2 Laterality Index (LI)

Figure 6.2 shows the LIs for each peak estimated with the conventional and 128-channel method. An amplitude difference between left and right side stimulation of 50% results in a LI of 0.20 and a difference of 100% results in a LI of 0.33. According to figure 6.2 only a few subjects had an LI estimated with the 128-channel method that exceeded 0.33. One patient with CBGD, one patient with MSA and one patient with an unclear diagnosis also had an N20 LI larger than 0.33. This patient with CBGD together with another patient with CBGD had a P27 LI higher

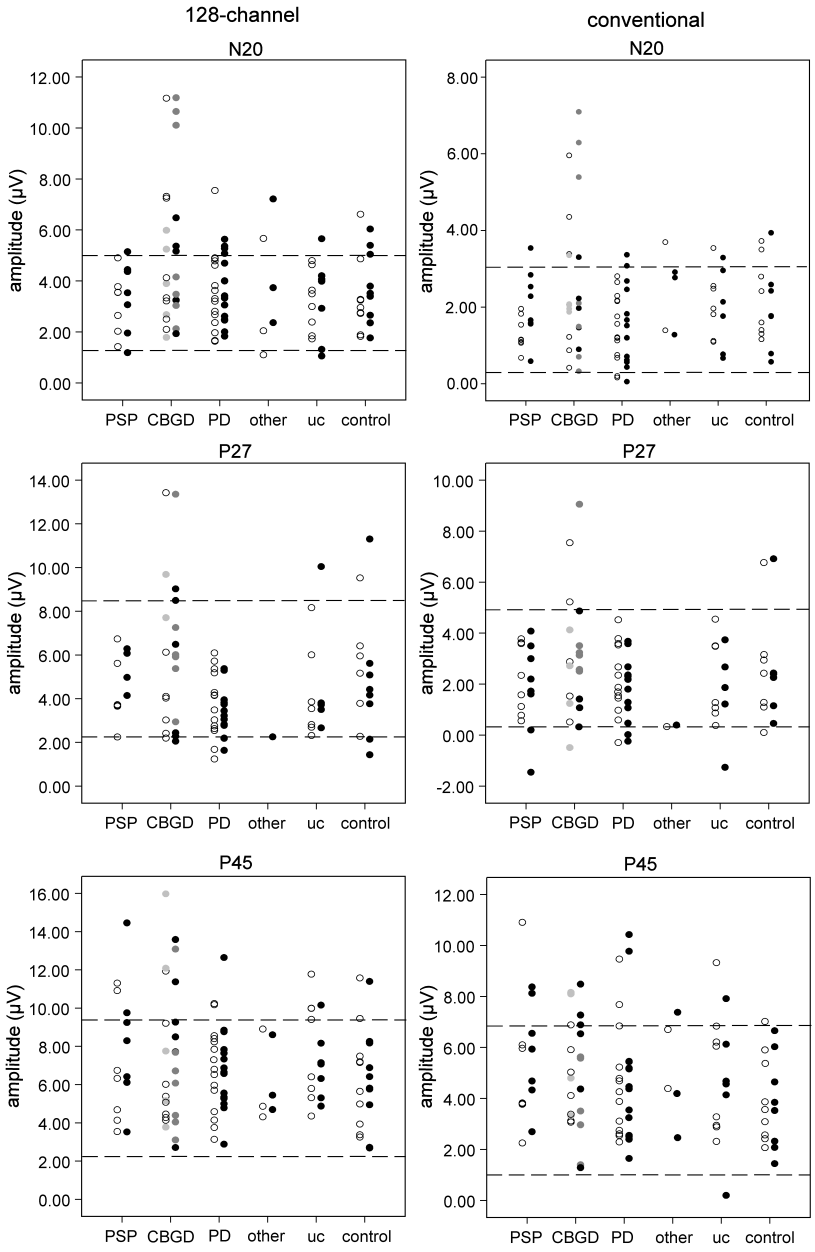

Figure 6.1: SEP peak amplitudes (N20, P27, P45) estimated with the 128-channel method (left) and the conventional method (right). Each circle represents the SEP amplitude of left or right side stimulation of one subject. Open circle: left side stimulation; black closed circles: right side stimulation; grey closed circles: affected side in patients with CBGD; uc: unclear diagnosis. The horizontal dashed lines represent the 5th and 95th percentile of amplitude estimates in a group of 47 healthy subjects (van de Wassenberg et al., 2008b).

than 0.33. The P45 LI was higher than 0.33 in one patient with an unclear diagnosis and in one healthy control.
LIs obtained with the conventional method were considerably larger compared to the 128-channel method. These results are consistent with our earlier study in which we determined LIs of tibial nerve SEP in healthy subjects (van de Wassenberg et al., 2008a). A likely reason for this is that the position of maximum amplitude differs between hemispheres due to differences in SEP source location and orientation. In general, the LI could not differentiate between parkinsonian disorders.

6.3.3 Intraclass correlation (ICC)

The ICC of the GFP of left and right side stimulation is displayed in figure 6.3 for all subjects. Three healthy subjects had no reproducible butterfly plots and GFPs on one side due to low SNR and were therefore excluded. Low ICC (<0.5) was only found in three patients with CBGD. On the other hand, one patient with PSP, one patient with PD, two patients with MSA, one patient with unclear diagnosis and one healthy subject also had a low ICC. All patients with a low ICC had a normal SNR (>4), except the patient with PD, who had a SNR in the left side SEP recording of 2.99.
Figure 6.4 shows the butterfly plots and GFPs of two patients with CBGD; one with a high ICC and one with a low ICC.

6.4 Discussion

In this study we investigated SEP symmetry and SEP amplitude in patients with parkinsonian disorders. We recorded SEPs in patients with parkinsonism who were suspected to have CBGD or PSP and in patients with PD. In total we included 47 patients. We compared SEP symmetry and parietal peak amplitudes of the patients by grouping them based on the clinical diagnosis after 1-5 years of follow-up. In nine subjects diagnosis remained unclear.
To compare SEP symmetry we used LI as well as a new method in which the ICC of the GFP of left and right median nerve SEP is calculated. A high ICC reflects a high symmetry of the SEP. Because CBGD is often associated with asymmetric atrophy of the pre- and post-central areas, we hypothesized that patients with CBGD have less symmetric median nerve SEPs compared to patients with PSP and PD and healthy subjects and thus have a lower ICC.
However, in this study only three out of 13 patient with CBGD had a small ICC, while other patients showed low ICCs as well (one patient with PSP, one patient with PD, two patients with MSA, one patient with a diagnosis that is still unclear). Only for the patient with PD the low ICC could be due to a low SNR. Furthermore, in contrast with previous studies that report unilaterally increased and decreased

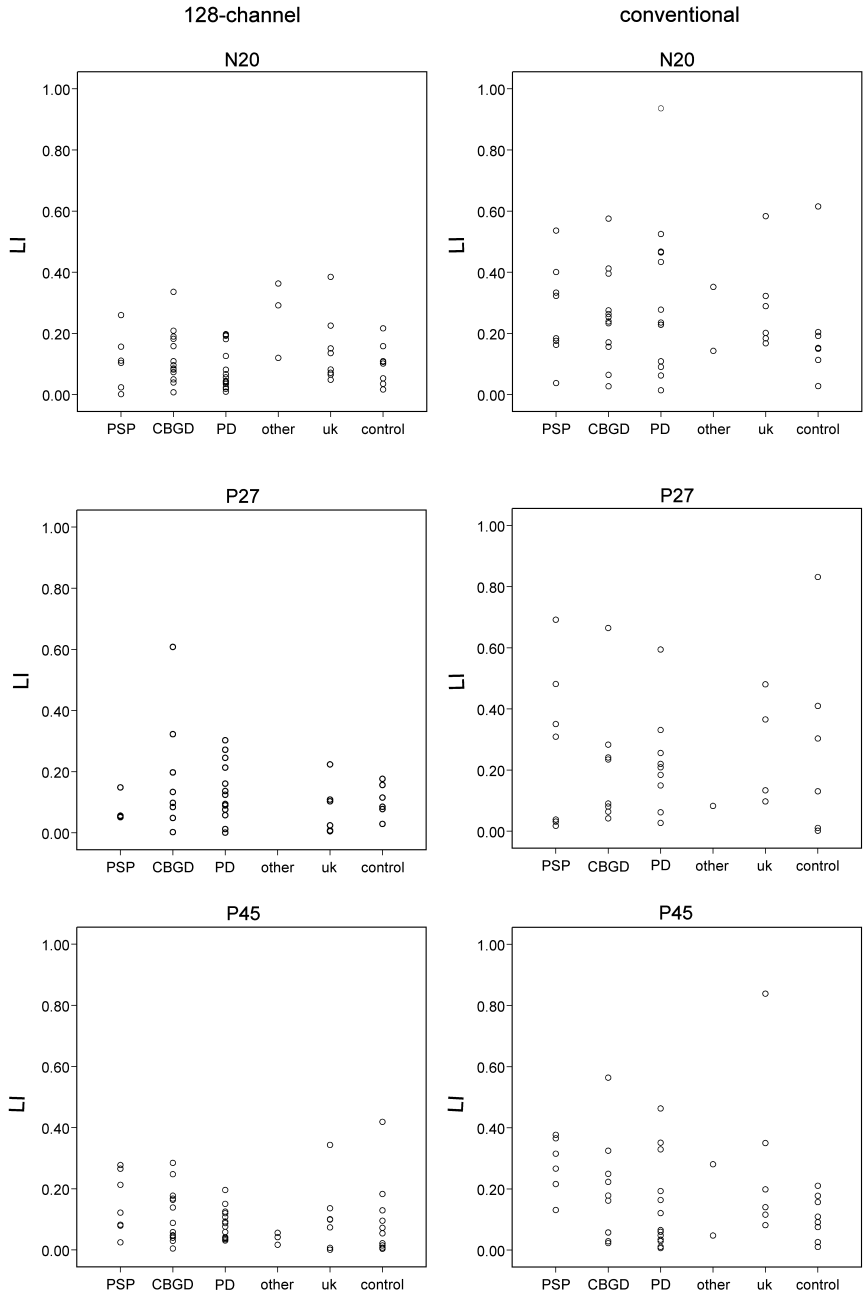

Figure 6.2: SEP peak laterality indices (LIs) estimated with the 128-channel method (left) and the conventional method (right). Each circle represents the LI of one subject. uc: unclear diagnosis.

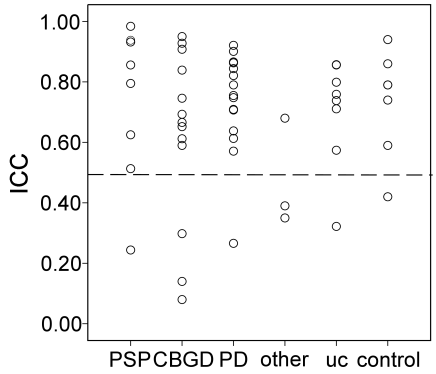

Figure 6.3: ICCs of all subjects. Each circle represents the ICC of one subject. uc: unclear diagnosis.

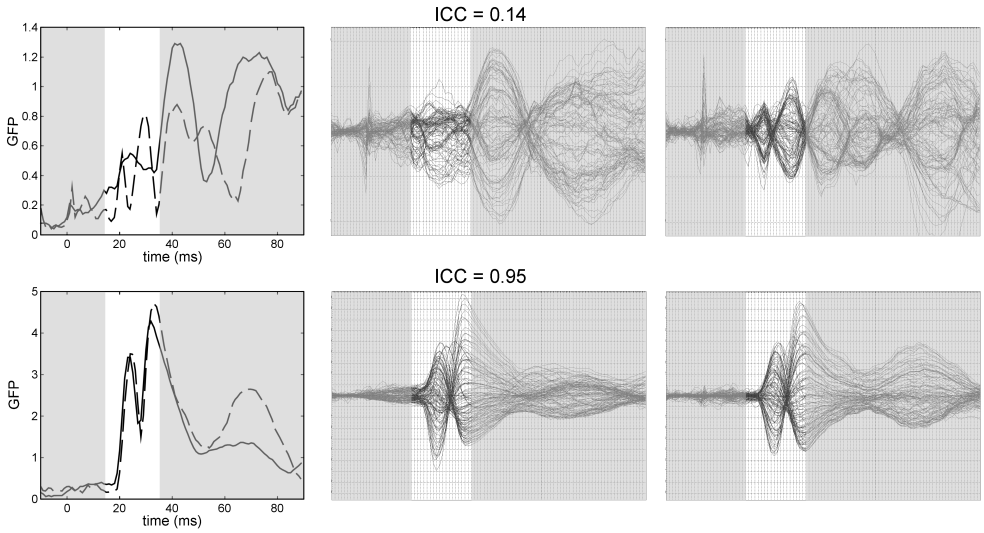

Figure 6.4: GFPs and butterfly plots of left and right median nerve SEP of two patients with CBGD; one with a low ICC (upper plots) and one with a high ICC (lowest plots). Left plots show GFPs of left side stimulation (solid line) and right side stimulation (dashed line). Middle and right plots show the butterflyplots of left and right median nerve SEP, respectively. Analysis interval (16-35 ms) is indicated in all figures.

amplitudes contralateral or ipsilateral to the most affected side in some patients with CBGD (Thompson et al., 1994; Brunt, 1995; Carella et al., 1997; Monza, 2003; Klodowska-Duda et al., 2006), we found comparable LIs for all patient groups and the healthy control group. Thus, SEP symmetry has a very low sensitivity and specificity for differentiating CBGD from other parkinsonian disorders and healthy controls.

Compared to the other patients with CBGD, the three with low ICC had clinical symptoms at the time of the SEP that might be related to degeneration of the sensory cortex; two patients suffered from sensory loss (patient 1 and 5, Table 6.2) and one patient had an alien limb (patient 2, Table 6.2). The latter symptom might also originate from frontal dysfunction (Bundick and Spinella, 2000; Biran and Chatterjee, 2004; Fitzgerald et al., 2007) and thus does not have to be related to degeneration of the sensory cortex in this subject. The low number of subjects with sensory problems is consistent with an earlier study. That study followed patients with CBGD for some years and reported sensory symptoms in 37% of the patients after an average disease duration of 5.2 years, while at disease onset only 8% had sensory problems (Rinne et al., 1994).

The number of patients with CBGD and a low ICC might thus be small, because the location of the SEP generators, which lie around the post central gyri, might only be affected in a small number of patients. The atrophy in this area might still be limited, because many of our patients were in an early stage of the disease. As far as we know little is known about the process of pathological progression in CBGD.

On the other hand, when investigating SEP amplitudes for each side separately, we found extremely high N20 amplitudes after stimulation of the most affected side in three patients with CBGD (patients 4, 8 and 12, Table 6.2) compared to the other subjects. One of these three patients, the one with the longest disease duration, also had extremely high N20 amplitude after stimulation of the less affected side. These three patients still had a left-right N20 amplitude difference within the normal range. In general, there was no clear relationship between the N20 amplitude and the clinical symptoms in patients with CBGD.

In contrast to several previous studies (Brunt, 1995; Carella et al., 1997; Klodowska-Duda et al., 2006), we did not find unilaterally reduced N20 amplitude in any of our patients with CBGD compared to healthy subjects and other parkinsonian disorders. A reason for this might be that these earlier studies included more advanced patients with CBGD, at a time that their diagnosis based on clinical features was clear, while in many of our patients the diagnosis was still unclear at the time of the SEP. Accordingly, our subjects were in an earlier stage of the disease and therefore cortical atrophy may be limited. However, other studies also described patients diagnosed with CBGD without reduced N20 amplitude (Thompson et al., 1994; Okuda et al., 1998; Monza, 2003).

In our study we found low ICCs not only in patients with CBGD, but also in one

patient with possible PSP, one patient with PD, two patients with MSA and in one patient with an unclear diagnosis. These findings are in disagreement with our hypothesis, since these disorders supposedly have similar neuropathological changes bilaterally and previous studies reported normal or bilaterally abnormal SEP amplitudes (Abbruzzese et al., 1991; Mauguière et al., 1993; Huttunen and Teravainen, 1993; Rossini et al., 1995; Abbruzzese et al., 1997; Kofler, 2000; Miwa and Mizuno, 2002). Therefore, we describe these patients with a low ICC in detail in the appendix. The differences between left and right butterfly plots of these patients with low ICC were similar compared to the differences found in patients with CBGD and low ICC.

A matter of debate in this study and other studies that investigate the same parkinsonian disorders is the correctness of the diagnosis of the patients. This is also illustrated in the patient descriptions in the appendix. A definite diagnosis can only be made by autopsy (Cornford et al., 1995; Mitra et al., 2003; Mahapatra et al., 2004). However, in our and many other studies autopsy was not performed. Two studies have compared clinical diagnosis and pathological diagnosis in a large group of parkinsonian disorders. In the study of Hughes et al. (2002), the positive predictive value (PPV) of the clinical diagnosis was 99% for PD and 80% for PSP, while sensitivity was 91% and 84% respectively. A high PPV of clinical diagnosis of PSP was also found by Josephs et al. (2006), while sensitivity in this study was 61%. The latter study also included patients with CBGD. The PPV and sensitivity of the clinical diagnosis of CBGD were only 48% and 47%, respectively. According to these results a clinical diagnosis of CBGD might be different from the pathological diagnosis. This discrepancy might have partly caused the different SEP findings between studies as well as between patients with CBGD.

By using FDG PET as an additional diagnostic criterion, we believe that we have partly overcome the problem of misdiagnosis. However, as far as we know no study compared FDG PET scans with a diagnosis based on post-mortem examination.

In this study we used the GFP that includes contralateral electrodes to estimate the ICC, because in a pilot study interhemispheric differences were observed in the SEP butterfly plots of patients with CBGD. However for future studies, it might be interesting to include only frontal electrodes or parietal electrodes for ICC estimation. In this way, possible unilateral frontal PD abnormalities can be better distinguished from unilateral parietal SEP abnormalities in patients with CBGD.

In conclusion, the ICC of median nerve SEP peak was abnormal in three out of 13 patients with CBGD. However, similar abnormalities were also found in patients with possible PSP, PD and MSA. Furthermore, we found extremely high N20 amplitudes in three other patients with CBGD, while LI was normal in all patients with CBGD. Therefore, cortical median nerve SEP symmetry and parietal amplitude have a low sensitivity and specificity for differentiating CBGD from other parkinsonian disorders in an early stage of the disease. A possible reason for this may be that the hand area of the primary somatosensory cortex is not affected

in many patients with CBGD in an early stage of their disease.

6.5 Appendix: Clinical features of patients with a low ICC and a disorder other than CBGD.

Patient with possible PSP (patient 3, Table 6.3)
The patient with possible PSP, who had a normal FDG PET scan and a low ICC showed larger amplitudes after right side stimulation in the butterfly plots and GFP waveform. She suffered from postural instability with falls, saccadic eye movements, impaired optokinetic nystagmus, axial rigiditity as well as rigidity of the extremities (right more than left), limited facial expression and bradykinesia at the time of the SEP.

Patient with PD (patient 6, Table 6.1)
The patient with PD and an ICC of 0.27 had PD for eight years and showed large differences in the butterfly plot and the GFP waveform. The differences in the butterfly plots were not only limited to the N30 but the P27 and P45 showed differences in amplitudes as well. In this patient, the disease started with a hypokinetic rigid syndrome on the left side of the body. The patient responded well to levodopa medication. At the time of the SEP his medication was stable and he had limited rigidity on the left side and hyperkinesias of the trunk, both arms and legs.

Patients with MSA (patients 1 and 2, Table 6.4)
The patients with MSA and a low ICC both showed reduced amplitude after left side stimulation around 20 ms and between 20 and 35 ms. In patient 1 the disease started with rigidity and pain of the left arm, rigidity of the legs and problems when standing up. She did not respond to parkinsonian medication. At the time of the SEP, three years after the start of the disease, she had a dystonic left arm, she was incontinent and sometimes choked. FDG PET scan showed hypometabolism of cerebellum and putamen.
Patient 2 with MSA had rigidity that started in the left leg and extended to the right leg, the arms and neck. At the time of the SEP she also suffered from bradykinesia, postural instability, urine incontinence and choking. The FDG PET scan showed hypometabolism of putamen and parietal lobe.

Patient with unclear diagnosis (patient 7, Table 6.4)
The patient whose diagnosis was unclear and had an ICC of 0.32, showed large amplitude differences in the butterflyplots and GFP waveform. At the time of the SEP she had a dystonic and rigid right arm and shoulder. FDG PET scan showed only slightly reduced bilateral hypometabolism in the parietal lobe. During

follow-up she had a good response to Levodopa. However, a myoclonus appeared in the right arm. The myoclonus, dystonia and the asymmetry are typical for CBGD, but a good L-dopa response is not often seen in patients with CBGD.

7

Multichannel recording of tibial nerve somatosensory evoked potentials

This chapter is accepted for publication as:
Multichannel recording of tibial nerve somatosensory evoked potentials.
W.J.G. van de Wassenberg, W.J. Kruizinga, J.H. van der Hoeven, K.L. Leenders, N.M. Maurits. Neurophysiology Clinique.

Abstract

Objectives. The topography of the peaks of the tibial nerve somatosensory evoked potential (SEP) varies among healthy subjects, most likely because of differences in position and orientation of the cortical generator(s). Therefore, amplitude estimation with a standard one or two-channel derivation is likely to be inaccurate and might partly cause the low sensitivity of SEP amplitude for pathological changes. In this study, we investigate whether 128-channel tibial nerve SEP recordings can improve the amplitude estimation and reduce the coefficient of variation.
Methods. We recorded tibial nerve SEPs using a 128-channel EEG system in 48 healthy subjects (20-70 years), of which one subject was excluded for further analyses. We compared P39, N50 and P60 amplitudes as obtained with a 128-channel analysis method (based on butterfly plots and spatial topographies) with those obtained using a one-channel conventional configuration and analysis. Scalp and earlobe references were compared.
Results. Tibial nerve SEP amplitudes obtained with the 128-channel method were significantly higher as compared to the one-channel conventional method. Consequently the coefficient of variation was lower for the 128-channel method. In addition, in both methods the N50 peak amplitude was sometimes hard to identify, because of its low amplitude. Besides, in some subjects the N50 peak, obtained with the conventional method, rather seems to be a period between two activation peaks than an activation peak on itself.
Conclusions. The 128-channel method can measure tibial nerve SEP amplitude more accurately and might therefore be more sensitive to pathological changes. Our results indicate that the N50 component is less useful for clinical practice.

7.1 Introduction

Somatosensory evoked potentials (SEPs) are mostly used clinically to evaluate conduction in somatosensory pathways. For this purpose, analyses of (inter)peak *latencies* are performed. Cortical SEP amplitude has been proven to be clinically useful for monitoring during carotid and scoliosis surgery and for prognostic applications (Florence et al., 2004; Luk et al., 2001; Manninen et al., 2004; Tzvetanov et al., 2004; Tzvetanov and Rousseff, 2003). Regarding diagnosis, applications of SEP amplitude are restricted to cortical myoclonus (Cassim and Houdayer, 2006; Ng and Jones, 2007; Shibasaki, 2006). The limited number of diagnostic SEP amplitude applications might result from the high intersubject amplitude variability in healthy subjects (Chiappa, 1997; Ferri et al., 1996; Gardill and Hielscher, 2001; Tsuji et al., 1984). Intersubject variation in size, shape and topography of the somatosensory cortical areas is thought to be one of the causes of this variability among subjects (Chiappa, 1997; Geyer et al., 1999; Miura et al., 2003; Uylings et al., 2005).

In our previous 128-channel median nerve SEP study, we showed that the position of maximum median nerve SEP amplitude at the scalp varies considerably among subjects and that a standard one channel recording underestimates the maximum amplitude at the scalp considerably (van de Wassenberg et al., 2008b). Furthermore, we found lower alternative coefficients of variation (aCOV) for amplitudes of the 128-channel compared to the one-channel method. These results suggest that 128-channel recordings can measure median nerve SEP amplitude more accurately and might therefore be more sensitive to pathological changes.

Studies investigating the tibial nerve SEP already showed a large variety of P39 topographies among healthy subjects (Chiappa, 1997; Emerson and Pedley, 2003; Miura et al., 2003; Seyal et al., 1983). The maximum P39 amplitude can be found either just posterior to Cz or at adjacent sites ipsilateral to the stimulated leg.

One first cause of this intersubject P39 variability might be that more sources with different positions and/or orientations are active around 40 ms. (Baumgartner et al., 1998; Valeriani et al., 1997, 1998, 2001). The relative contribution of the different sources to the P39 amplitude can vary between subjects due to variation in source strength, position, orientation and latency and thus can result in differences in the position of maximum SEP amplitudes.

A second cause may be the intersubject variation in position of the primary sensory areas for the leg and foot on the medial part of the postcentral gyrus within the interhemispheric fissure. If the leg area is located at the superficial edge of the interhemispheric fissure, the orientation of the pyramidal cells would be radial to the scalp, which results in a large positive field at the midline. On the contrary, if the position of the leg area lies deeper in the interhemispheric fissure, the orientation of the pyramidal cells would be more tangential with a positive field ipsilateral and a negative field contralateral to the side of stimulation (Seyal et al., 1983).

In some cases, this may lead to the absence of the P39 component in the CPz-Fz derivation. Therefore, previous researchers and guidelines recommend to use multiple leads for accurate peak *latency* estimation; for example CPz-Fpz and CPi-Fpz (Emerson and Pedley, 2003). However, SEP peak *amplitude* varies much more over adjacent electrodes compared to SEP latency. As a result, an even higher density of electrodes might be necessary for accurate amplitude estimation of tibial nerve SEP peaks.
The above results have been obtained for P39 only; less is known about the intersubject variability in position of N50 and P60 peaks that follow the P39.
In this study, we investigate if 128-channel recordings reduce the aCOVs of cortical tibial nerve SEP amplitudes. We compared SEP amplitudes and positions obtained using the electrode configuration proposed by Mauguire et al. (1999) with one cortical channel to SEP amplitudes obtained by 128-channel recordings in healthy subjects. Furthermore, we compared scalp and earlobe references.
In addition, we investigated the effect of age on 128-channel SEP amplitude. Previous studies with limited number of electrodes report different results about the amplitude-age relation (Kakigi, 1987; Kakigi and Shibasaki, 1992; Miura et al., 2003; Romani et al., 1992). If 128-channel recordings reduce the intrasubject variability, this method will probably also better quantify the effect of age on amplitude.

7.2 Materials and methods

7.2.1 Subjects

Tibial nerve SEPs were recorded from 48 right-handed healthy volunteers. For each decade between 20 and 70 years 9 or 10 subjects were included of which at least four males and four females. None of the subjects had a history of head injury or other neurological conditions. All subjects gave their informed consent. The protocol was approved by the medical-ethical board of the University Medical Center Groningen.

7.2.2 SEP recording

The subjects were sitting in a comfortable chair in a warm and quiet room and were instructed to relax and keep their eyes open. We stimulated the tibial nerve at both ankles 500 times, one side at a time, and repeated each recording once. The stimuli were square wave impulses of 0.2 ms, which were delivered at a frequency of 2.1 Hz. The stimulus intensity was slightly above motor threshold, producing a small twitch of the big toe. We placed Ag/AgCl electrodes in the popliteal fossa of the knee and recorded EEG from the scalp using a 128-electrode cap, which was connected to a 128-channel headbox (Twente Medical Systems BV, Enschede, Netherlands). Impedance values were kept below 10 kΩ. Complete preparation time for this

recording was approximately 30 minutes and preparation and recordings were well tolerated by all subjects. We used Onyx software (Silicon Biomedical Instruments BV, Westervoort, The Netherlands) to record the data at a sampling frequency of 1000 Hz. Data from the popliteal fossa were recorded, segmented, amplified and averaged with the Medelec Synergy N-EP system (Oxford Instruments Medical, Concord, USA) to check peripheral conductivity.
The raw EEG data was processed off-line using Brain Vision Analyzer 1.05 (Brain Products GmbH, München, Germany). Data were first high-pass filtered at 3 Hz (12 dB/octave, zero-phase shift Butterworth filter) and then segmented into epochs of 100 ms, including a 10 ms pre-stimulus interval. Artifact rejection was set at $\pm$ 100 μV and a baseline correction procedure was performed using the pre-stimulus interval. Channels with muscle artifacts that obscured the SEP were excluded for further analysis.
On each stimulation side, we used the recording with the highest signal-to-noise ratio for further analysis. The signal-to-noise ratio was calculated by dividing the mean global field power (GFP) between 30 and 80 ms by the mean GFP baseline amplitude (between -10 and 0 ms). The GFP was calculated by:

$$GFP(t) = \sqrt{\frac{1}{N}\sum_{n=1}^{N}[V_n(t)]^2} \tag{7.1}$$

where N is the number of electrodes and $V_n(t)$ is the potential measured at electrode n and timepoint t.
The complete protocol was repeated in 5 subjects, one from each decade, within 6 months to assess long-term intrasubject reproducibility.

7.2.3 SEP analysis

Conventional SEP analysis

We considered both CPz-Fz (conventional scalp reference) and CPz-Ei (conventional earlobe reference) for estimation of P39, N50 and P60 latency and amplitude for left/right side stimulation. The largest positive peak around 39 ms was identified as the P39. The main prominent negative peak succeeding the P39 was recognized as the N50 and the P60 was the main prominent positive peak following the N50. Peaks were only identified and used for analyses if they were reproducible and visually exceeded the noise level. All amplitudes were defined as peak-to-baseline amplitudes.

128-channel SEP analysis

The averaged data were exported to ASA 2.21 (ANT software BV, Enschede, The Netherlands) using either an average (dataset 1) or earlobe reference (dataset 2).

The results of the subsequent analysis on dataset 1 were compared to the conventional scalp reference results. The results of the analysis on dataset 2 were compared to the conventional earlobe reference results.
For both 128-channel analyses we searched for negative (N50) and positive peaks (P39 and P60) in the butterfly plot between 35 and 75 ms and checked if the corresponding map met the criteria we defined for P39, N50 and P60. These criteria were a centroparietal positive field at the midline or a positive field ipsilateral and a contralateral negative parietal field for both the P39 and P60 maps and a centroparietal negative field at the midline in combination with a contralateral positive parietal field for the N50 map. In both analyses we used the topographic map with average reference, which is the reference of choice for these maps (Pascual-Marqui and Lehmann, 1993b).
If the map matched, we used the difference between maximum and minimum amplitude at the time of the peak as (total) amplitude in the analysis of dataset 1. In the analysis of dataset 2 we used the peak to baseline amplitude as (total) amplitude at the time of the peak (Fig. 7.1).
Peak latencies in the 128-channel method were defined as the time between stimulus onset and the peak maximum.

7.2.4 Statistics

We used the intraclass correlation coefficient (ICC) and Bland-Altman plots to test the intrasubject amplitude variability of two successive recordings on the same day (Bland and Altman, 1986; Rousson et al., 2002). The Bland-Altman plot shows the amplitude difference between two subsequent recordings as a function of the mean amplitude and is used here to analyze the absolute agreement of successive recordings.
For the statistical analysis of both scalp and earlobe reference analyses we divided the subjects in different age groups. To include at least 10 persons in each age group and because we mainly expected age effects from 30 years onwards we divided the subjects in the following age groups: 1) 20-30 years, 2) 30-50 years and 3) 50-70 years.
We used the Wilcoxon signed ranks test for comparison of latencies and amplitudes between methods. Additionally, we compared latencies and amplitudes of the different age groups using the Kruskal-Wallis test. Post hoc testing was performed using the Kolmogorov-Smirnov Z test with subsequent Bonferroni correction. Furthermore, regression analysis was performed to examine the effect of age on amplitude. All parameters were described in terms of medians and interquartile ranges.
The coefficient of variation (COV) is a ratio between the variability and the central tendency of the data. In principle, any measure of variability and central tendency of the data can be used. For normally distributed data the COV is typically defined as the ratio between variance and mean. Since SEP amplitude is not normally

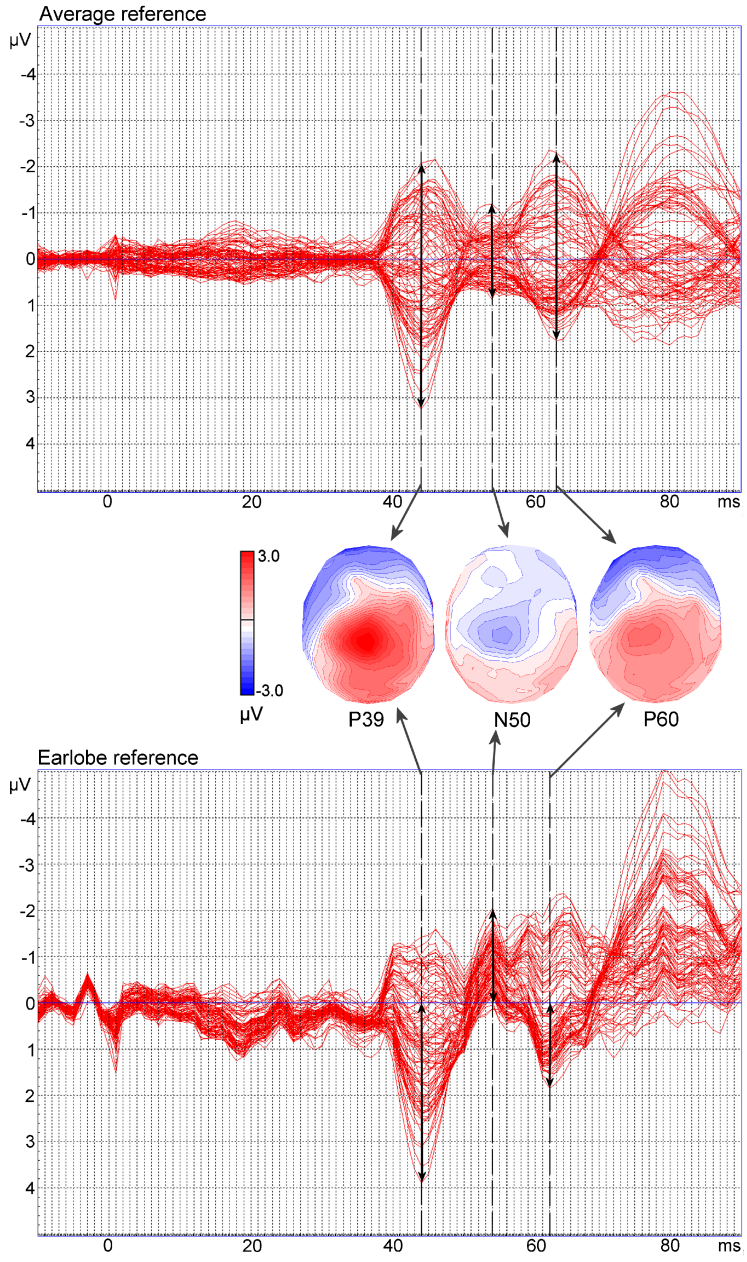

Figure 7.1: 128-channel analysis technique for scalp and earlobe reference analyses. Topographic maps that correspond with peaks in the butterfly plot are compared with a reference map. These reference maps are plotted using an average reference. For the scalp reference the difference between maximum and minimum amplitude at the time of the peak is used as (total) amplitude (top butterfly plot). For the earlobe reference the maximum amplitude to baseline is used as (total) amplitude (bottom butterfly plot).

distributed we introduce an alternative coefficient of variation (aCOV), which is defined as the interquartile range divided by the median. We compared aCOV of the 128-channel analyses to the conventional analyses for both scalp and earlobe references. A lower aCOV is indicative for a better sensitivity/specificity when evaluating patients.
In addition, we investigated whether the 128-channel method reduces the within-subject variability between the measure of left and right tibial SEP peak amplitude. We compared the left-right SEP amplitude difference of the 128-channel method and the conventional method with scalp reference by calculating the absolute amplitude difference and the absolute laterality index for each SEP peak. The laterality index is defined as the amplitude difference between left and right median nerve SEP, divided by the sum of both amplitudes (Jung et al., 2003).

7.3 Results

One out of 48 subjects (female; 35 years old) was excluded for further analysis, because a large left-right difference in N8 latency was found and no cortical components could be observed. We analyzed the SEP data of the remaining 47 subjects according to the conventional and 128-channel method. P39, N50 and P60 could not be identified in all subjects. Table 7.2 shows the number of detected components. P39 was identified in more subjects with the 128-channel method, while N50 and P60 were identified more often with the conventional method.

Table 7.1: Subject characteristics

Age group	Number	Age
20-30	10	26.0 ± 2.8
30-40	9	33.8 ± 3.2
40-50	9	45.2 ± 2.5
50-60	10	54.2 ± 3.1
60-70	9	62.9 ± 2.7

Age is given in years as mean ± sd.

Table 7.2: Number of observed components per SEP peak in 47 healthy subjects for both scalp and earlobe reference analyses.

		P39		N50		P60	
Method		L	R	L	R	L	R
Scalp	Con	38	43	38	44	40	46
	128	44	46	27	33	37	38
Earlobe	Con	38	39	38	39	39	40
	128	40	41	19	21	35	37

Con: conventional method; 128: 128-channel method.
L: left side stimulation; R: right side stimulation.

7.3.1 Reproducibility

We tested amplitude reproducibility by calculating the ICC of the SEP components identified in two successive recordings on the same day. Values ranged from 0.66 to 0.94 for the 128-channel method and from 0.62 to 0.89 for the conventional method, except for the N50 when using the 128-channel earlobe reference (ICC=0.20).
According to the criteria proposed by Lee et al. (1989) peaks with an ICC higher than 0.75 represent a good reliability. In this study, only the ICC of the N50 peaks is below this threshold.
Figure 7.2 shows the Bland-Altman plots (Bland and Altman, 1986) for peak amplitudes of two successive recordings at the same day and for two recordings obtained with a time interval of two to six months. It appears that successive recordings differences were in most cases smaller than 1.0 μV. Furthermore, differences between recordings at separate days were in the same range as differences between two successive recordings on the same day. However, one person showed larger differences in right side P60 amplitude between recordings at separate days compared to recordings at the same day although in both recordings a twitch was present.

7.3.2 Comparison between conventional and 128-channel analyses

Amplitudes and latencies for both scalp and earlobe reference analyses are displayed in tables 7.3 and 7.4. Median amplitudes as obtained with 128-channel analyses were significantly higher than amplitudes obtained with conventional analyses. However, no significance was reached for left and right N50 amplitude with earlobe reference in respectively two and one age groups. In these cases, in only two or three subjects an N50 was found with the 128-channel method.
Interquartile ranges of the conventional and 128-channel method were typically similar. Consequently, in general aCOV was lower for the 128-channel method compared to the conventional method (Table 7.5).
Latencies showed only significant differences between conventional and 128-channel analyses with scalp reference for two peaks in the 30-50 age group, one peak in the 50-70 age group and three peaks in the total group and with earlobe reference for one peak in the 20-30 age group and two peaks in the total group. In cases with a significant difference in latency, median latency differed less than 1 ms, except for P39 left side stimulation (age group 30-50).
Further investigation of the maximum amplitude position showed that the maximum amplitude was found in a widespread area for all SEP components (Fig. 7.3). Maximum amplitudes found at the outer electrode layer were always part of a more widespread potential field of the same polarity.

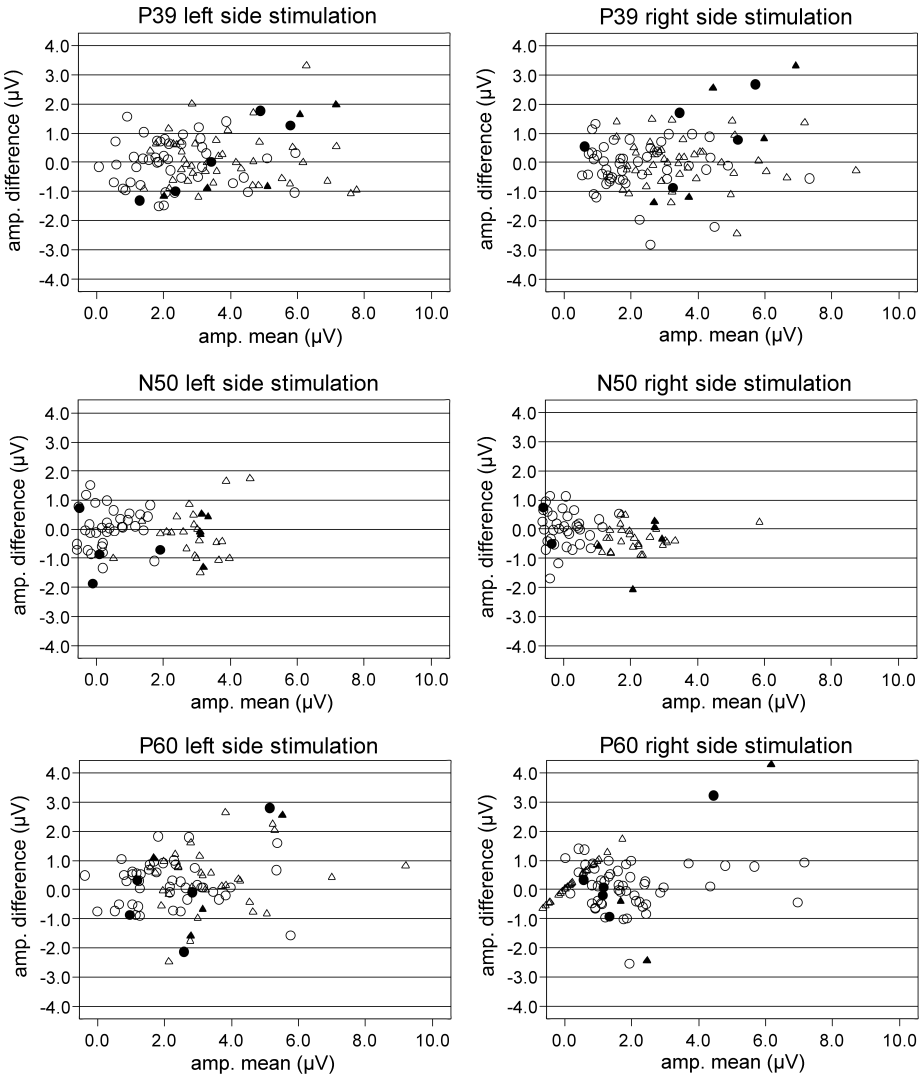

Figure 7.2: Difference versus mean of two successive recordings at the same day and two recordings with a time interval of 2-6 months for the scalp reference analyses. Open circle: conventional (same day); closed circle: conventional (2-6 months interval); open triangle: 128-channel (same day); closed triangle: 128-channel (2-6 months interval).

Table 7.3: Median and interquartile range (IQR) for peak amplitudes in μV (A) and latencies in ms (B) per age group and for the entire group of subjects obtained with scalp reference analyses.

Amplitude		20-30				30-50				50-70				Total			
		Median		IQR		Median		IQR		Median		IQR		Median		IQR	
Peak	Method	L	R	L	R	L	R	L	R	L	R	L	R	L	R	L	R
P39	Con	2.18	1.70	1.07	1.65	2.21	1.40	1.51	1.90	2.47	1.54	2.04	1.32	2.21	1.54	1.48	1.49
	128	3.62	2.92	2.14	1.36	3.54	3.63	2.48	1.94	2.88	2.34	2.27	1.83	3.35	3.05	2.31	1.59
N50	Con	0.57	0.13	1.95	0.83	0.21	0.25	1.28	1.29	0.34	0.05	1.11	1.00	0.27	0.13	1.31	0.94
	128	2.27	1.79	0.69	1.29	2.41	2.35	1.61	1.12	2.08	1.86	1.31	0.94	2.35	1.94	1.24	1.01
P60	Con	1.27	1.37	1.03	1.50	2.41	1.71	2.07	2.04	2.62	1.60	1.75	1.17	2.13	1.55	1.86	1.21
	128	2.80	2.42	0.29	1.63	3.48	3.19	2.20	2.33	3.641	3.24	1.20	2.14	3.37	2.95	1.35	1.80

A

Latency		20-30				30-50				50-70				Total			
		Median		IQR		Median		IQR		Median		IQR		Median		IQR	
Peak	Method	L	R	L	R	L	R	L	R	L	R	L	R	L	R	L	R
P39	Con	41.0	42.5	3.0	2.0	48.0^{*1}	46.5	3.8	4.3	45.0	46.0*	5.5	4.0	45.0*	45.0*	5.3	4.0
	128	41.0	42.0	2.0	2.0	45.0^{1}	46.0^{1}	4.5	4.5	44.01	45.0^{1}	5.3	5.8	44.0	44.0	5.5	5.0
N50	Con	52.0	51.0	3.5	3.3	55.01	54.0*	5.0	4.5	55.0	54.0	7.8	6.3	54.0	53.0*	5.3	4.0
	128	52.0	53.0	2.0	2.0	56.0	55.0	2.5	4.0	57.0	57.0^{1}	6.0	6.0	55.0	54.0	5.0	5.0
P60	Con	61.0	61.0	3.5	3.5	66.0	65.5	5.0	6.3	68.0	67.5^{1}	9.5	6.5	65.0	65.0	7.0	8.0
	128	62.5	61.0	2.0	3.5	65.0^{1}	66.5^{1}	5.0	6.0	67.0	67.0^{1}	3.8	6.3	65.0	65.0	5.0	6.3

B

Con: conventional method; 128: 128-channel method.
L: left side stimulation; R: right side stimulation.
Amplitudes are all significantly higher for the 128-channel method than for the conventional method.
[1] significant difference with age group 20-30 ($p < 0.05$).
* significant latency difference between both methods.

Table 7.4: Median and interquartile range (IQR) for peak amplitudes in μV (A) and latencies in ms (B) per age group and for the entire group of subjects obtained with earlobe reference analyses.

		20-30				30-50				50-70				Total			
		Median		IQR		Median		IQR		Median		IQR		Median		IQR	
Peak	Method	L	R	L	R	L	R	L	R	L	R	L	R	L	R	L	R
P39	Con	3.02	1.81	1.79	1.30	2.20	2.04	2.18	1.42	2.32	1.49	2.29	1.07	2.30	1.80	2.00	1.09
	128	3.57	2.34	1.84	1.45	2.29	2.27	2.37	1.77	2.75	2.04	2.54	0.84	2.75	2.29	1.32	2.13
N50	Con	0.52	0.60	2.53	0.79	0.52	1.16	1.11	1.37	1.01	0.06	1.41	1.74	0.37	0.70	1.45	1.47
	128	2.03	1.36	0.38	0.54	1.93	1.79	1.81	0.79	2.55	2.03	1.42	1.18	2.06	1.78	0.78	0.96
P60	Con	1.92	1.46	1.11	1.50	1.82	1.95	2.14	1.19	2.52	2.17	2.05	1.59	2.08	1.79	1.79	1.24
	128	2.28	1.85	0.62	1.15	2.15	2.65	2.24	2.28	3.28	3.07	1.47	1.63	2.71	2.41	1.64	1.69

A

		20-30				30-50				50-70				Total			
		Median		IQR		Median		IQR		Median		IQR		Median		IQR	
Peak	Method	L	R	L	R	L	R	L	R	L	R	L	R	L	R	L	R
P39	Con	43.0*	43.0	2.0	2.0	45.0[1]	45.0	5.0	3.0	45.0[1]	44.0	6.0	3.3	44.0*	44.0	5.3	3.0
	128	42.0	43.0	1.5	2.5	44.0[1]	45.0[1]	6.0	4.3	43.5	44.5[1]	5.3	6.3	43.5	44.0	5.8	4.5
N50	Con	53.0	50.5	3.0	3.5	55.0	55.0[1]	5.0	4.8	55.0	55.0	9.5	8.0	54.5	54.0*	5.3	6.0
	128	52.0	54.0	1.5	5.0	57.0	55.0	6.8	5.0	52.0	56.0	1.5	9.0	53.0	55.0	5.0	2.5
P60	Con	62.0	60.5	2.0	3.3	66.5[1]	67.0[1]	4.0	4.8	67.0[1]	68.0[1]	6.3	6.0	65.0	65.0	6.0	7.0
	128	62.0	61.0	1.0	3.0	65.0[1]	67.0[1]	5.0	5.0	67.0[1]	67.0[1]	5.5	4.0	65.0	66.0	5.0	6.0

B

Con: conventional method; 128: 128-channel method.
L: left side stimulation; R: right side stimulation.
Amplitudes are all significantly higher for the 128-channel method than for the conventional method except for N50 left side (age group 20-30 and 50-70) and N50 right side (age group 50-70).
[1] significant difference with age group 20-30 ($p < 0.05$).
* significant latency difference between both methods.

Table 7.5: Alternative coefficient of variation (aCOV) of amplitude for each SEP peak for

		Scalp		Earlobe	
Peak	Method	L	R	L	R
P39	Con	0.67	0.97	0.87	0.61
	128	0.69	0.52	0.77	0.58
N50	Con	4.82	7.23	3.92	2.10
	128	0.53	0.52	0.47	0.44
P60	Con	0.87	0.78	0.86	0.69
	128	0.40	0.61	0.62	0.68

Con: conventional method; 128: 128-channel method.
L: left side stimulation; R: right side stimulation.

Additionally, we estimated for 10 subjects the P39 amplitude when only 64 or 32 channels were used and compared these with 128-channel amplitudes (Fig. 7.4). On average 64 and 32-channel amplitude estimation resulted in an underestimation of 5% and 12% respectively. In one subject a reduction to 32 channels resulted in an amplitude underestimation of 19%.

7.3.3 Age effect

When evaluating the age effect, we observed no significant differences in amplitude between age groups. Regression analysis resulted in only two significant, but small, positive age-effects (128-channel P60 left side with scalp reference ($\beta = 0.042$, $R^2 = 0.117$, $p = 0.028$) and conventional P60 right side with earlobe reference ($\beta = 0.035$, $R^2 = 0.089$, $p = 0.047$).

7.3.4 Left-right differences

No significant differences were found between absolute left-right amplitude differences obtained from conventional and 128-channel analyses with scalp reference. On the other hand, P39 and N50 absolute laterality indices were significantly smaller ($p<0.001$) for the 128-channel method.

7.4 Discussion

In this study we examined whether 128-channel recordings can measure cortical tibial nerve SEP amplitude more accurately than the conventional method. We hypothesized that a 128-channel recording would decrease the intersubject variability in amplitude, since it potentially overcomes the discrepancy caused by intersubject variation in position and orientation of cortical SEP generators with respect to the fixed, conventional recording position. However, as in our previous

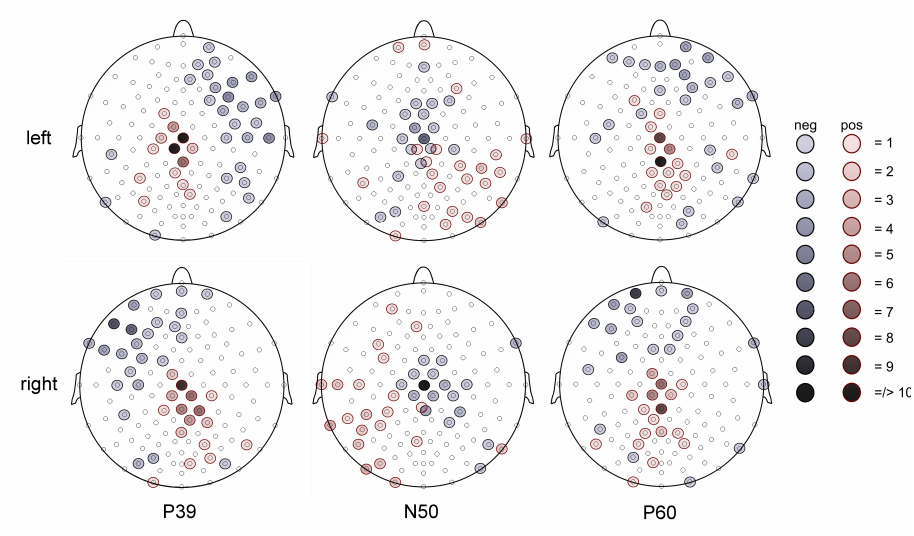

Figure 7.3: Positions of maximum amplitude for the different SEP components for the 128-channel scalp reference analysis. The darkness of the color indicates the number of subjects where the maximum amplitude was found at this electrode. The position of the maximum amplitudes, although centered around electrodes used in conventional analyses, was found in a widespread area for all SEP components.

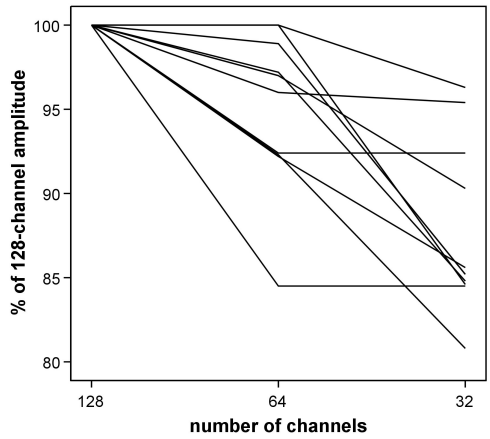

Figure 7.4: Left P39 amplitude, when obtained with 64 and 32 channels for 10 subjects. Amplitudes are given as percentage of the 128-channel amplitude. Since reduction of the number of electrodes to 32 channels can result in an amplitude decrease of 19%, a minimum of 64 channels is advised for accurate amplitude estimation.

study on median nerve SEP (van de Wassenberg et al., 2008b) we found similar intersubject amplitude variability for the conventional and 128-channel method. Nevertheless, amplitudes obtained with the 128-channel method were considerably higher (Tables 7.3 and 7.4), because the electrode position where the SEP amplitude was maximal differed in most subjects from the electrode position used in the conventional method (Fig. 7.3). Furthermore, we found a lower aCOV for the 128-channel method. A lower aCOV is indicative for a better differentiation between groups. Therefore, the 128-channel method is likely to be more sensitive to pathological changes than the conventional method.

As expected, in most cases no significant latency difference was observed between both methods. If there was a significant latency difference the median latency differed only 1 ms, which is within measurement accuracy. However, left P39 (age group 30-50) latency obtained with scalp reference differed significantly with a median latency difference of 3 ms between the conventional and 128-channel method. Further investigation of this difference showed that three subjects had a much higher conventional than 128-channel latency (differences 3, 8 and 9 ms). The large differences in these subjects were caused by the fact that, after the positive field around CPz had reached its maximum, a (more) negative field arose around Fz. As a result, the positive peak in the CPz-Fz derivations around 39 ms did not correspond with the moment of maximum positive field around CPz. According to these results, in some subjects P39 latency can be determined more accurately with the 128-channel method compared to the conventional method with Fz as reference.

Amplitude reproducibility of the 128-channel method, as assessed using the ICC and Bland-Altman plots (Fig. 7.2), were good and comparable with the conventional method except for N50 left side stimulation obtained with earlobe reference. One other study investigated the ICC of test-retest tibial nerve SEP amplitude with an interval of one week. They used peak-to-peak amplitude and found ICC values of 0.80 and 0.86 for respectively N30-P40 and P40-N50 amplitude (Romani et al., 1993), which lie in the same range as our ICC values.

The ICC of the left N50 obtained with the 128-channel method and earlobe reference is very low (0.2) compared to the other ICCs. This might be caused by the limited number of detected SEP peaks and the low N50 amplitude, which makes this peak more sensitive for the artifacts that are more present in the earlobe channel.

In this study, we also determined amplitude differences between recordings at separate days, because these might not only be related to physiological factors but also to the experimental set up, i.e. re-placement of the cap, stimulation position and intensity and impedance. We found that differences in amplitude between two recordings at separate days were in the same range as the differences between two successive recordings on the same day except in one person, where the P60 after right side stimulation differed more than 3.0 μV even though the conditions in both

measurements were the same; in both recordings a twitch was present and similar stimulus intensity and position were used.
In contrast to several other studies (Kakigi, 1987; Miura et al., 2003; Romani et al., 1992; Valeriani et al., 2000), tibial nerve SEP peaks were missing in a number of subjects for both methods. It is reported that the P39 might be of low amplitude or indistinct when using the conventional CPz-Fz derivation, depending on the position of the primary sensory areas for the leg and foot on the postcentral gyrus within the interhemispheric fissure (Chiappa, 1997; Mauguière et al., 1999; Miura et al., 2003).
From the 13 P39 peaks (four right side stimulation, nine left side stimulation) that could not be detected in the CPz-Fz derivation nine recordings had a positive field that was positioned more anterior than Cpz. In these cases the P39 was observable with a Cz-Fz derivation however. In two cases the P39 was not defined, because the recording was not reproducible. In the other two recordings the P39 could not be detected despite a low noise level.
In previous studies, where no peaks were missing, a channel with an electrode ipsilateral or contralateral to the side of stimulation was used except in the study of Kakigi (1987). Furthermore, not all these studies investigated the N50 (Kakigi, 1987; Pascual-Marqui and Lehmann, 1993b; Valeriani et al., 2000) and P60 (Kakigi, 1987; Pascual-Marqui and Lehmann, 1993b). In this study, we have followed the standard derivation recommended by Mauguiere et al.(1999). Other guidelines recommend to use an extra derivation e.g. CPi-Fpz (Emerson and Pedley, 2003). This might have increased the number of detected peaks in the conventional method. However, for accurate amplitude estimation more channels are necessary, since the position of maximum amplitude varies over a wide area among subjects (Fig. 7.3). Furthermore, Tsuji et al. (1984) stated that high pass filters lower than 30 Hz make identification of P39 and N50 components and thus amplitude estimation more difficult. However, for accurate measurement of cortical tibial nerve peak amplitudes a lower high pass filter is necessary, because lower frequencies also contribute to peak amplitudes. Therefore, we chose to use a high pass filter of 3 Hz.
A possible explanation of the lower number of detected peaks in the CPz-earlobe derivation compared to the CPz-Fz derivation may be a higher noise level in the earlobe channels in some subjects. In those cases small peaks will not exceed the noise level.
In this study, the 128-channel method identified P39 peaks more often, but N50 and P60 peaks less often than the conventional method. The latter effect might be partly explained by the extra criteria, i.e. the correspondence to the reference map, in the 128-channel method. The peaks assigned as N50 and P60 with the conventional method do not all correspond to the reference maps as defined in this paper. For example, in some subjects the conventional N50 peak rather seems to be a period between two activation peaks than an activation peak on itself and does not show a centroparietal negative field at the midline. A second cause of the lower

number of detected N50 peaks in the 128-channel method is its low amplitude, which might not always rise above the noise level of all channels and thus might not result in a peak in the butterflyplot.
The relatively low median N50 amplitudes are partly caused by the fact that some subjects had a W-shape (P39-N50-P60) in the conventional derivation with a N50 peak that did not cross the baseline; after the positive P39 the potential decreases, but not to a negative value. This phenomenon has been reported earlier in other studies (Desmedt and Bourguet, 1985; Tinazzi et al., 1997). In these subjects, we used the positive value as peak N50 amplitude. In some subjects the N50 had a positive value in the first recording, while a negative value was obtained in the second recording.
Furthermore, the extreme high aCOV for N50 obtained with the conventional method is caused by low median N50 amplitudes. These median N50 amplitudes are lower than when obtained with the 128-channel method, not only because of the less optimal electrode position, but also because very low amplitudes are sometimes more difficult to detect with the 128-channel method.
We also investigated the effect of age on amplitude. Previous tibial nerve SEP studies showed an increase of cortical amplitudes with age (Kakigi, 1987; Kakigi and Shibasaki, 1992), although others reported no significant age effect on cortical amplitude (Miura et al., 2003; Romani et al., 1992). In our study, a comparison of amplitude between age groups did not result in significant differences. Furthermore, there was no significant correlation between age and amplitude for the tibial nerve SEP components, except for P60 right side stimulation obtained with the conventional method (earlobe and scalp reference) and for P60 left side stimulation obtained with the 128-channel method (scalp reference). However, these correlations were very small.
Finally, we compared left-right SEP amplitude differences and found significantly smaller absolute laterality indices for the 128-channel method. Probably, sources in both hemispheres differ (slightly) in orientation and/or location, resulting in (small) interhemispheric differences in position of maximum amplitude. Therefore, the 128-channel method can estimate interhemispheric symmetry more accurately than the conventional method.
In conclusion, this study shows that tibial nerve SEP amplitudes can be estimated more accurately with multichannel recordings than with the conventional method. In this study, we used 128 electrodes, which resulted in much higher amplitudes. We found (Fig. 7.4) that a reduction to 64 and 32 channels leads to an average amplitude decrease of 5% and 12% respectively. Therefore, we recommend to use at least 64 channels if accurate estimation of tibial nerve SEP amplitude is required. The same number was recommended for median nerve SEP based on the Nyquist criteria (Spitzer et al., 1989). Furthermore, this more accurate estimation might lead to a higher sensitivity of SEP amplitude for pathological changes, depending on amplitude and variability changes in patients, and might result in new clinical

applications. Based on our experience, multichannel EEG recordings are clinically feasible, since preparation time for 64 channels is only 20 minutes and no additional problems occur during preparation or recording compared to conventional recordings, neither in healthy subjects, nor in patients. So far, we have successfully recorded 128-channel EEGs in patients with dementia, movement disorders, brain tumours and pain syndromes, but results are not reported here.
Alternatively, instead of 64 or 128-channel recordings a limited number of electrodes can be used with a high electrode density centroparietally. To achieve similar accuracy as with a 64 channel recording and based on our results displayed in figure 7.4, we advise to use at least 18 electrodes; FC1, FCz, FC2, C3, C1, Cz, C2, C4, CP3, CP1, CPz, CP2, CP4, P3, P1, Pz, P2, P4. However, when 64 or 128 channels are used additional advantages are that an average reference can be used and that source localization to estimate source strengths and differentiate sources is feasible. Moreover, with 64- or 128-channel recordings every derivation can be made off-line, e.g. the derivations suggested by Valeriani et al. (2000) that might distinguish the two components that contribute to the P39. On the other hand, if one is only interested in SEP latency, standard recordings using only a few electrodes are sufficient.
Furthermore, according to our results, the N50 amplitude identified in the conventional method does not always correspond to the expected topography and in these cases the N50 peak rather seems to be a period between two activation peaks than an activation peak on itself. In addition, the N50 is sometimes difficult to identify, because of its low amplitude. Therefore, we believe that the N50 peak is less useful for clinical purposes.

8

Feasibility of 128-channel recordings of attention- and movement-related lateralized potentials in patients with Parkinson's disease

W.J.G. van de Wassenberg, J.H. van der Hoeven, K.L. Leenders, N.M. Maurits.

Abstract

Introduction. Recent event-related potential (ERP) studies have shown that directing attention and movement preparation produce similar frontocentral and occipitotemporal lateralized ERPs (L-ERPs), i.e. the anterior-directing-attention negativity (ADAN) and the late directing-attention positivity (LDAP). Parkinson's disease is associated with motor deficits as well as deficits in spatial attention. A previous study already reported a reduced ADAN in patients with PD during an attention task with a limited number of electrodes. These L-ERPs can be investigated in more detail by additionally using also a motor preparation task and 128-channel EEG recordings. However, patients with PD have more difficulties with suppressing eye movements than age-matched healthy controls, which is essential for reliable estimation of these L-ERPs. Here, we investigated whether recording of ADAN and LDAP in patients with PD with a protocol previously used in young subjects is feasible and, in particular, whether patients with PD are able to suppress their eye movements in an attention and motor preparation task.
Methods. We used a cue-target task in which the cue gives information about the location of the target (attention task) or about the response appropriate to the target (motor task).
Results. Eight out of eleven patients had major problems with suppressing horizontal eye movements in the attention as well as in the motor task. In addition, for one patient the task was too complicated ($> 20\%$ errors).
Conclusion. Patients with PD have problems with suppressing saccades, possibly because the patients experience the task as more difficult or because of dysfunc-

tion of frontostriatal circuits. Accordingly, performing spatial attention tasks and estimation of reliable ADAN and LDAP in patients with PD is a challenge. For future studies with patients with PD, we therefore recommend to make the task easier to perform and we have provided some suggestions.

8.1 Introduction

Idiopathic Parkinson's disease (PD) is a progressive neurological disorder associated with degeneration of dopaminergic neurons in the substantia nigra leading to dysfunction of the basal ganglia. PD is characterized by motor impairment, such as bradykinesia, tremor or rigidity. Besides motor symptoms, also several cognitive deficits, such as deficits in attention shifting, planning and memory can be observed in patients with PD. These cognitive and motor problems are suggested to be caused by dysfunction of frontostriatal circuits (Taylor et al., 1986; Gotham et al., 1988; Owen, 2004; Zgaljardic et al., 2006; Tinaz et al., 2008).
To further investigate the origin of these motor and cognitive deficits in patients with PD, event-related potentials (ERPs) and reaction time tasks have been used. Previous studies found abnormal movement-related cortical potentials (MRCPs) as well as abnormal ERPs and reaction times during cognitive tasks in patients with PD. Two MRCPs that are reduced in amplitude in patients with PD are the readiness potential (Dick et al., 1989; Vieregge et al., 1994; Cunnington et al., 1995; Jahanshahi et al., 1995) and the contingent negative variation (CNV) (Wright et al., 1993; Praamstra et al., 1996). The readiness potential is a slow negative potential occurring 1-2 s prior to self-paced movements generated by the primary and supplementary motor areas (SMA). The CNV is a slow negative potential which develops in the interval between a warning stimulus and a target stimulus and reflects motor preparation as well as cognitive processes (Rohrbaugh et al., 1976; Elbert et al., 1994). The CNV is thought to be generated by the supplementary motor area (SMA), anterior cingulate, thalamus and bilateral insula (Nagai et al., 2004).
Reaction times and ERPs in cognitive task studies showed that patients with PD have problems retaining covert attention (Wright et al., 1993; Bennett et al., 1995; Yamaguchi et al., 1998) and exhibit abnormalities in stimulus analysis (abnormal P300) (Bennett et al., 1995; Poceta, 2006).
Recently ERP studies have shown that directing attention and movement preparation produce similar frontocentral and occipitotemporal lateralized ERPs (L-ERPs) (Verleger et al., 2000; Praamstra et al., 2005; Eimer et al., 2005). During a cue-target task, in which a first stimulus (cue) gives information about the location of the second stimulus or about the response appropriate to the second stimulus (target), a lateralized frontocentral negativity and a lateralized occipitotemporal positivity have been found. The frontocentral L-ERP is named anterior

directing-attention negativity (ADAN) and the occipitotemporal L-ERP is called late directing-attention positivity (LDAP). ADAN and LDAP have been suggested to originate in the lateral premotor cortex and lateral occipital cortex respectively (Praamstra et al., 2005).

To investigate the spatial attention and motor deficits in PD in more detail and to investigate the role of the basal ganglia in attention and motor processes we intend to perform the same attention and motor task as Praamstra et al. (2005) performed in healthy subjects, but now in patients with PD and older healthy controls. Attention related L-ERPs in patients with PD have only be studied by Yamaguchi and Kobayashi (1998), while ADAN and LDAP during motor intention tasks have not been studied in patients with PD. They reported absence of L-ERPs in the frontocentral area in patients with PD during a covert attention task. The major difference in the attention task between the study of Yamaguchi and Kobayashi and the study of Praamstra et al. is the fact that in the first study the response is always given with the right index finger, while in the second study the response is given by left or right index finger and the side is determined by the target. This assures that no lateralized motor preparation occurs during the cue-target interval of the attention task. On the other hand, this approach possibly makes the task more difficult to perform, especially for patients with PD. In this study we tested if patients with PD and older subjects were able to perform the task.

Furthermore, in contrast to the study by Yamaguchi and Kobayashi that did not report problems with eye saccades, three studies that investigated ADAN and LDAP in a covert attention task with healthy young subjects mentioned that some of the subjects were excluded, because of too many horizontal eye movements towards the cued side (Nobre et al., 2000; Eimer and van Velzen, 2002; van der Lubbe et al., 2006). Apparently some subjects have difficulties with directing attention and at the same time maintaining their eyes focused on a central fixation point. However, for estimation of ADAN and LDAP during a covert attention task it is important that saccades are suppressed. Firstly, saccades would affect task performance, because covert attention requires suppressing of saccades. Furthermore, saccades can affect the EEG signal due to volume conduction, particularly on the frontal electrodes, where the ADAN can be found (Kennett et al., 2007). Because saccades also change the task performance (from covert attention to overt attention), it is not advisable to use eye movement correction methods, such as principal component analysis (PCA) (Lins et al., 1993; Lagerlund et al., 1997), independent component analysis (ICA) (Vigario, 1997), regression (Gratton et al., 1983; Elbert et al., 1985) or source localization (Berg and Scherg, 1994) to remove the electrooculogram (EOG) from the EEG signal.

Another method to remove eye movement artifacts is by rejecting trials with large horizontal EOG (HEOG) deviations. Kennett et al. (2007) showed that after applying this method to healthy young subjects only small residual gaze shifts can remain that have only a limited effect on the amplitude of ADAN. However, remov-

ing trials also reduces the signal-to-noise ratio (SNR) and should thus be limited. It is unclear if older subjects and patients with PD are able to suppress eye movements in the attention task used by Praamstra et al. It has already been reported that patients with PD have more difficulties than control subjects to suppress eye movements in a Simon task (Praamstra and Plat, 2001) and have difficulties with suppressing reflex saccades in an antisaccade task (Kitagawa et al., 1994; Crevits and De, 1997; Chan et al., 2005; Amador et al., 2006). Furthermore, as the tasks are expected to be more demanding for patients with PD than for healthy controls, eye movement suppression may be even more difficult.
In this study, we investigated whether the protocol used by Praamstra et al. is feasible to investigate attention-related and movement-related lateralized potentials in patients with PD and older subjects and in particular, whether they are able to suppress saccades. Furthermore, we investigated whether ADAN and LDAP are observable in older subjects and patients with PD. We used 128-channel EEG recordings, which enables us to compare ERP and L-ERP topographies between patients and controls in more detail.
When performing group analyses of ERPs or L-ERPs it is very important to use the same analysis for all subjects. Therefore, it is usually recommended to perform the same automatic artefact rejection over all subjects. However, the quality of data can be very different between subjects, which makes manual artefact rejection appealing. After all, the goal is to obtain reliable data of as many subjects as possible. In this study, we have attempted to apply automatic artefact rejection. Subsequently, we investigated the effect of manual eye movement rejection with fixed criteria and of individual artifact rejection.

8.2 Materials and methods

The data for this study has been collected at the Behavioural Brain Science Center at the University of Birmingham between May and July 2007.

8.2.1 Subjects

Eleven patients (10 male: age 62.1 $\pm$ 4.4 years) with a clinical diagnosis of Parkinson's disease according to the UK Parkinson's Disease Society Brain Bank (Hughes et al., 1992) and twelve age- and gender matched healthy control subjects (10 male: age 63.7 $\pm$ 5.7 years) participated in this study. All participants gave informed consent and the study was approved by the local ethical committee. Two patients were left handed. All patients used Parkinson medication (Table 8.1). Disease duration ranged between 2 and 10 years. Patients were tested after overnight withdrawal (>10 hr after medication) and their motor performance was tested in this state, using the Unified Parkinson's Disease Rating Scale (Lang and Fahn, 1989) (mean 31.9 $\pm$ 6, range 22-41).

Table 8.1: Patient characteristics

Pt	age (years)	Sex	Disease duration (years)	UPDRS[1]	daily medication
1	57	m	4	33	L-Dopa 300 mg
2	67	m	7	41	L-Dopa 800 mg, Entacapone 800 mg
3	64	m	8	32	L-Dopa 300 mg, Ropinirol 21 mg, Selegiline 10 mg
4	65	m	4	23	Pramipexol 0.75 mg
5	67	m	10	37	L-Dopa 400 mg, Pramipexol 3 mg
6	60	m	6	22	Pergolide 3.75 mg
7	59	m	8	31	L-Dopa 800 mg Entacapone 600 mg
8	56	m	2	33	Ropinirol 6 mg
9	64	f	5	36	L-Dopa 450 mg
10	62	m	6	28	L-Dopa 450 mg, Ropinirol 16 mg
11	57	m	2	24	L-Dopa 300 mg, Selegiline 10 mg

Pt = patient number; f = female; m = male
[1] Unified Parkinson's Disease Rating Scale (UPDRS: off medication for at least 10 h)

8.2.2 Tasks

The experiments consisted of three attention/response precueing tasks, each consisting of three blocks of 80 trials preceded by a practice block of 50 trials. The trial structure was the same in each task. Throughout each trial, two square boxes were displayed in the left and right lower quadrant of the computer screen. In these boxes the target stimuli appeared. At the start of each trial, a centrally presented directional cue (left or right pointing arrow) or a nondirectional cue (overlapping arrows pointing in opposite directions) was presented. The directional cue pointed to the left or right box with equal probability. After a cue-target interval of 1000 ms, a target appeared in one of the two boxes or in both boxes. Participants had to make a manual response to the target stimulus as quickly and accurately as possible, according to instructions set out for each task. The three tasks differed in the directional information provided by the cue (Fig. 8.1). The order of the tasks was counterbalanced across subjects.

Attention task

The arrow cue is directed to the hemifield, in which the target stimulus will appear. The subsequent target stimulus is an arrow in one of the two boxes directed to the left or to the right, requiring a response with the left or right hand, respectively. The cue was valid in 90% of the trials.

Neutral Task

A nondirectional cue was presented by overlaying left and right arrows. The subsequent target stimulus appeared with equal probability in the left or right hemifield

and consisted of an equiprobable left or right pointing arrow, requiring a left or right hand response, respectively.

Motor task

The same arrow cue as in the attention task instructed here to select and prepare a left or right hand response. There was no need to direct spatial attention, as the imperative stimulus was identical on both sides. The target stimulus was a set of horizontal lines and indicated that the prepared response could be initiated. Ten percent of all trials were Nogo trials, in which the stimulus consisted of vertical lines on both sides.

The stimuli were presented on a computer monitor in white on a gray background. The brackets surrounding the cue, enclosing a square of $0.75° \times 0.75°$ of visual angle, were displayed permanently and served as fixation signal. The boxes had a size of $1.0° \times 1.0°$ and the horizontal distance between both boxes was 2.5°. The vertical separation between the position of the cue and imperative stimulus was 1.5°. Cues and targets were displayed for 200 ms.
During the experiment subjects were seated upright in a comfortable armchair, with their eyes 100 cm from the monitor. Responses were made by pressing a button underneath the left or right index finger. The subject was asked to keep his/her eyes focused on the fixation point during the complete block. In the attention task, they were further instructed to direct their attention to the cued location without moving their eyes.

8.2.3 Electrophysiological recordings

EEG was recorded continuously with Ag/AgCl electrodes from 128 standard locations according to the 10-5 extension of the international 10-10 electrode system (American Electroencephalographic Society, 1994; Oostenveld and Praamstra, 2001). Electrodes were mounted in a nylon cap. Eye movements were monitored by bipolar horizontal and vertical EOG derivations. EEG and EOG signals were amplified with a band-pass of 0-128 Hz by BioSemi Active-Two amplifiers (Biosemi, Amsterdam, The Netherlands) and sampled at 512 Hz.

8.2.4 Electrophysiological analyses

During off-line visual inspection of the raw data, EEG channels with many artifacts that would affect the averaged signal were removed. Since these channels were positioned on the outer layer of the electrode cap and thus didn't contribute to the CNV, ADAN or LDAP, they were not interpolated. Next, the continuous EEG recordings were off-line segmented in epochs from 500 ms before cue-onset to

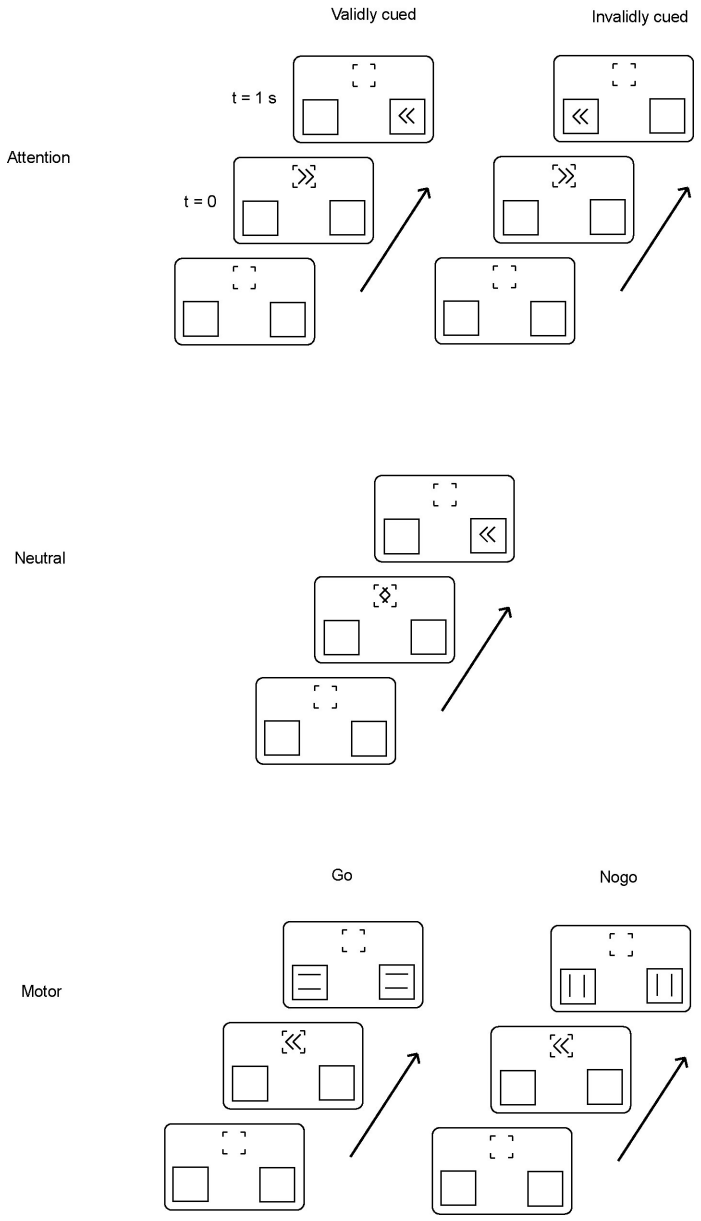

Figure 8.1: Trial structures. Cue-target interval was 1000 ms. Both cue and target stimuli were presented for 200 ms.

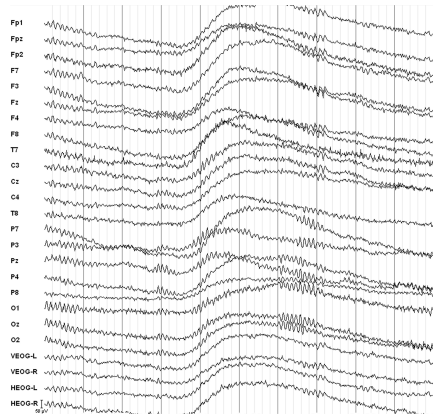

Figure 8.2: Drifts during EEG recordings.

2000 ms after target-onset. Subsequently, automatic artifact rejection, manual eye movement rejection and individual correction were performed.

Automatic artifact rejection

Since some subjects suffered from drifts in the EEG signal (Fig 8.2), automatic artifact rejection started with the rejection of trials in which the max-min amplitude exceeded 250 μV in at least one of the EEG signals. Individual trials with eye blinks and large eye movements were removed by excluding trials in which VEOG or HEOG exceeded 150 μV. Trials were removed for individual channels when the maximum difference within a trial exceeded 120 μV.

Manual eye movement rejection

After the automatic artifact rejection small horizontal saccades were still present in the majority of the datasets. Horizontal saccades are characterized by block shifts in the HEOG channel (Fig. 8.3). We manually removed trials with HEOG block shifts in the cue-target interval that exceeded $\pm$ 30 μV and that had a duration of at least 100 ms. A deviation of 30 μV is thought to equate approximately $\pm$ 2.5°.

Individual correction

Subsequently, we performed additional or adapted artifact rejection procedures in some individuals, depending on the quality of the data after the previous artifact rejection procedures.
Individuals were excluded if the averaged HEOG signal difference between left and right cue trials exceeded 4 μV within the cue-target interval or if more than half of the trials were removed by artifact rejection.

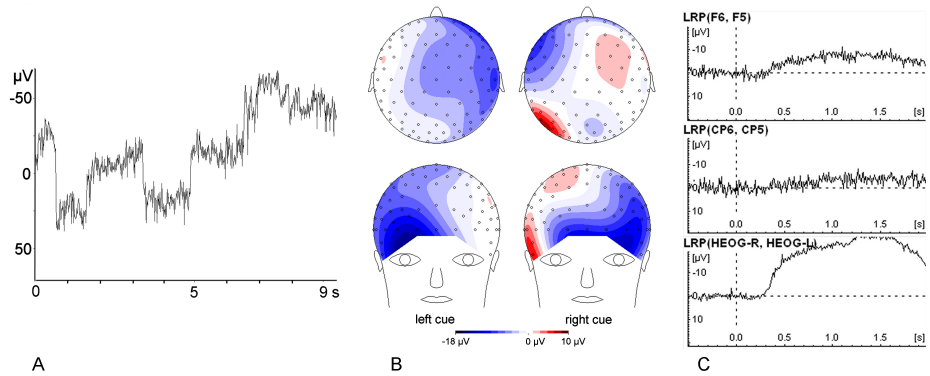

Figure 8.3: Example of eye movement artifact in a patient with PD. A: saccades in horizontal electrooculogram (HEOG) channel. B: topography of ERP. The lateralized frontal negative field is mainly caused by eye movements. C: L-ERP derivations obtained by subtracting ipsilateral from contralateral activity for both cue directions. A large deviation after 300 ms is observable in the F6/F5 derivation due to eye movements. The deviation is consistent with the onset of deviation in the HEOG L-ERP derivation.

In this study, we are interested in movement-related and attention-related lateralized potentials that occur between cue and target presentation. Therefore, for each task separately we averaged the remaining trials with the same cue except for the neutral task, in which trials were averaged per target side, since cues are the same over all trials. In this way ERPs were obtained. ADAN and LDAP were determined by calculating the difference potentials between homologous electrodes contra- and ipsilateral to the side of movement or attention and by subsequently averaging these difference potentials associated with left and right cue conditions.

8.2.5 Behavioural analyses

Performance was evaluated in terms of reaction time and accuracy. Reaction times were measured from the onset of the target until the response. Reaction times exceeding mean +/- 2.5 standard deviation within the subject were excluded. Reaction times were compared between subjects, between tasks and within tasks. Data were evaluated with repeated measures ANOVAs and posthoc t-tests (2-sided) with Bonferroni corrected significance levels.

8.2.6 Grand average ERP analyses

For each EEG artifact rejection step, we counted the number of subjects that did not meet our criteria of HEOG deviation and number of trials. Subsequently we made grand averages of the ERP and L-ERP for each group from the data obtained after all artifact rejection procedures. Because many patients had to be excluded

due to eye movement or artefacts in the EEG, statistical analysis on the EEG data was not possible.

8.3 Results

The task appeared to be very difficult for the subjects, especially for the patients. For one patient the motor and attention tasks were too difficult, since he made too many errors (> 20%) and after some trials he got confused and forgot the task he had to perform. Another patient showed too many horizontal saccades towards the direction of the arrow cue, which was already obvious during the recording. One recording of a healthy subject failed due to large drifts in EEG signals during the entire recording. These subjects were excluded for further analysis.

8.3.1 Reaction times and error rates

Reaction times (Table 8.2) were compared between tasks and groups with ANOVA. Reaction times were significantly different between tasks [$F(1.53, 27.51) = 52.40$, $p < 0.001$]. There was no difference in reaction time between the neutral and attention task [$t = -1.52$, $p = 0.14$], which is consistent with findings in young healthy subjects (Praamstra et al., 2005). There was no group effect [$F(1, 18) = 1.929$, $p=0.182$] or interaction effect of task and group [$F(1.53, 27.51) = 2.613$, $p = 0.103$].
Within tasks, reaction times were significantly faster when target side and response side were the same than when they were different, both in the neutral task [$F(1,18) = 153.49$, $p < 0.001$] and in the attention task [$F(1,18) = 70.66$, $p < 0.001$]. These results are in agreement with a previous study performed in young healthy subjects (Praamstra et al., 2005). There was no interaction effect of group and stimulus-response congruency for the neutral task [$F(1,18) = 2.41$, $p = 0.138$] nor for the attention task [$F(1,18) = 0.450$, $p = 0.51$].
Furthermore, subjects made more errors when stimulus side and response side were different in both the neutral task [$F(1,18) = 36.69$ $p < 0.001$] and the attention task [$F(1,18) = 10.66$, $p < 0.005$]. In the neutral task patients made significantly more errors than controls [$(F(1,18) = 122.26$, $p < 0.001$], which was not the case for the attention task [$(F(1,18) = 2.46$, $p = 0.134$].

8.3.2 Artefact rejection

Automatic artefact rejection

After the automatic artefact rejection step, in which we removed large drifts, eye blinks and large eye movements still nine patients and two healthy subjects exceeded the average HEOG criteria of 4.0 μV in at least one of the tasks, because of

Table 8.2: Mean ± sd of reaction times (ms) and error rates (%) in the healthy control group and patient group.

Task	Cue direction/ Target location	response side		controls		patients	
Neutral	Target left	left	RT	592.8	± 123.6	634.7	± 86.0
			error	1.9	± 2.0	2.4	± 3.0
	Target right	left	RT	652.6	± 129.9	697.3	± 90.9
			error	3.3	± 2.2	5.8	± 2.7
	Target right	right	RT	552.1	± 90.0	639.6	± 140.2
			error	1.0	± 0.9	2.1	± 1.5
	Target left	right	RT	615.0	± 96.9	734.8	± 148.2
			error	3.8	± 2.9	5.8	± 2.5
Motor	Cue left	left	RT	492.5	± 101.3	503.3	± 62.5
			error	4.8	± 3.0	4.8	± 3.0
	Cue right	right	RT	501.8	± 97.9	539.4	± 172.6
			error	4.1	± 1.4	5.2	± 3.0
Attention	Cue left	left	RT	587.1	± 107.5	647.3	± 77.7
			error	1.5	± 1.2	1.9	± 1.1
	Cue right	left	RT	650.4	± 131.1	715.2	± 105.9
			error	3.2	± 2.8	4.2	± 2.8
	Cue right	right	RT	562.9	± 86.7	678.7	± 173.7
			error	1.5	± 1.0	2.3	± 1.4
	Cue left	right	RT	630.6	± 119.8	764.5	± 160.3
			error	3.1	± 3.3	3.8	± 2.4

RT = reaction time; error = error rate.

too many saccades in the direction of the arrow cue after the cue was presented. In one patient and two healthy subjects too many trials (more than half of the trials) were removed in at least one task by these procedures (Table 8.3).

Eye movement rejection

To remove remaining eye movements, manual eye movement artefact rejection was performed. All trials with HEOG saccadic deviations exceeding ± 30 μV were removed. After this procedure still seven patients and one healthy control exceeded the average HEOG criteria of 4.0 μV in at least one of the tasks.

Individual artefact rejection

Hence, we performed additional individual artefact removing procedures to increase the number of subjects and to remove artefacts still present in the data. In two healthy controls and one patient drifts affected the ERP and L-ERP. Therefore, we removed these drifts manually by removing all trials with slow drifts exceeding 30 μV/s. However, this resulted in too few trials (less than half of all trials) for these subjects.
One patient had too few trials due to a tremor in the face, which caused artefacts in the VEOG channels and a large number of rejected trials in the automatic protocol.

Table 8.3: Quality of remaining data after each artefact rejection procedure for all subjects and all tasks.

	Step 1 automatic			Step 2 manual eye movement			Step 3 individual artefacts		
	A	M	N	A	M	N	A	M	N
Pt									
1	eye	eye							
2	eye	eye		eye	eye		eye	eye	
3	eye	eye		eye,trial	eye		eye,trial	eye	
4		eye			eye			eye	
5	eye			eye			eye		
6	too many saccades already visible during recording in attention and motor task								
7	too many errors in motor and attention task								
8	eye	eye,drift			eye,drift			eye,trial	
9	trial,eye	trial,eye	trial	trial,eye	trial,eye	trial	trial,eye	trial,eye	
10	eye	eye		eye	eye		eye	eye	
11		eye							
Hc									
1									
2	too many drifts in EEG recording								
3						trial			
4			drift			drift			trial
5	eye	eye	eye	eye	eye	eye	eye	eye	eye
6		eye							
7		drift			drift			trial	
8	trial		trial	trial		trial			
9									
10									
11	trial			trial					
12									

Pt = patient number; Hc = healthy control number.
A = Attention task; M = motor task; N = neutral task.
eye = average HEOG difference left cue versus right cue > 4.0 μV.
trial = more than half of the trials removed, drift = drift in ERP/L-ERP.

We therefore changed the VEOG threshold from 150 μV to 185 μV. However, this subject still had a too large HEOG difference between left and right cues.
One healthy subject had too few trials due to eye blinks. These eye blinks occurred mainly after the target presentation. Therefore, we performed eye blink correction semi-automatically instead of automatic eye blink correction. We searched for trials that exceeded the threshold and in case the blink or eye movement shift appeared after target presentation we did not remove the trial.
Another healthy subject had many drifts on the mastoid reference electrodes, which caused rejection of too many trials in the automatic artefact rejection procedure. Therefore, we changed the reference electrodes in this subject to TP7 and TP8. Yet, of all subjects, only two patients and eight healthy controls met our criteria. This low remaining number of subjects, in particular in the patient group, makes statistical comparison of both groups impossible.

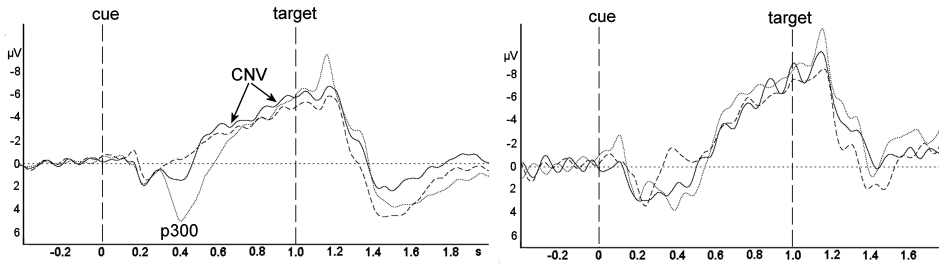

Figure 8.4: Grand average ERPs of the control group (left) and patient group (right) at electrode Pz pooled with its four neighbour electrodes (CPP1h, CPP2h, PPO1h and PPO2h). solid line = attention task, dotted line = motor task, dashed line = neutral task. For display purposes ERPs have been filtered with a low-pass filter of 10 Hz.

8.3.3 ERP

Figure 8.4 shows the grand average ERPs of the healthy subject group (8 subjects) and patient group (2 patients) for the different tasks. For both groups P300 was maximal in the motor task and was not present in the neutral task. The CNV of both groups was of similar amplitude.

8.3.4 L-ERP

We also investigated the lateralized ADAN and LDAP. The ADAN and LDAP could not be detected in the patient group, because of low signal to noise ratio (SNR). Therefore, topographic mappings and L-ERPs are only shown for the healthy control group (Fig. 8.5). In the healthy control group we found ADAN in the motor task, while in the attention task this L-ERP could not be detected. LDAP could not be observed in the healthy controls possibly due to a low SNR.

8.4 Discussion

In this study, we investigated if recording of attention-related and movement-related lateralized potentials using the protocol reported by Praamstra et al. (2005) in patients with PD and older subjects is feasible. In particular, we studied whether patients with PD were able to suppress their eye movements. In addition, we investigated whether ADAN and LDAP are observable in older subjects and patients with PD.

Eight out of eleven patients had major difficulties controlling their eye movements during the attention and motor task, while this was only the case in one age-matched control subject. In these tasks the patients made many saccades towards the direction where the arrow cue was pointing to, directly after the cue was presen-

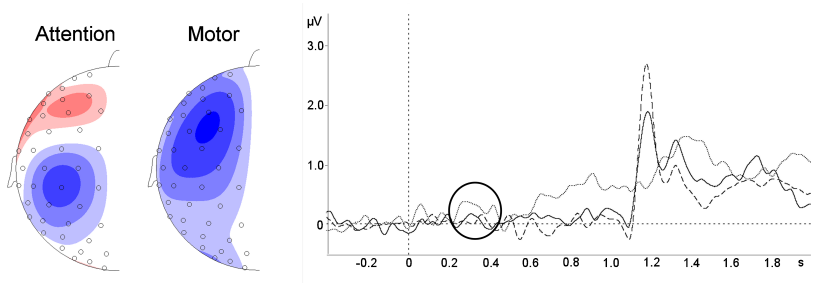

Figure 8.5: Left: Topography of the ADAN for the healthy subjects in the attention and motor task. The topography is based on the interval between 250 and 350 ms. Right: The L-ERP graph is generated from pooled electrode pairs (F1/F2, F3/F4, FC3/FC4, FCC1h/FCC2h, FCC3h/FCC4h, FCC5h/FCC6h). ADAN is visible around 300 ms in the motor task. Solid line = attention task, dotted line = motor task, dashed line = neutral task. For display purposes L-ERPs have been filtered with a low-pass filter of 10 Hz.

ted. Even after manual rejection of eye movement artefacts, these patients had an average HEOG difference between left cue and right cue that exceeded 4 μV. Probably, eye movements were small, but present in many trials. These eye movements were not only present in the attention task, but often also in the motor task. In the motor task, however, directing attention was not needed, since the stimulus appeared on both sides. According to these findings, patients with PD move their eyes not (only) because of the task to direct attention, but also as a direct response to the arrow cue. The large amount of eye movements might be due to the fact that the tasks are more difficult for patients compared to age-matched controls, which is confirmed by the larger number of errors in the patient group. One patient was even excluded, because the task was too difficult (errors $> 20\%$ and after some trials he got confused and forgot the task he had to perform). Because of the difficulty of the tasks, patients might be less focused on inhibiting their eye movements.

This hypothesis is supported by the fact that Yamaguchi and Kobayashi (1998) reported no problems with eye saccades in a task that is possibly easier to perform. However, the absence of saccades in their study could also be related to the medication that was used by their patients, while in our study patients were tested after overnight withdrawal.

If the difficulty of the tasks is one of the causes for the large eye movement artefacts, these artefacts might be reduced by increasing the cue-target interval, by increasing the presentation time of cue and target or by enlarging the stimuli. In this way, the task is possibly easier to perform for the patients with PD.

On the other hand, patients with PD might in general have problems to inhibit reflexive saccades. It was long believed that predictive central arrows only generate volitional behaviour and that non-predictive peripheral cues only generate reflexive behaviour. However, recent studies suggest that also reflexive behaviour

is generated by central arrows cues as well (Hommel et al., 2001; Tipples, 2002; Ristic and Kingstone, 2006). Furthermore, Fielding et al. (2006) already showed that patients with PD made more reflex saccades in the direction of a peripheral cue compared to age-matched healthy controls, even when they were instructed to fixate on a central fixation point. The saccades in our patients start after approximately 300 ms (Fig. 8.3) which corresponds with the latency found in reflex saccade tasks of patients with PD (Briand et al., 1999; Kingstone et al., 2002; Chan et al., 2005; Hood et al., 2007). Therefore, we hypothesize that the saccades made by the patients in this study might partly be reflex saccades, which could not be suppressed.

If the saccades made by the patients with PD were reflex saccades, these saccades might be absent when using letter instead of arrow cues, since letters are thought to only generate volitional saccades. Letter cues have been used previously in a cue-target task by Praamstra et al. (1996) to investigate the CNV and lateralized readiness potential (LRP) and they reported no difficulties with saccades in patients with PD. However, based on a previous study by Eimer et al. (1995) it might be the case that the ADAN is only elicited by reflexive attention shifts. In that study, they found no ADAN when colours were used as cue instead of arrows and colours are thought to only generate volitionally attention shifts. Similar to the colour cues, letters are thought to only generate volitional attention shifts, which would possibly result in no ADAN.

Before averaging ERP trials, it is common to remove trials with artefacts. In general, automatic artefact rejection is favourable, because this results in the same analysis for all subjects. In this study, we have attempted to apply automatic artefact rejection to remove drifts, eye blinks, large eye movements and other artefacts. However, automatic artefact rejection excluded some subjects unnecessarily. For example, one patient in our study had a tremor in the face, which resulted in large EMG artefacts in mainly the EOG channels. Consequently, the EOG artefact rejection removed extra trials and less than half of the trials were left. In another subject more than half of the trials were rejected, because of eye blinks. However, most eye blinks occurred after the target was presented and did not influence the L-ERPs of our interest. On the other hand, two subjects were not excluded, even though their L-ERPs and ERPs were affected by drift artefacts. These drifts are possibly cephalic skin potentials (Picton and Hillyard, 1972). In addition, many subjects still had a considerable number of eye movements after this trial rejection procedure.

Therefore, we performed additional eye movement artefact correction. Accurate automatic rejection of eye movements is difficult, since the SNR ratio of the HEOG channels is too high to remove all trials with eye movements with an automatic rejection that uses a threshold for maximum deviation without removing other trials. In addition, ERP signals and drifts might also be present in the HEOG channels that can cause rejection of additional trials. Therefore, eye movements

can sometimes be better detected by visual inspection. In this study, we manually removed trials with block shifts in the HEOG channel that exceeded 30 μV. Previous studies that investigated ADAN and LDAP in younger healthy controls removed trials, when HEOG deviation exceeded 30 μV relative to baseline (Eimer et al., 2002; van Velzen et al., 2006). However, due to drifts in the HEOG channel and possible ERP contribution to the HEOG signal this was not possible in our analysis. In these previous studies, subjects were excluded if the average HEOG deviation exceeded 2 or 3 μV. Since in some of our subjects drifts were present, we used a more lenient criterion and excluded subjects if the difference in averaged HEOG between left and right cue trials exceeded 4 μV. This criterion was also used by others (Eimer et al., 2002; Eimer and van Velzen, 2002; van Velzen et al., 2002). In this way, subjects with drifts on HEOG channels were not excluded, since drifts were similar for left and right cue trials. Accordingly, depending on the data, manual artefact rejection might sometimes be desirable. However, when performing manual artefact rejection, it is advisable to use fixed criteria. In this way, artefact rejection is not subjective and results are always reproducible.
Due to eye movements we excluded eight out of eleven patients for analysis of ERPs and L-ERPs. Another patient was excluded, because of too many errors in the attention task and motor task. The small number of patients makes reliable comparison with age-matched controls impossible. Therefore, we only shortly discuss the L-ERP results in the control group. ADAN was present in the healthy control group during the motor task. However, in the attention task no ADAN could be observed. Furthermore, compared to the study of Praamstra et al. (2005) with healthy young subjects, where ADAN occurred around 400 ms after cue presentation, ADAN in our older subjects arose around 300 ms and preceded the P300. It remains unclear why ADAN appeared earlier in the older subjects. A possible explanation may be the small differences between used protocols.
The reaction times were not significantly different between both groups, but we found different error rates for the neutral task. Previous studies with comparable tasks found slower (Wright et al., 1993; Yamaguchi et al., 1998) as well as similar reaction times (Bennett et al., 1995) in patients with PD compared to healthy controls. However, in our study the patients showed considerably more eye movements compared to healthy controls. This might have influenced the reaction times of the patients. Therefore, it might be better to remove all trials with eye movements, but this would lead to an enormous reduction of trials and to even more variable results.
In conclusion, this study showed that patients with PD have problems with controlling their horizontal eye movements during a visuospatial attention and motor task, in which an arrow cue is presented. Even after manual rejection of eye movement artifacts, the HEOG deviation of these patients exceeded the threshold used as rejection criteria. These eye movements probably affect the ADAN in two ways. First of all, eye movements affect the EEG, especially on the lateral frontal side,

where ADAN can be found. In addition, due to eye movements, lateralization of spatial attention might be reduced resulting in smaller ADAN amplitude.
There may be at least two causes for the abundance of horizontal eye movements in patients with PD. They may experience the task as more difficult than healthy subjects. In addition, patients with PD might in general have problems to inhibit reflexive saccades due to dysfunction of the basal ganglia (Fielding et al., 2006).
For future studies with patients with PD we recommend to use a longer presentation time of cue and target, larger stimuli and a longer cue-target interval. In this way, the task is possibly easier to perform for the patients with PD. Furthermore, one could perform the task in patients with shorter disease duration, who are less affected.

9

Summary

EEG is a non-invasive technique that can be used to measure the electrical activity produced by nerve cells in the brain using electrodes placed on the scalp. A disadvantage of EEG compared to other techniques such as CT, MRI, SPECT and PET is its low spatial resolution, which may be a cause of the limited number of clinical applications. However, with the development of multichannel EEG systems ($>$ 64 electrodes) around 1990 spatial resolution has increased considerably. So far, multichannel EEG has been used mainly for fundamental research (Huber et al., 2004; Jackson et al., 2004; Massimini et al., 2004; Sabbagh et al., 2004; Pae et al., 2003; Ruchsow et al., 2003; Youn et al., 2003; Praamstra et al., 2005). In contrast to what may be expected of a technique that has demonstrated its value in diagnostic neurology when using a few electrodes, only a limited number of studies report clinical neurological applications of multichannel EEG (Elting et al., 2005; Lantz et al., 2003a,b; Michel et al., 2004a). The aim of this thesis is to develop new clinical applications of multichannel EEG, in particular evoked potentials (EPs) and event related potentials (ERPs), by introducing new analysis techniques.

A standard clinical analysis technique for EPs and ERPs is estimating peak amplitudes and latencies. In chapter 2 an overview is given of other analysis techniques in the time domain as well as in the frequency domain. So far, analysis techniques such as wavelet analysis and single trial analysis have only been used for fundamental research. However, these techniques might also be clinically useful.

In chapter 3 an overview is given of the wide range of source localization techniques that require multichannel recordings. These methods are mainly used for fundamental research as well, whereas they may also be clinically relevant. As mentioned in the introduction source localization has only been used clinically for localization of epileptogenic lesions and diagnosis and quantification of cognitive disorders after acute brain injury. However, source localization techniques may also be used to separate E(R)P components that overlap in time. In this way, latencies and amplitudes of overlapping components may be determined more accurately, which may result in less variable components.

In contrast to latency, E(R)P amplitude has hardly been used for diagnostic purposes, probably because of its large variability among healthy subjects and patients. Usually, only extremely high peaks or absent peaks are defined as abnormal. The

variety among healthy subjects might be due to a combination of anatomical variation and the limited number of electrodes used on specific positions. In chapter 4 we investigated whether 128-channel recordings reduce the intersubject amplitude variability of median nerve somatosensory EPs (SEPs). Peak amplitudes of the 128-channel recordings were obtained by combining butterfly plots (potential plot, in which all channels are superimposed) and potential maps to find the location at which the SEP peak amplitude is maximal. We showed that the position of maximum peak amplitude varies enormously among subjects and that the 128-channel recordings can estimate peak amplitude more accurately than conventional recordings with a limited number of electrodes. Therefore, the 128-channel amplitude estimate might be more sensitive to pathological changes. Furthermore, we estimated normal values and found that there was no significant effect of age on SEP amplitude.

In chapter 5 we introduced a new 128-channel technique to quantify interhemispheric symmetry and applied this method to median nerve SEPs of healthy subjects. This method compares left and right stimulated SEPs by calculating the intraclass correlation coefficient (ICC) of the global field powers (GFPs) of left and right median nerve SEP. GFP is a quantity for the total amount of activity over all electrodes at each timepoint. In this way, the similarity of median nerve SEP activity patterns is quantified without being sensitive for small interhemispheric differences in position and orientation of sources. We showed that this measure is appropriate for quantifying SEP interhemispheric symmetry. In contrast to what is usually thought, we found less symmetric SEPs even in a number of healthy subjects, which were due to differences in amplitude, absence of a peak or shape differences. We found no correlation between age and this measure of symmetry. This technique can be useful for detection of unilateral abnormalities in somatosensory cortical processing.

In chapter 6 the methods introduced in chapters 4 and 5 are applied to SEPs of patients with different parkinsonian disorders to investigate if these techniques can be used as a diagnostic tool. Clinical practice shows that the differential diagnosis of parkinsonian disorders, such as Parkinson's Disease (PD), progressive supranuclear palsy (PSP) and corticobasal ganglionic degeneration (CBGD), can be difficult, especially in an early stage of the disease. Previous studies with a limited number of electrodes already found small abnormalities in median nerve SEP in different parkinsonian disorders. However, so far these abnormalities were too small or present in a too few patients to be clinically useful. This chapter shows that even with our 128-channel method only a few patients with CBGD had abnormally asymmetric SEPs. In addition, similar abnormalities were found in patients with other parkinsonian disorders. As a result, SEP symmetry had a low sensitivity and specificity for differentiating CBGD from other parkinsonian disorders. Furthermore, SEP amplitudes obtained with 128-channel recordings also had a low sensitivity and specificity and therefore cannot contribute to the differential diagnosis of parkin-

sonian disorders either.
Another SEP recording that is often used clinically is the tibial nerve SEP. It is already known that one of its peaks differs enormously in position among healthy subjects. In chapter 7, we applied the same technique as used in chapter 4 to analyse SEP tibial nerve SEP. Similar to the results of our analysis of median nerve SEP we found large variability in position of maximum tibial nerve SEP amplitude. Accordingly, the 128-channel method also estimates tibial nerve SEP amplitude more accurately than recordings with a limited number of electrodes. Furthermore, we found that in some subjects one of the SEP components (N50) defined with conventional recordings, rather seems to be a period between two activations than an activation on itself.
ERPs have mainly been used for fundamental research. Recently, Elting et al. (2003) showed that when recorded with 128-channels the P300, an ERP generated during a standard oddball task, can improve diagnosis and quantification of cognitive disorders after acute brain injury. The results suggest that other ERPs might be clinically useful as well. A disadvantage of ERPs is that they depend on subject performance. Previous studies in young subjects showed that a movement preparation task and a directing attention task generate partly similar lateralized ERPs (L-ERPs). Since PD is characterized by motor deficits as well as attention deficits, we hypothesized that it would be interesting to investigate these L-ERPs in this patient group. However, the question was whether patients with PD were able to perform the task that generates these L-ERPs. In chapter 8 we showed that patients with PD had many more problems while performing these tasks compared to age-matched healthy controls. Especially, eye fixation was very difficult for these patients probably due to a dysfunction of frontostriatal circuits. Therefore, other easier tasks should be used to investigate these attention and motor related ERPs.

10

Future perspectives

Usually, when a new medical technique is developed, its precise applicability in and value for clinical practice still need to be established, even when its theoretical improvement with regard to existing technologies may be quite obvious. One example of such a (relatively) new technique is multichannel EEG. In this thesis its value for clinical practice and - to a lesser extent - its feasibility in a clinical setting, have been investigated. Even though it is immediately clear that a 64- or 128-channel EEG recording provides much more information than a conventional EEG recording with up to 32 channels, the question remains whether this additional information is clinically relevant. More channels take more preparation time, which is less convenient for the patient, and more channels require a more expensive EEG recording system. Therefore, the main motivation for this thesis has been the question 'Does measuring more mean knowing more?'.

So far, multichannel EEG has only limited clinical neurological applications, as described in more detail in the introduction of this thesis. This might be partly due to the fact that many clinicians have the impression that multichannel EEG may be suitable for research purposes, but is not feasible in clinical practice. However, in the course of the research performed for this thesis and other projects more than 150 128-channel recordings have been performed in our department in patients with various disorders, ranging from movement disorders, to multiple sclerosis, dementia and mild head injury. This experience has learned us that the technique is well suited for recordings in patients, since - when the electrode cap is in experienced hands - preparation time can be limited to 20 minutes (for 64 channels) or 30 minutes (for 128 channels). Furthermore, placing (multichannel) caps is patient friendly and multichannel EEG recordings are cheap compared to imaging methodologies such as (f)MRI. Implementation of 64- or 128-channel EEG recordings therefore seems feasible for any clinical lab that is experienced in conventional EEG recordings.

Although there are only a few clinical applications, multichannel EEG has extensively been used for fundamental research (see introduction). In these studies results are limited to group comparisons, whereas estimates of sensitivity and

specificity are rare, even though high sensitivity and specificity are essential for introducing a technique in clinical practice. In this thesis we developed new analysis techniques for multichannel EPs, aiming at clinical introduction of the techniques. We showed that 128-channel recordings can measure SEP amplitudes more accurately than conventional recordings with only a limited number of electrodes. Theoretically, more accurate amplitude estimation should improve sensitivity and specificity for physiological and pathological changes in SEPs. We applied these techniques to multichannel SEPs obtained in patients with parkinsonian disorders to investigate if the use of these techniques can indeed improve the differential diagnosis. Unfortunately, for this group of patients this multichannel recording and analysis technique did not contribute to the differential diagnosis. Possible causes of this result may be sought at different levels.

First of all, assuming that 128-channel recording is sufficient (based on spatial sampling arguments (Spitzer et al., 1989)), the used analysis technique may not be optimal. Secondly, it is possible that underlying pathology is either not as expected or that the pathological effect of various parkinsonian disorders on SEP parameters is so small that it can not even be measured with 128-channel recordings.

A first possible improvement on the analytical level is to enhance the symmetry measure for application in parkinsonian disorders by calculating separate global field powers for frontal and parietal electrodes. In this way frontal SEP components, which are thought to be abnormal in patients with Parkinson's disease (Mauguière et al., 1993; Bostantjopoulou et al., 2000; Garcia et al., 1995; Rossini et al., 1995), can be investigated separately from parietal components that are thought to be abnormal in patients with corticobasal degeneration (Brunt, 1995; Klodowska-Duda et al., 2006; Carella et al., 1997; Okuda et al., 1998; Monza, 2003; Takeda et al., 1998; Thompson et al., 1994).

On the other hand, for improvement at the recording level, it might be worthwhile to test other SEP protocols, such as double stimulation in which two nerves are stimulated simultaneously or stimulation during hand movements to induce the so-called gating effect (the modulation of sensory information processes during movement). Such protocols resulted in abnormal conventional SEPs in patients with dystonia and hand tremor (Restuccia et al., 2003; Tinazzi et al., 2000). Although our symmetry measure and amplitude estimation did not improve the differential diagnosis of parkinsonian disorders, these techniques can still be useful in other neurological applications. One of the clinical applications of the symmetry measure for multichannel SEPs may be the estimation of sensory impairment in stroke patients as prediction for clinical outcome (Rossini et al., 2003; Huang et al., 2004). The multichannel amplitude technique might also be useful for monitoring disease progression or estimating the effect of medication or surgical intervention in patients with e.g., multiple sclerosis, spinal cord compression, neuropathy, diabetes or amyotrophic lateral sclerosis.

In addition, other signal analysis techniques may be applied to both EPs and ERPs in general and to the SEP and attention and motor-related ERPs in this thesis in particular. For example, wavelet analysis (Chapter 2) might be useful for a more objective description and comparison of E(R)P waveforms. In this way, other features than amplitude and latency of the E(R)P waveform can be extracted and used for clinical purposes.
Furthermore, single trial analysis can be clinically relevant when pathological changes are associated with habituation, fatigue or other sources of intertrial variability. For example, in elderly subjects, it has already been found that the variability of single trial P3a amplitude is increased (Fjell and Walhovd, 2007).
The few existing neurological applications of multichannel EEG are based on source localization. This analysis technique can only be applied to multichannel recordings. As shown by Elting et al. (2006) this technique can differentiate the P3a and P3b peaks obtained with an oddball task. Not only these peaks, but also other peaks that overlap in time and space can possibly be separated using source localization techniques resulting in a better amplitude and latency estimation of the different peaks.
So far, the P300 is one of the few ERPs that is routinely used clinically. Another, less frequently used ERP is the Bereitschaftspotential or readiness potential (Shibasaki and Hallett, 2006). The use of multichannel recordings might increase the possible clinical applications of ERPs. However, while EPs reflect primary stimulus processing and are therefore reliable and easy to interpret, ERPs reflect many different processes and depend on subject attention and effort. Therefore, possibly new paradigms or recording protocols may need to be developed that are reliable and that control subject attention and effort.

Recently, MR-compatible multichannel EEG systems have become commercially available from multiple suppliers. By combining fMRI and EEG, the high temporal resolution of EEG can be combined with the high spatial resolution of fMRI, in principle providing more information about brain functioning than EEG or fMRI alone. So far, this combination has only been used clinically for localizing epileptic seizures. Yet, the combination of these techniques has the potential to be useful for other clinical problems as well. However, fMRI is an expensive technique compared to EEG and has some additional problems related to e.g. reliability of individual recordings. In addition, fMRI can not be performed in all patients, whereas EEG usually can. Thus, although potentially very powerful, much work remains to be done before individual EEG-fMRI recordings may be expected in clinical routine work-up.

Further development of neurological applications of multichannel EEG and EEG-MRI recordings requires close cooperation and considerable effort of neurologists, neurophysiologists and engineers. By using engineering, mathematical and

computational techniques, new developments may be expected in the future that can help solve clinical neurological problems. This thesis provides a step in this direction.

APPENDIX A

Electrode configuration

The 128-channel electrode caps we used for the measurements described in chapters 4-7 have an electrode configuration as given in figure A.1. The position of the electrode cap on the skull is related to anatomical landmarks; the inion, which is the lowest point of the skull on the back of the head and is normally indicated by a prominent bump, and the nasion, which is the point between the forehead and the nose. There are different sizes of the cap. The capsize used depends on the circumference of the head.

Each electrode position is characterized by one or more letters to identify the underlying brain area and a number or letter z to identify the hemisphere. The letters F,T, P and O stand for frontal, temporal, parietal and occipital lobe. The letter C refers to the central sulcus and the letters Fp refer to a prefrontal electrode. Electrodes anterior to the frontal (F) electrodes are named anterior frontal (AF). Electrodes that are positioned between frontal and central electrodes (frontocentral electrodes), central and parietal electrodes (centroparietal electrodes), parietal and occipital electrodes (parieto-occipital electrodes), parietal and temporal electrodes (parietotemporal electrodes) and frontal and temporal electrodes (frontotemporal electrodes) are labeled FC, CP, PO, TP and FT respectively. In a similar way, electrodes between F and FC electrodes are named FFC, etc.

The letter z stands for zero. Electrodes with the letter z are positioned on the midline. Even numbers refer to electrode positions on the right hemisphere, whereas odd numbers refer to those on the left hemisphere.

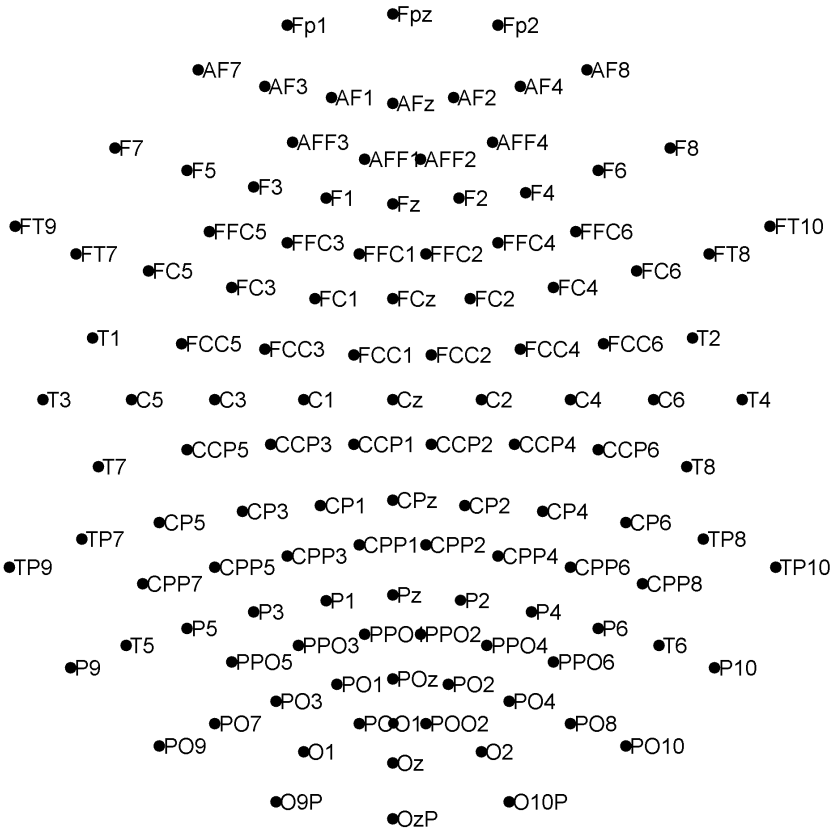

Figure A.1: Electrode configuration of the 128-channel electrode cap used in chapters 4-7. Besides these electrodes one electrode is positioned on each earlobe (A1, A2) and six electrooculography (EOG) electrodes are connected to the electrode cap (two horizontal EOG and four vertical EOG channels). (ten Caat, 2008)

References

Abbruzzese, G., Marchese, R., and Trompetto, C. (1997). Sensory and motor evoked potentials in multiple system atrophy: a comparative study with Parkinson's disease. *Mov Disord.*, 12(3):315–321.

Abbruzzese, G., Tabaton, M., Morena, M., Dall'Agata, D., and Favale, E. (1991). Motor and sensory evoked potentials in progressive supranuclear palsy. *Mov Disord.*, 6(1):49–54.

Amador, S., Hood, A., Schiess, M., Izor, R., and Sereno, A. (2006). Dissociating cognitive deficits involved in voluntary eye movement dysfunctions in Parkinson's disease patients. *Neuropsychologia*, 44(8):1475–1482.

Amunts, K., Jancke, L., Mohlberg, H., Steinmetz, H., and Zilles, K. (2000). Interhemispheric asymmetry of the human motor cortex related to handedness and gender. *Neuropsychologia*, 38(3):304–312.

Andrew, C. (1996). Event-related coherence as a tool for studying dynamic interaction of brain regions. *Electroencephalography and Clinical Neurophysiology*, 98(2):144–148.

Babiloni, F., Babiloni, C., Carducci, F., Fattorini, L., Onorati, P., and Urbano, A. (1996). Spline laplacian estimate of EEG potentials over a realistic magnetic resonance-constructed scalp surface model. *Electroencephalogr.Clin.Neurophysiol.*, 98(4):363–373.

Babiloni, F., Babiloni, C., Fattorini, L., Carducci, F., Onorati, P., and Urbano, A. (1995). Performances of surface Laplacian estimators: a study of simulated and real scalp potential distributions. *Brain Topogr.*, 8(1):35–45.

Babiloni, F., Cincotti, F., Carducci, F., Rossini, P., and Babiloni, C. (2001). Spatial enhancement of EEG data by surface Laplacian estimation: the use of magnetic resonance imaging-based head models. *Clin.Neurophysiol.*, 112(5):724–727.

Başar, E., Demir, N., Gnder, A., and Ungan, P. (1979a). Combined dynamics of EEG and evoked potentials. I. studies of simultaneously recorded EEG-epograms in the auditory pathway, reticular formation, and hippocampus of the cat brain during the waking stage. *Biol Cybern*, 34(1):1–19.

Başar, E., Durusan, R., Gnder, A., and Ungan, P. (1979b). Combined dynamics of EEG and evoked potentials. II. studies of simultaneously recorded EEG-epograms in the auditory pathway, reticular formation, and hippocampus of the cat brain during sleep. *Biol Cybern*, 34(1):21–30.

Başar, E., Schurmann, M., Basar-Eroglu, C., and Karakas, S. (1997). Alpha oscillations in brain functioning: an integrative theory. *Int.J.Psychophysiol.*, 26(1-3):5–29.

Baillet, S. and Garnero, L. (1997). A Bayesian approach to introducing anatomo-functional priors in the EEG/MEG inverse problem. *IEEE Trans.Biomed.Eng*, 44(5):374–385.

Baillet, S., Mosher, J., and Leahy, R. (2001). Electromagnetic brain mapping. *Ieee Signal Processing Magazine*, 18(6):14–30.

Baumgartner, U., Vogel, H., Ellrich, J., Gawehn, J., Stoeter, P., and Treede, R. (1998). Brain electrical source analysis of primary cortical components of the tibial nerve somatosensory evoked potential using regional sources. *Electroencephalogr.Clin.Neurophysiol.*, 108(6):588–599.

Bell, A. and Sejnowski, T. (1995). An information-maximization approach to blind separation and blind deconvolution. *Neural Comput.*, 7(6):1129–1159.

Bennett, K., Waterman, C., Scarpa, M., and Castiello, U. (1995). Covert visuospatial attentional mechanisms in Parkinson's disease. *Brain*, 118 (Pt 1):153–166.

Berg, P. and Scherg, M. (1994). A multiple source approach to the correction of eye artifacts. *Electroencephalogr.Clin.Neurophysiol.*, 90(3):229–241.

Biran, I. and Chatterjee, A. (2004). Alien hand syndrome. *Arch.Neurol.*, 61(2):292–294.

Bland, J. and Altman, D. (1986). Statistical methods for assessing agreement between two methods of clinical measurement. *Lancet*, 1(8476):307–310.

Bostantjopoulou, S., Katsarou, Z., Zafiriou, D., Gerasimou, G., Alevriadou, A., Georgiadis, G., Kiosseoglou, G., and Kazis, A. (2000). Abnormality of N30 somatosensory evoked potentials in Parkinson's disease: a multidisciplinary approach. *Neurophysiologie Clinique/Clinical Neurophysiology*, 30(6):368–376.

Briand, K., Strallow, D., Hening, W., Poizner, H., and Sereno, A. (1999). Control of voluntary and reflexive saccades in Parkinson's disease. *Exp.Brain Res.*, 129(1):38–48.

Brown, G. D., Yamada, S., and Sejnowski, T. J. (2001). Independent component analysis at the neural cocktail party. *Trends in Neurosciences*, 24(1):54–63.

Brunt, E. (1995). Unique myoclonic pattern in corticobasal degeneration. *Movement disorders*, 10(2):132–142.

Buchner, H., Ludwig, I., Veldkamp, R., Willmes, K., and Ferbert, A. (1992). Topography of the early median nerve SEP, results for the diagnostic method in the routine. *Eeg-Emg-Zeitschrift fur Elektroenzephalographie Elektromyographie und Verwandte Gebiete*, 23(4):203–209.

Buchner, H., Ludwig, I., Waberski, T., Wilmes, K., and Ferbert, A. (1995). Hemispheric asymmetries of early cortical somatosensory evoked potentials revealed by topographic analysis. *Electromyogr.Clin.Neurophysiol.*, 35(4):207–215.

Bundick, T., J. and Spinella, M. (2000). Subjective experience, involuntary movement, and posterior alien hand syndrome. *J.Neurol.Neurosurg.Psychiatry*, 68(1):83–85.

Calhoun, V., Adali, T., Pearlson, G., and Pekar, J. (2001). Spatial and temporal independent component analysis of functional MRI data containing a pair of task-related waveforms. *Hum.Brain Mapp.*, 13(1):43–53.

Carella, F., Ciano, C., Panzica, F., and Scaioli, V. (1997). Myoclonus in corticobasal degeneration. *Mov Disord*, 12(4):598–603.

Cassim, F. and Houdayer, E. (2006). Neurophysiology of myoclonus. *Neurophysiol Clin*, 36(5-6):281–291.

Chan, F., Armstrong, I., Pari, G., Riopelle, R., and Munoz, D. (2005). Deficits in saccadic eye-movement control in Parkinson's disease. *Neuropsychologia*, 43(5):784–796.

Chiappa, K. (1997). *Evoked Potentials in clinical medicine*, volume 3. Lippincott-Raven, Philadelphia.

Clochon, P., Fontbonne, J., Lebrun, N., and Etevenon, P. (1996). A new method for quantifying EEG event-related desynchronization:amplitude envelope analysis. *Electroencephalogr.Clin.Neurophysiol.*, 98(2):126–129.

Cornford, M., Chang, L., and Miller, B. (1995). The neuropathology of parkinsonism: an overview. *Brain Cogn*, 28(3):321–341.

Crevits, L. and De, R. K. (1997). Disturbed striatoprefrontal mediated visual behaviour in moderate to severe parkinsonian patients. *J.Neurol.Neurosurg.Psychiatry*, 63(3):296–299.

Cunnington, R., Iansek, R., Bradshaw, J., and Phillips, J. (1995). Movement-related potentials in Parkinson's disease. Presence and predictability of temporal and spatial cues. *Brain*, 118 (Pt 4):935–950.

Darvas, F., Pantazis, D., Kucukaltun-Yildirim, E., and Leahy, R. (2004). Mapping human brain function with MEG and EEG: methods and validation. *NeuroImage*, In Press, Corrected Proof:–.

de Peralta Menendez, R. G. and Andino, S. L. G. (1994). Single dipole localization: some numerical aspects and a practical rejection criterion for the fitted parameters. *Brain Topogr*, 6(4):277–282.

de Peralta Menendez, R. G., Andino, S. L. G., Morand, S., Michel, C. M., and Landis, T. (2000). Imaging the electrical activity of the brain: ELECTRA. *Hum Brain Mapp*, 9(1):1–12.

Delberghe, X., Mavroudakis, N., Zegers de, B. D., and Brunko, E. (1990). The effect of stimulus frequency on post- and pre-central short-latency somatosensory evoked potentials (SEPs). *Electroencephalogr.Clin.Neurophysiol.*, 77(2):86–92.

Desmedt, J. and Bourguet, M. (1985). Color imaging of parietal and frontal somatosensory potential fields evoked by stimulation of median or posterior tibial nerve in man. *Electroencephalogr.Clin.Neurophysiol.*, 62(1):1–17.

Desmedt, J. and Cheron, G. (1980). Somatosensory evoked potentials to finger stimulation in healthy octogenarians and in young adults: wave forms, scalp topography and transit times of parietal and frontal components. *Electroencephalogr.Clin.Neurophysiol.*, 50(5-6):404–425.

Desmedt, J. and Cheron, G. (1981). Non-cephalic reference recording of early somatosensory potentials to finger stimulation in adult or aging normal man: differentiation of widespread N18 and contralateral N20 from the prerolandic P22 and N30 components. *Electroencephalogr.Clin.Neurophysiol.*, 52(6):553–570.

Desmedt, J., Nguyen, T., and Bourguet, M. (1987). Bit-mapped color imaging of human evoked potentials with reference to the N20, P22, P27 and N30 somatosensory responses. *Electroencephalogr.Clin.Neurophysiol.*, 68(1):1–19.

Desmedt, J. and Tomberg, C. (1990). Topographic analysis in brain mapping can be compromised by the average reference. *Brain Topogr.*, 3(1):35–42.

Dick, J., Rothwell, J., Day, B., Cantello, R., Buruma, O., Gioux, M., Benecke, R., Berardelli, A., Thompson, P., and Marsden, C. (1989). The Bereitschaftspotential is abnormal in Parkinson's disease. *Brain*, 112 (Pt 1):233–244.

Dickson, D. (1999). Neuropathologic differentiation of progressive supranuclear palsy and corticobasal degeneration. *J.Neurol.*, 246 Suppl 2:II6–15.

Dickson, D., Bergeron, C., Chin, S., Duyckaerts, C., Horoupian, D., Ikeda, K., Jellinger, K., Lantos, P., Lippa, C., Mirra, S., Tabaton, M., Vonsattel, J., Wakabayashi, K., and Litvan, I. (2002). Office of rare diseases neuropathologic

criteria for corticobasal degeneration. *J.Neuropathol.Exp.Neurol.*, 61(11):935–946.

Eckert, T., Barnes, A., Dhawan, V., Frucht, S., Gordon, M., Feigin, A., and Eidelberg, D. (2005). FDG PET in the differential diagnosis of parkinsonian disorders. *Neuroimage.*, 26(3):912–921.

Eimer, M. (1995). Stimulus-response compatibility and automatic response activation: evidence from psychophysiological studies. *J.Exp.Psychol.Hum.Percept.Perform.*, 21(4):837–854.

Eimer, M., Forster, B., van Velzen, J., and Prabhu, G. (2005). Covert manual response preparation triggers attentional shifts: ERP evidence for the premotor theory of attention. *Neuropsychologia*, 43(6):957–966.

Eimer, M., Van, V. J., and Driver, J. (2002). Cross-modal interactions between audition, touch, and vision in endogenous spatial attention: ERP evidence on preparatory states and sensory modulations. *J.Cogn Neurosci.*, 14(2):254–271.

Eimer, M. and van Velzen, J. (2002). Crossmodal links in spatial attention are mediated by supramodal control processes: evidence from event-related potentials. *Psychophysiology*, 39(4):437–449.

Elbert, T., Lutzenberger, W., Rockstroh, B., and Birbaumer, N. (1985). Removal of ocular artifacts from the EEG–a biophysical approach to the EOG. *Electroencephalogr.Clin.Neurophysiol.*, 60(5):455–463.

Elbert, T., Rockstroh, B., Hampson, S., Pantev, C., and Hoke, M. (1994). The magnetic counterpart of the contingent negative variation. *Electroencephalogr.Clin.Neurophysiol.*, 92(3):262–272.

Elting, J. (2006). *Biochemical and Neurophysiological Parameters of Acute Brain Injury*. PhD thesis.

Elting, J., van der, N. J., van Weerden, T., De Keyser, J., and Maurits, N. (2005). P300 after head injury: pseudodelay caused by reduced P3a amplitude. *Clin.Neurophysiol.*, 116(11):2606–2612.

Elting, J., Van Weerden, W., Van der Naalt, J., De Keyser, A., and Maurits, N. (2003). P300 component identification using source analysis techniques: reduced latency variability. *Journal of clinical neurophysiology*, 20(1):26–34.

Emerson, R. and Pedley, T. (2003). Somatosensory evoked potentials. In Ebersole, J. and Pedley, T., editors, *Current practice of clinical electroencephalography*, volume third edition, pages 892–922. Lippincot Williams & Wilkins, Philiadelphia.

Fein, G., Raz, J., Brown, F., and Merrin, E. (1988). Common reference coherence data are confounded by power and phase effects. *Electroencephalogr.Clin.Neurophysiol.*, 69(6):581–584.

Ferri, R., Del Gracco, S., Elia, M., Musumeci, S., Spada, R., and Stefanini, M. (1996). Scalp topographic mapping of middle-latency somatosensory evoked potentials in normal aging and dementia. *Neurophysiol.Clin.*, 26(5):311–319.

Fielding, J., Georgiou-Karistianis, N., and White, O. (2006). The role of the basal ganglia in the control of automatic visuospatial attention. *J.Int.Neuropsychol.Soc.*, 12(5):657–667.

Fitzgerald, D., Drago, V., Jeong, Y., Chang, Y., White, K., and Heilman, K. (2007). Asymmetrical alien hands in corticobasal degeneration. *Mov Disord.*, 22(4):581–584.

Fjell, A. M. and Walhovd, K. B. (2007). Stability of brain potentials, mental abilities, and cortical thickness. *Neuroreport*, 18(8):725–728.

Florence, G., Guerit, J.-M., and Gueguen, B. (2004). Electroencephalography (eeg) and somatosensory evoked potentials (sep) to prevent cerebral ischaemia in the operating room. *Neurophysiol Clin*, 34(1):17–32.

Fujii, M., Yamada, T., Aihara, M., Kokubun, Y., Noguchi, Y., Matsubara, M., and Yeh, M. (1994). The effects of stimulus rates upon median, ulnar and radial nerve somatosensory evoked potentials. *Electroencephalogr.Clin.Neurophysiol.*, 92(6):518–526.

Garcia, P. A., Aminoff, M. J., and Goodin, D. S. (1995). The frontal n30 component of the median-derived SEP in patients with predominantly unilateral Parkinson's disease. *Neurology*, 45(5):989–992.

Gardill, K. and Hielscher, H. (2001). Multichannel derived median nerve SEP compared to EEG in patients with vascular cerebral lesions. *Electromyogr.Clin.Neurophysiol.*, 41(4):215–223.

Geddes, L. and Baker, L. (1967). Specific resistance of biological material-a compendum of data for biomedical engineer and physiologist. *Medical & Biological Engineering*, 5(3):271–&.

Gerloff, C., Richard, J., Hadley, J., Schulman, A., Honda, M., and Hallett, M. (1998). Functional coupling and regional activation of human cortical motor areas during simple, internally paced and externally paced finger movements. *Brain*, 121 (Pt 8):1513–1531.

Gevins, A., Bressler, S., Morgan, N., Cutillo, B., White, R., Greer, D., and Illes, J. (1989). Event-related covariances during a bimanual visuomotor task. I. methods and analysis of stimulus- and response-locked data. *Electroencephalogr.Clin.Neurophysiol.*, 74(1):58–75.

Gevins, A., Morgan, N., Bressler, S., Cutillo, B., White, R., Illes, J., Greer, D., Doyle, J., and Zeitlin, G. (1987). Human neuroelectric patterns predict performance accuracy. *Science*, 235(4788):580–585.

Geyer, S., Schleicher, A., and Zilles, K. (1999). Areas 3a, 3b, and 1 of human primary somatosensory cortex. *NeuroImage*, 10(1):63–83.

Gorodnitsky, I. F., George, J. S., and Rao, B. D. (1995). Neuromagnetic source imaging with FOCUSS: a recursive weighted minimum norm algorithm. *Electroencephalogr Clin Neurophysiol*, 95(4):231–251.

Gotham, A., Brown, R., and Marsden, C. (1988). 'frontal' cognitive function in patients with Parkinson's disease 'on' and 'off' levodopa. *Brain*, 111 (Pt 2):299–321.

Gratton, G., Coles, M., and Donchin, E. (1983). A new method for off-line removal of ocular artifact. *Electroencephalogr.Clin.Neurophysiol.*, 55(4):468–484.

Grave de Peralta, M. R., Gonzalez, A. S., Lantz, G., Michel, C., and Landis, T. (2001). Noninvasive localization of electromagnetic epileptic activity. I. method descriptions and simulations. *Brain Topogr.*, 14(2):131–137.

Grave de Peralta Menendez, R., Murray, M. M., Michel, C. M., Martuzzi, R., and Gonzalez Andino, S. L. (2004). Electrical neuroimaging based on biophysical constraints. *NeuroImage*, 21(2):527–539.

Gross, J., Kujala, J., Hamalainen, M., Timmermann, L., Schnitzler, A., and Salmelin, R. (2001). Dynamic imaging of coherent sources: Studying neural interactions in the human brain. *Proc.Natl.Acad.Sci.U.S.A*, 98(2):694–699.

Hämäläinen, M. (1995). Discrete and distributed source estimates. in: Skrandies W, editor. source localization: continuing discussion of the inverse problem. *ISBET newsletter*, 6:9–12.

Hämäläinen, M. S. and Ilmoniemi, R. J. (1994). Interpreting magnetic fields of the brain: minimum norm estimates. *Med Biol Eng Comput*, 32(1):35–42.

Heinrich, H., Dickhaus, H., Rothenberger, A., Heinrich, V., and Moll, G. (1999). Single-sweep analysis of event-related potentials by wavelet networks–methodological basis and clinical application. *IEEE Trans.Biomed.Eng*, 46(7):867–879.

Helmholtz, H. (1853). Ueber einige gesetze der vertheilung elektrischer ströme in körperlichen leitern mit anwendung auf die thierisch-elektrischen versuche. *Ann. Physik und Chemie*, 89:211–33, 354–77.

Hjorth, B. (1975). An on-line transformation of EEG scalp potentials into orthogonal source derivations. *Electroencephalogr.Clin.Neurophysiol.*, 39(5):526–530.

Hjorth, B. (1991). Principles for transformation of scalp EEG from potential field into source distribution. *J.Clin.Neurophysiol.*, 8(4):391–396.

Hoehn, M. and Yahr, M. (1967). Parkinsonism: onset, progression and mortality. *Neurology*, 17(5):427–442.

Hommel, B., Pratt, J., Colzato, L., and Godijn, R. (2001). Symbolic control of visual attention. *Psychol.Sci.*, 12(5):360–365.

Hood, A., Amador, S., Cain, A., Briand, K., Al-Refai, A., Schiess, M., and Sereno, A. (2007). Levodopa slows prosaccades and improves antisaccades: an eye movement study in Parkinson's disease. *J.Neurol.Neurosurg.Psychiatry*, 78(6):565–570.

Huang, M., Davis, L. E., Aine, C., Weisend, M., Harrington, D., Christner, R., Stephen, J., Edgar, J. C., Herman, M., Meyer, J., Paulson, K., Martin, K., and Lee, R. R. (2004). MEG response to median nerve stimulation correlates with recovery of sensory and motor function after stroke. *Clin Neurophysiol*, 115(4):820–833.

Huber, R., Ghilardi, M., Massimini, M., and Tononi, G. (2004). Local sleep and learning. *Nature*, 430(6995):78–81.

Hughes, A., Daniel, S., Ben-Shlomo, Y., and Lees, A. (2002). The accuracy of diagnosis of parkinsonian syndromes in a specialist movement disorder service. *Brain*, 125(Pt 4):861–870.

Hughes, A., Daniel, S., Kilford, L., and Lees, A. (1992). Accuracy of clinical diagnosis of idiopathic Parkinson's disease: a clinico-pathological study of 100 cases. *J.Neurol.Neurosurg.Psychiatry*, 55(3):181–184.

Huizenga, H., van Zuijen, T., Heslenfeld, D., and Molenaar, P. (2001). Simultaneous MEG and EEG source analysis. *Phys.Med.Biol.*, 46(7):1737–1751.

Huttunen, J. and Teravainen, H. (1993). Pre- and postcentral cortical somatosensory evoked potentials in hemiparkinsonism. *Mov Disord.*, 8(4):430–436.

Hyvarinen, A. and Oja, E. (2000). Independent component analysis: algorithms and applications. *Neural Netw.*, 13(4-5):411–430.

Iriarte, J., Urrestarazu, E., Valencia, M., Alegre, M., Malanda, A., Viteri, C., and Artieda, J. (2003). Independent component analysis as a tool to eliminate artifacts in EEG: a quantitative study. *J.Clin.Neurophysiol.*, 20(4):249–257.

Jackson, G., Swainson, R., Mullin, A., Cunnington, R., and Jackson, S. (2004). ERP correlates of a receptive language-switching task. *Q.J.Exp.Psychol.A*, 57(2):223–240.

Jahanshahi, M., Jenkins, I., Brown, R., Marsden, C., Passingham, R., and Brooks, D. (1995). Self-initiated versus externally triggered movements. I. an investigation using measurement of regional cerebral blood flow with PET and movement-related potentials in normal and Parkinson's disease subjects. *Brain*, 118 (Pt 4):913–933.

Josephs, K., Petersen, R., Knopman, D., Boeve, B., Whitwell, J., Duffy, J., Parisi, J., and Dickson, D. (2006). Clinicopathologic analysis of frontotemporal and corticobasal degenerations and PSP. *Neurology*, 66(1):41–48.

Jung, P., Baumgartner, U., Bauermann, T., Magerl, W., Gawehn, J., Stoeter, P., and Treede, R. D. (2003). Asymmetry in the human primary somatosensory cortex and handedness. *NeuroImage*, 19(3):913–923.

Jung, T., Makeig, S., Lee, T., McKeown, M., Brown, G., Bell, A., and Sejnowski, T. (2000). Independent component analysis of biomedical signals.

Kakigi, R. (1987). The effect of aging on somatosensory evoked potentials following stimulation of the posterior tibial nerve in man. *Electroencephalogr.Clin.Neurophysiol.*, 68(4):277–286.

Kakigi, R. and Shibasaki, H. (1991). Effects of age, gender, and stimulus side on scalp topography of somatosensory evoked potentials following median nerve stimulation. *J.Clin.Neurophysiol.*, 8(3):320–330.

Kakigi, R. and Shibasaki, H. (1992). Effects of age, gender, and stimulus side on the scalp topography of somatosensory evoked potentials following posterior tibial nerve stimulation. *J.Clin.Neurophysiol.*, 9(3):431–440.

Kalcher, J. and Pfurtscheller, G. (1995). Discrimination between phase-locked and non-phase-locked event-related EEG activity. *Electroencephalogr.Clin.Neurophysiol.*, 94(5):381–384.

Kanovsky, P., Streitova, H., Dufek, J., and Rektor, I. (1997). Lateralization of the P22/N30 component of somatosensory evoked potentials of the median nerve in patients with cervical dystonia. *Mov Disord.*, 12(4):553–560.

Kazis, A., Vlaikidis, N., Pappa, P., Papanastasiou, J., Vlahveis, G., and Routsonis, K. (1983). Somatosensory and visual evoked potentials in human aging. *Electromyogr.Clin.Neurophysiol.*, 23(1-2):49–59.

Kennett, S., Van, V. J., Eimer, M., and Driver, J. (2007). Disentangling gaze shifts from preparatory ERP effects during spatial attention. *Psychophysiology*, 44(1):69–78.

Kingstone, A., Klein, R., Morein-Zamir, S., Hunt, A., Fisk, J., and Maxner, C. (2002). Orienting attention in aging and Parkinson's disease: distinguishing modes of control. *J.Clin.Exp.Neuropsychol.*, 24(7):951–967.

Kisley, M. and Gerstein, G. (1999). Trial-to-trial variability and state-dependent modulation of auditory-evoked responses in cortex. *J.Neurosci.*, 19(23):10451–10460.

Kitagawa, M., Fukushima, J., and Tashiro, K. (1994). Relationship between antisaccades and the clinical symptoms in Parkinson's disease. *Neurology*, 44(12):2285–2289.

Klodowska-Duda, G., Slowinski, J., Opala, G., Gorzkowska, A., Jasinska-Myga, B., Wszolek, Z. K., and Dickson, D. W. (2006). Corticobasal degeneration – clinico-pathological considerations. *Folia Neuropathol*, 44(4):257–264.

Kofler, M. (2000). Somatosensory evoked potentials in progressive supranuclear palsy. *Journal of the Neurological Sciences*, 179(S 1-2):85–91.

Koles, Z. J. (1998). Trends in EEG source localization. *Electroencephalography and Clinical Neurophysiology*, 106(2):127–137.

Kresch, E., Levitan, M., Baran, E., Mandel, S., Whitenack, S., Betz, R., and Brown, A. (1998). Correlation analysis of somatosensory evoked potential waveforms: clinical applications. *Arch.Phys.Med.Rehabil.*, 79(2):184–190.

Lachaux, J., Rodriguez, E., Martinerie, J., and Varela, F. (1999). Measuring phase synchrony in brain signals. *Hum.Brain Mapp.*, 8(4):194–208.

Lagerlund, T., Sharbrough, F., and Busacker, N. (1997). Spatial filtering of multichannel electroencephalographic recordings through principal component analysis by singular value decomposition. *J.Clin.Neurophysiol.*, 14(1):73–82.

Lang, A. and Fahn, A. (1989). Assessment of Parkinson's disease. In Munsat, T., editor, *Quantification of neurological deficit*, pages 285–309. Butterworths, Boston.

Lange, D., Pratt, H., and Inbar, G. (1997). Modeling and estimation of single evoked brain potential components. *IEEE Trans.Biomed.Eng*, 44(9):791–799.

Lantz, G., Grave, d. P., Spinelli, L., Seeck, M., and Michel, C. (2003a). Epileptic source localization with high density EEG: how many electrodes are needed? *Clin.Neurophysiol.*, 114(1):63–69.

Lantz, G., Spinelli, L., Seeck, M., Peralta Menendez, R., Sottas, C., and Michel, C. (2003b). Propagation of interictal epileptiform activity can lead to erroneous source localizations: a 128-channel EEG mapping study. *J.Clin.Neurophysiol.*, 20(5):311–319.

Lee, J., Koh, D., and Ong, C. (1989). Statistical evaluation of agreement between two methods for measuring a quantitative variable. *Comput.Biol.Med.*, 19(1):61–70.

Legatt, A., Bronx, N., Emerson, R., Labar, D., and Pedley, T. (1987). Surface near-field mapping of the median nerve SEP N20 component. *Neurology*, 37(Suppl 1):366–.

Legatt, A. and Kader, A. (2000). Topography of the initial cortical component of the median nerve somatosensory evoked potential. Relationship to central sulcus anatomy. *J.Clin.Neurophysiol.*, 17(3):321–325.

Lehmann, D. and Skrandies, W. (1984). Spatial analysis of evoked potentials in man–a review. *Prog.Neurobiol.*, 23(3):227–250.

Lins, O., Picton, T., Berg, P., and Scherg, M. (1993). Ocular artifacts in recording EEGs and event-related potentials.II: Source dipoles and source components. *Brain Topogr.*, 6(1):65–78.

Litvan, I., Agid, Y., Calne, D., Campbell, G., Dubois, B., Duvoisin, R., Goetz, C., Golbe, L., Grafman, J., Growdon, J., Hallett, M., Jankovic, J., Quinn, N., Tolosa, E., and Zee, D. (1996). Clinical research criteria for the diagnosis of progressive supranuclear palsy (Steele-Richardson-Olszewski syndrome): report of the NINDS-SPSP international workshop. *Neurology*, 47(1):1–9.

Litvan, I., Booth, V., Wenning, G., Bartko, J., Goetz, C., McKee, A., Jankovic, J., Jellinger, K., Lai, E., Brandel, J., Verny, M., Chaudhuri, K., Pearce, R., and Agid, Y. (1998). Retrospective application of a set of clinical diagnostic criteria for the diagnosis of multiple system atrophy. *J.Neural Transm.*, 105(2-3):217–227.

Litvan, I., Grimes, D., Lang, A., Jankovic, J., McKee, A., Verny, M., Jellinger, K., Chaudhuri, K., and Pearce, R. (1999). Clinical features differentiating patients with postmortem confirmed progressive supranuclear palsy and corticobasal degeneration. *J.Neurol.*, 246 Suppl 2:II1–II5.

Luk, K. D., Hu, Y., Wong, Y. W., and Cheung, K. M. (2001). Evaluation of various evoked potential techniques for spinal cord monitoring during scoliosis surgery. *Spine*, 26(16):1772–1777.

Mahapatra, R., Edwards, M., Schott, J., and Bhatia, K. (2004). Corticobasal degeneration. *Lancet Neurol.*, 3(12):736–743.

Makeig, S. (1993). Auditory event-related dynamics of the EEG spectrum and effects of exposure to tones. *Electroencephalogr.Clin.Neurophysiol.*, 86(4):283–293.

Manninen, P., Sarjeant, R., and Joshi, M. (2004). Posterior tibial nerve and median nerve somatosensory evoked potential monitoring during carotid endarterectomy. *Can J Anaesth*, 51(9):937–941.

Massimini, M., Huber, R., Ferrarelli, F., Hill, S., and Tononi, G. (2004). The sleep slow oscillation as a traveling wave. *J.Neurosci.*, 24(31):6862–6870.

Mauguière, F., Allison, T., Babiloni, C., Buchner, H., Eisen, A., Goodin, D., Jones, S., Kakigi, R., Matsuoka, S., Nuwer, M., Rossini, P., and Shibasaki, H. (1999). Somatosensory evoked potentials. The International Federation of Clinical Neurophysiology. *Electroencephalogr.Clin.Neurophysiol.Suppl*, 52:79–90.

Mauguière, F., Broussolle, E., and Isnard, J. (1993). Apomorphine-induced relief of the akinetic-rigid syndrome and early median nerve somatosensory evoked potentials (SEPs) in Parkinson's disease. *Electroencephalogr.Clin.Neurophysiol.*, 88(4):243–254.

Mauguière, F., Merlet, I., Forss, N., Vanni, S., Jousmaki, V., Adeleine, P., and Hari, R. (1997). Activation of a distributed somatosensory cortical network in the human brain: a dipole modelling study of magnetic fields evoked by median nerve stimulation. part II: Effects of stimulus rate, attention and stimulus detection. *Electroencephalogr.Clin.Neurophysiol.*, 104(4):290–295.

McFarland, D. and Cacace, A. (2004). Separating stimulus-locked and unlocked components of the auditory event-related potential. *Hear.Res.*, 193(1-2):111–120.

Mcgraw, K. and Wong, S. (1996). Forming inferences about some intraclass correlations coefficients (vol 1, pg 30, 1996). *Psychological Methods*, 1(4):390–390.

Michalewski, H., Prasher, D., and Starr, A. (1986). Latency variability and temporal interrelationships of the auditory event-related potentials (N1, P2, N2, and P3) in normal subjects. *Electroencephalogr.Clin.Neurophysiol.*, 65(1):59–71.

Michel, C., Lantz, G., Spinelli, L., De Peralta, R., Landis, T., and Seeck, M. (2004a). 128-channel EEG source imaging in epilepsy: clinical yield and localization precision. *J.Clin.Neurophysiol.*, 21(2):71–83.

Michel, C., Murray, M., Lantz, G., Gonzalez, S., Spinelli, L., and Grave, d. P. (2004b). EEG source imaging. *Clin.Neurophysiol.*, 115(10):2195–2222.

Mitra, K., Gangopadhaya, P., and Das, S. (2003). Parkinsonism plus syndrome–a review. *Neurol India*, 51(2):183–188.

Miura, T., Sonoo, M., and Shimizu, T. (2003). Establishment of standard values for the latency, interval and amplitude parameters of tibial nerve somatosensory evoked potentials (SEPs). *Clinical Neurophysiology*, 114(7):1367–1378.

Miwa, H. and Mizuno, Y. (2002). Enlargements of somatosensory-evoked potentials in progressive supranuclear palsy. *Acta Neurologica Scandinavica*, 106(4):209–212.

Monza, D. (2003). Neurophysiological features in relation to clinical signs in clinically diagnosed corticobasal degeneration. *Neurological sciences*, 24(1):16–23.

Mosher, J., Baillet, S., and Leahy, R. (1999). EEG source localization and imaging using multiple signal classification approach. *Journal of clinical neurophysiology*, 16(3):225–238.

Mosher, J. and Leahy, R. (1999). Source localization using recursively applied and projected (rap) music. *IEEE Tans Signal Proc*, 47:332–40.

Mosher, J., Lewis, P., and Leahy, R. (1992). Multiple dipole modeling and localization from spatio-temporal MEG data. *IEEE Trans.Biomed.Eng*, 39(6):541–557.

Nagai, Y., Critchley, H., Featherstone, E., Fenwick, P., Trimble, M., and Dolan, R. (2004). Brain activity relating to the contingent negative variation: an fMRI investigation. *Neuroimage.*, 21(4):1232–1241.

Ng, K. and Jones, S. (2007). The "enhanced N35" somatosensory evoked potential: its associations and potential utility in the clinical evaluation of dystonia and myoclonus. *J Neurol*, 254(1):46–52.

Nikolaev, A., Ivanitsky, G., Ivanitsky, A., Posner, M., and Abdullaev, Y. (2001). Correlation of brain rhythms between frontal and left temporal (Wernicke's) cortical areas during verbal thinking. *Neurosci.Lett.*, 298(2):107–110.

Nishida, S., Nakamura, M., Suwazono, S., Honda, M., and Shibasaki, H. (1997). Estimate of physiological variability of peak latency in single sweep P300. *Electroencephalogr.Clin.Neurophysiol.*, 104(5):431–436.

Nobre, A., Sebestyen, G., and Miniussi, C. (2000). The dynamics of shifting visuospatial attention revealed by event-related potentials. *Neuropsychologia*, 38(7):964–974.

Nogawa, T., Katayama, K., Tabata, Y., Ohshio, T., and Kawahara, T. (1976). Changes in amplitude of the EEG induced by a photic stimulus. *Electroencephalogr.Clin.Neurophysiol.*, 40(1):78–88.

Nunez, P. (1997). EEG coherency. I: Statistics, reference electrode, volume conduction, laplacians, cortical imaging, and interpretation at multiple scales. *Electroencephalography and Clinical Neurophysiology*, 103(5):499–515.

Nunez, P. and Pilgreen, K. (1991). The spline-Laplacian in clinical neurophysiology: a method to improve EEG spatial resolution. *J.Clin.Neurophysiol.*, 8(4):397–413.

Nunez, P., Silberstein, R., Cadusch, P., Wijesinghe, R., Westdorp, A., and Srinivasan, R. (1994). A theoretical and experimental study of high resolution EEG based on surface Laplacians and cortical imaging. *Electroencephalogr.Clin.Neurophysiol.*, 90(1):40–57.

Nunez, P. L. (1990). Localization of brain activity with electroencephalography. *Adv Neurol*, 54:39–65.

Okuda, B., Tachibana, H., Takeda, M., Kawabata, K., and Sugita, M. (1998). Asymmetric changes in somatosensory evoked potentials correlate with limb apraxia in corticobasal degeneration. *Acta Neurol Scand*, 97(6):409–412.

Oostenveld, R., Praamstra, P., Stegeman, D. F., and van Oosterom, A. (2001). Overlap of attention and movement-related activity in lateralized event-related brain potentials. *Clin Neurophysiol*, 112(3):477–484.

Owen, A. (2004). Cognitive dysfunction in Parkinson's disease: the role of frontostriatal circuitry. *Neuroscientist.*, 10(6):525–537.

Pae, J., Kwon, J., Youn, T., Park, H., Kim, M., Lee, B., and Park, K. (2003). LORETA imaging of P300 in schizophrenia with individual MRI and 128-channel EEG. *NeuroImage*, 20(3):1552–1560.

Palva, S., Linkenkaer-Hansen, K., Naatanen, R., and Palva, J. (2005). Early neural correlates of conscious somatosensory perception. *J.Neurosci.*, 25(21):5248–5258.

Pascual-Marqui, R. (1999). Review of methods for solving the EEG inverse problem. *International Journal of biomagnetism*, 1(1):75–86.

Pascual-Marqui, R. (2002). Standardized low-resolution brain electromagnetic tomography (sLORETA): technical details. *Methods Find.Exp.Clin.Pharmacol.*, 24 Suppl D:5–12.

Pascual-Marqui, R., Michel, C., and Lehmann, D. (1994). Low resolution electromagnetic tomography: a new method for localizing electrical activity in the brain. *Int.J.Psychophysiol.*, 18(1):49–65.

Pascual-Marqui, R. D. and Lehmann, D. (1993a). Comparison of topographic maps and the reference electrode: comments on two papers by Desmedt and collaborators. *Electroencephalogr Clin Neurophysiol*, 88(6):530–1, 534–6.

Pascual-Marqui, R. D. and Lehmann, D. (1993b). Topographic maps, source localization inference, and the reference electrode: comments on a paper by Desmedt et al. *Electroencephalogr Clin Neurophysiol*, 88(6):532–536.

Penhune, V., Zatorre, R., MacDonald, J., and Evans, A. (1996). Interhemispheric anatomical differences in human primary auditory cortex: probabilistic mapping and volume measurement from magnetic resonance scans. *Cereb.Cortex*, 6(5):661–672.

Perrin, F., Bertrand, O., and Pernier, J. (1987). Scalp current density mapping: value and estimation from potential data. *IEEE Trans Biomed Eng*, 34(4):283–288.

Perrin, F., Pernier, J., Bertrand, O., and Echallier, J. (1989). Spherical splines for scalp potential and current density mapping. *Electroencephalogr.Clin.Neurophysiol.*, 72(2):184–187.

Pfefferbaum, A. and Ford, J. (1988). ERPs to stimuli requiring response production and inhibition: effects of age, probability and visual noise. *Electroencephalogr.Clin.Neurophysiol.*, 71(1):55–63.

Pfurtscheller, G. (1977). Graphical display and statistical evaluation of event-related desynchronization (ERD). *Electroencephalogr.Clin.Neurophysiol.*, 43(5):757–760.

Pfurtscheller, G. (1992). Event-related synchronization (ERS): an electrophysiological correlate of cortical areas at rest. *Electroencephalogr.Clin.Neurophysiol.*, 83(1):62–69.

Pfurtscheller, G. and Andrew, C. (1999). Event-related changes of band power and coherence: methodology and interpretation. *J.Clin.Neurophysiol.*, 16(6):512–519.

Pfurtscheller, G. and Lopes da Silva, F. (1999). Event-related EEG/MEG synchronization and desynchronization: basic principles. *Clin.Neurophysiol.*, 110(11):1842–1857.

Picton, T. and Hillyard, S. (1972). Cephalic skin potentials in electroencephalography. *Electroencephalogr.Clin.Neurophysiol.*, 33(4):419–424.

Poceta, L. (2006). Reader asks for support of medical marijuana. *Oncol.Nurs.Forum*, 33(6):1053–.

Praamstra, P., Boutsen, L., and Humphreys, G. (2005). Frontoparietal control of spatial attention and motor intention in human EEG. *J.Neurophysiol.*, 94(1):764–774.

Praamstra, P., Meyer, A., Cools, A., Horstink, M., and Stegeman, D. (1996). Movement preparation in Parkinson's disease. Time course and distribution of movement-related potentials in a movement precueing task. *Brain*, 119 (Pt 5):1689–1704.

Praamstra, P. and Plat, F. (2001). Failed suppression of direct visuomotor activation in Parkinson's disease. *J.Cogn Neurosci.*, 13(1):31–43.

Quian, Q. R. and Garcia, H. (2003). Single-trial event-related potentials with wavelet denoising. *Clin.Neurophysiol.*, 114(2):376–390.

Quian, Q. R., Sakowitz, O., Basar, E., and Schurmann, M. (2001). Wavelet transform in the analysis of the frequency composition of evoked potentials. *Brain Res.Brain Res.Protoc.*, 8(1):16–24.

Restuccia, D., Valeriani, M., Barba, C., Pera, D. L., Bentivoglio, A., Albanese, A., Rubino, M., and Tonali, P. (2003). Abnormal gating of somatosensory inputs in essential tremor. *Clin Neurophysiol*, 114(1):120–129.

Rinne, J., Lee, M., Thompson, P., and Marsden, C. (1994). Corticobasal degeneration. a clinical study of 36 cases. *Brain*, 117 (Pt 5):1183–1196.

Ristic, J. and Kingstone, A. (2006). Attention to arrows: pointing to a new direction. *Q.J.Exp.Psychol.(Colchester.)*, 59(11):1921–1930.

Rodionov, V., Goodman, C., Fisher, L., Rosenstein, G., and Sohmer, H. (2002). A new technique for the analysis of background and evoked EEG activity: time and amplitude distributions of the EEG deflections. *Clin.Neurophysiol.*, 113(9):1412–1422.

Roerdink, J. (1993). *Wavelets for signal and image processing.* University of Groningen.

Rohrbaugh, J., Syndulko, K., and Lindsley, D. (1976). Brain wave components of the contingent negative variation in humans. *Science*, 191(4231):1055–1057.

Romani, A., Bergamaschi, R., Versino, M., Delnevo, L., Callieco, R., and Cosi, V. (1992). Spinal and cortical potentials evoked by tibial nerve stimulation in humans: effects of sex, age and height. *Boll.Soc.Ital.Biol.Sper.*, 68(11):691–698.

Romani, A., Bergamaschi, R., Versino, M., Sartori, I., Callieco, R., and Cosi, V. (1993). One-week test-retest reliability of spinal and cortical somatosensory evoked potentials by tibial nerve stimulation. *Boll.Soc.Ital.Biol.Sper.*, 69(10):601–607.

Rossini, P. (1994). Analysis of interhemispheric asymmetries of somatosensory evoked magnetic fields to right and left median nerve stimulation. *Electroencephalography and Clinical Neurophysiology*, 91(6):476–482.

Rossini, P. (2004). Does cerebrovascular disease affect the coupling between neuronal activity and local haemodynamics? *Brain*, 127(Pt 1):99–110.

Rossini, P., Babiloni, F., Bernardi, G., Cecchi, L., Johnson, P., Malentacca, A., Stanzione, P., and Urbano, A. (1989). Abnormalities of short-latency somatosensory evoked potentials in parkinsonian patients. *Electroencephalogr.Clin.Neurophysiol.*, 74(4):277–289.

Rossini, P., Bassetti, M., and Pasqualetti, P. (1995). Median nerve somatosensory evoked potentials. Apomorphine-induced transient potentiation of frontal components in Parkinson's disease and in parkinsonism. *Electroencephalogr.Clin.Neurophysiol.*, 96(3):236–247.

Rossini, P., Caramia, D., Bassetti, M., Pasqualetti, P., Tecchio, F., and Bernardi, G. (1996). Somatosensory evoked potentials during the ideation and execution of individual finger movements. *Muscle Nerve*, 19(2):191–202.

Rossini, P., Tecchio, F., Pizzella, V., Lupoi, D., Cassetta, E., and Pasqualetti, P. (2001). Interhemispheric differences of sensory hand areas after monohemispheric stroke: MEG/MRI integrative study. *NeuroImage*, 14(2):474–485.

Rossini, P. M., Calautti, C., Pauri, F., and Baron, J.-C. (2003). Post-stroke plastic reorganisation in the adult brain. *Lancet Neurol*, 2(8):493–502.

Rousson, V., Gasser, T., and Seifert, B. (2002). Assessing intrarater, interrater and test-retest reliability of continuous measurements. *Stat.Med.*, 21(22):3431–3446.

Ruchsow, M., Trippel, N., Groen, G., Spitzer, M., and Kiefer, M. (2003). Semantic and syntactic processes during sentence comprehension in patients with schizophrenia: evidence from event-related potentials. *Schizophr.Res.*, 64(2-3):147–156.

Sabbagh, M., Moulson, M., and Harkness, K. (2004). Neural correlates of mental state decoding in human adults: an event-related potential study. *J.Cogn Neurosci.*, 16(3):415–426.

Saeid Sanei, J. C. (2007). *EEG signal processing*. John Wiley & Sons.

Salmelin, R. and Hari, R. (1994). Spatiotemporal characteristics of sensorimotor neuromagnetic rhythms related to thumb movement. *Neuroscience*, 60(2):537–550.

Schmidt, D. M., George, J. S., and Wood, C. C. (1999). Bayesian inference applied to the electromagnetic inverse problem. *Hum Brain Mapp*, 7(3):195–212.

Seyal, M., Emerson, R., and Pedley, T. (1983). Spinal and early scalp-recorded components of the somatosensory evoked potential following stimulation of the posterior tibial nerve. *Electroencephalogr.Clin.Neurophysiol.*, 55(3):320–330.

Shibasaki, H. (2006). Neurophysiological classification of myoclonus. *Neurophysiol Clin*, 36(5-6):267–269.

Shibasaki, H. and Hallett, M. (2006). What is the Bereitschaftspotential? *Clin Neurophysiol*, 117(11):2341–2356.

Smulders, F., Kenemans, J., and Kok, A. (1994). A comparison of different methods for estimating single-trial P300 latencies. *Electroencephalogr.Clin.Neurophysiol.*, 92(2):107–114.

Soros, P., Knecht, S., Imai, T., Gurtler, S., Lutkenhoner, B., Ringelstein, E., and Henningsen, H. (1999). Cortical asymmetries of the human somatosensory hand representation in right- and left-handers. *Neurosci.Lett.*, 271(2):89–92.

Spitzer, A., Cohen, L., Fabrikant, J., and Hallett, M. (1989). A method for determining optimal interelectrode spacing for cerebral topographic mapping. *Electroencephalogr.Clin.Neurophysiol.*, 72(4):355–361.

Steinmetz, H., Volkmann, J., Jancke, L., and Freund, H. (1991). Anatomical left-right asymmetry of language-related temporal cortex is different in left- and right-handers. *Ann.Neurol.*, 29(3):315–319.

Strenge, H. (1986). [age changes in early somatosensory evoked potentials]. *EEG.EMG.Z.Elektroenzephalogr.Elektromyogr.Verwandte.Geb.*, 17(2):75–82.

Strenge, H. (1989). [variations in the configuration of somatosensory evoked potentials following stimulation of the median nerve]. *EEG EMG Z.Elektroenzephalogr.Elektromyogr.Verwandte Geb.*, 20(3):139–146.

Suwazono, S., Shibasaki, H., Nishida, S., Nakamura, M., Honda, M., Nagamine, T., Ikeda, A., Ito, J., and Kimura, J. (1994). Automatic detection of P300 in single sweep records of auditory event-related potential. *J.Clin.Neurophysiol.*, 11(4):448–460.

Takeda, M., Tachibana, H., Okuda, B., Kawabata, K., and Sugita, M. (1998). Electrophysiological comparison between corticobasal degeneration and progressive supranuclear palsy. *Clinical Neurology and Neurosurgery*, 100(2):94–98.

Taylor, A., Saint-Cyr, J., and Lang, A. (1986). Frontal lobe dysfunction in Parkinson's disease. The cortical focus of neostriatal outflow. *Brain*, 109 (Pt 5):845–883.

Tecchio, F., Pasqualetti, P., Pizzella, V., Romani, G., and Rossini, P. (2000). Morphology of somatosensory evoked fields: inter-hemispheric similarity as a parameter for physiological and pathological neural connectivity. *Neuroscience Letters*, 287(3):203–206.

ten Caat, M. (2008). *Multichannel EEG Visualization*. PhD thesis, University of Groningen.

Thatcher, R., Krause, P., and Hrybyk, M. (1986). Cortico-cortical associations and EEG coherence: a two-compartmental model. *Electroencephalogr.Clin.Neurophysiol.*, 64(2):123–143.

Theuvenet, P., van Dijk, B., Peters, M., van Ree, J., Lopes da Silva, F., and Chen, A. (2005). Whole-head MEG analysis of cortical spatial organization from unilateral stimulation of median nerve in both hands: no complete hemispheric homology. *NeuroImage*, 28(2):314–325.

Thomas, D., Neer, C., and Price, J. (1989). Analyses of single-trial N1 amplitude and latency variability and their influence on the average evoked potential. *Electroencephalogr.Clin.Neurophysiol.*, 74(3):228–235.

Thompson, P., Day, B., Rothwell, J., Brown, P., Britton, T., and Marsden, C. (1994). The myoclonus in corticobasal degeneration. Evidence for two forms of cortical reflex myoclonus. *Brain*, 117 (Pt 5):1197–1207.

Tinaz, S., Schendan, H., and Stern, C. (2008). Fronto-striatal deficit in Parkinson's disease during semantic event sequencing. *Neurobiol.Aging*, 29(3):397–407.

Tinazzi, M., Priori, A., Bertolasi, L., Frasson, E., Mauguire, F., and Fiaschi, A. (2000). Abnormal central integration of a dual somatosensory input in dystonia. evidence for sensory overflow. *Brain*, 123 (Pt 1):42–50.

Tinazzi, M., Zanette, G., Manganotti, P., Bonato, C., Polo, A., Fiaschi, A., and Mauguiere, F. (1997). Amplitude changes of tibial nerve cortical somatosensory evoked potentials when the ipsilateral or contralateral ear is used as reference. *J.Clin.Neurophysiol.*, 14(3):217–225.

Tipples, J. (2002). Eye gaze is not unique: automatic orienting in response to uninformative arrows. *Psychon.Bull.Rev.*, 9(2):314–318.

Tomberg, C., Desmedt, J., and Ozaki, I. (1991). Right or left ear reference changes the voltage of frontal and parietal somatosensory evoked potentials. *Electroencephalogr.Clin.Neurophysiol.*, 80(6):504–512.

Tomberg, C., Noel, P., Ozaki, I., and Desmedt, J. (1990). Inadequacy of the average reference for the topographic mapping of focal enhancements of brain potentials. *Electroencephalogr.Clin.Neurophysiol.*, 77(4):259–265.

Truccolo, W., Knuth, K., Shah, A., Bressler, S., Schroeder, C., and Ding, M. (2003). Estimation of single-trial multicomponent ERPs: differentially variable component analysis (dvca). *Biol.Cybern.*, 89(6):426–438.

Trujillo-Barreto, N. J., Aubert-Vazquez, E., and Valdes-Sosa, P. A. (2004). Bayesian model averaging in EEG/MEG imaging. *NeuroImage*, 21(4):1300–1319.

Tsuji, S., Luders, H., Lesser, R., Dinner, D., and Klem, G. (1984). Subcortical and cortical somatosensory potentials evoked by posterior tibial nerve stimulation: normative values. *Electroencephalogr.Clin.Neurophysiol.*, 59(3):214–228.

Tzvetanov, P., Milanov, I., Rousseff, R. T., and Christova, P. (2004). Can SSEP results predict functional recovery of stroke patients within the "therapeutic window"? *Electromyogr Clin Neurophysiol*, 44(1):43–49.

Tzvetanov, P. and Rousseff, R. T. (2003). Median SSEP changes in hemiplegic stroke: long-term predictive values regarding ADL recovery. *NeuroRehabilitation*, 18(4):317–324.

Uutela, K., Hmlinen, M., and Salmelin, R. (1998). Global optimization in the localization of neuromagnetic sources. *IEEE Trans Biomed Eng*, 45(6):716–723.

Uylings, H., Rajkowska, G., Sanz-Arigita, E., Amunts, K., and Zilles, K. (2005). Consequences of large interindividual variability for human brain atlases: converging macroscopical imaging and microscopical neuroanatomy. *Anat.Embryol.(Berl)*, 210(5-6):423–431.

Valeriani, M., Le Pera, D., and Tonali, P. (2001). Characterizing somatosensory evoked potential sources with dipole models: advantages and limitations. *Muscle Nerve*, 24(3):325–339.

Valeriani, M., Restuccia, D., Lazzaro, V. D., Barba, C., Pera, D. L., and Tonali, P. (1997). Dipolar generators of the early scalp somatosensory evoked potentials to tibial nerve stimulation in human subjects. *Neurosci Lett*, 238(1-2):49–52.

Valeriani, M., Restuccia, D., Lazzaro, V. D., Barba, C., Pera, D. L., and Tonali, P. (1998). Dissociation induced by voluntary movement between two different components of the centro-parietal P40 SEP to tibial nerve stimulation. *Electroencephalogr Clin Neurophysiol*, 108(2):190–198.

Valeriani, M., Restuccia, D., Le, P. D., Barba, C., and Tonali, P. (2000). Scalp distribution of the earliest cortical somatosensory evoked potential to tibial nerve stimulation: proposal of a new recording montage. *Clin.Neurophysiol.*, 111(8):1469–1477.

van de Berg, W., Rozemuller, J., and de Vos, R. (2007). Neuropathology in movement disorders. In Wolters, E., van Laar, T., and Berendse, H., editors, *Parkinsonism and related disorders*, volume first, pages 97–128. VU University Press.

van de Wassenberg, W., Kruizinga, W., van der Hoeven, J., Leenders, K., and Maurits, N. (2008a). Multichannel recording of tibial nerve somatosensory evoked potentials. *Neurophysiol Clin*, Accepted.

van de Wassenberg, W., van der Hoeven, J., Leenders, K., and Maurits, N. (2008b). Multichannel recording of median nerve somatosensory evoked potentials. *Neurophysiol Clin*, 38(1):9–21.

van de Wassenberg, W., van der Hoeven, J., Leenders, K., and Maurits, N. (2008c). Quantifying interhemispheric symmetry of somatosensory evoked potentials with the intraclass correlation coefficient. *J.Clin.Neurophysiol.*, 25(3):139–146.

van der Lubbe, R., Neggers, S., Verleger, R., and Kenemans, J. (2006). Spatiotemporal overlap between brain activation related to saccade preparation and attentional orienting. *Brain Res.*, 1072(1):133–152.

van Velzen, J., Eardley, A., Forster, B., and Eimer, M. (2006). Shifts of attention in the early blind: an erp study of attentional control processes in the absence of visual spatial information. *Neuropsychologia*, 44(12):2533–2546.

van Velzen, J., Forster, B., and Eimer, M. (2002). Temporal dynamics of lateralized ERP components elicited during endogenous attentional shifts to relevant tactile events. *Psychophysiology*, 39(6):874–878.

Verleger, R., Vollmer, C., Wauschkuhn, B., van der Lubbe, R., and Wascher, E. (2000). Dimensional overlap between arrows as cueing stimuli and responses?. Evidence from contra-ipsilateral differences in EEG potentials. *Brain Res.Cogn Brain Res.*, 10(1-2):99–109.

Vieregge, P., Verleger, R., Wascher, E., Stuven, F., and Kompf, D. (1994). Auditory selective attention is impaired in Parkinson's disease–event-related evidence from EEG potentials. *Brain Res.Cogn Brain Res.*, 2(2):117–129.

Vigario, R. (1997). Extraction of ocular artefacts from EEG using independent component analysis. *Electroencephalogr.Clin.Neurophysiol.*, 103(3):395–404.

Vigario, R., Sarela, J., Jousmaki, V., Hamalainen, M., and Oja, E. (2000). Independent component approach to the analysis of EEG and MEG recordings. *IEEE Trans.Biomed.Eng*, 47(5):589–593.

Vrba, J. and Robinson, S. (2001). Signal processing in magnetoencephalography. *Methods*, 25(2):249–271.

Wagner, M., Fuchs, M., and Kastner, J. (2004). Evaluation of sLORETA in the presence of noise and multiple sources. *Brain Topography*, 16(4):277–280.

Wastell, D. and Kleinman, D. (1980). N1-P2 correlates of reaction time at the single-trial level. *Electroencephalogr.Clin.Neurophysiol.*, 48(2):191–196.

Wright, M., Geffen, G., and Geffen, L. (1993). Event-related potentials associated with covert orientation of visual attention in Parkinson's disease. *Neuropsychologia*, 31(12):1283–1297.

Xu, X., Xu, B., and He, B. (2004). An alternative subspace approach to EEG dipole source localization. *Physics in Medicine and Biology*, 49(2):327–343.

Yamaguchi, S., Tsuchiya, H., and Kobayashi, S. (1998). Visuospatial attention shift and motor responses in cerebellar disorders. *J.Cogn Neurosci.*, 10(1):95–107.

Yao, D. (2002a). High-resolution EEG mapping: a radial-basis function based approach to the scalp laplacian estimate. *Clin.Neurophysiol.*, 113(6):956–967.

Yao, D. (2002b). The theoretical relation of scalp Laplacian and scalp current density of a spherical shell head model. *Phys.Med.Biol.*, 47(12):2179–2185.

Youn, T., Park, H., Kim, J., Kim, M., and Kwon, J. (2003). Altered hemispheric asymmetry and positive symptoms in schizophrenia: equivalent current dipole of auditory mismatch negativity. *Schizophr.Res.*, 59(2-3):253–260.

Zgaljardic, D., Borod, J., Foldi, N., Mattis, P., Gordon, M., Feigin, A., and Eidelberg, D. (2006). An examination of executive dysfunction associated with frontostriatal circuitry in Parkinson's disease. *J.Clin.Exp.Neuropsychol.*, 28(7):1127–1144.

Nederlandse samenvatting

Het elektro-encefalogram (EEG) onderzoek is een veel gebruikt onderzoek binnen de neurologie. Het is een registratie van de elektrische hersenactiviteit gemeten op het hoofd. Het EEG verandert wanneer iemand bijvoorbeeld zijn ogen sluit of slaapt. Daarnaast zijn bepaalde afwijkingen in het EEG kenmerkend voor specifieke neurologische ziektes zoals epilepsie. Een EEG onderzoek wordt meestal uitgevoerd met maximaal 21 elektrodes op het hoofd. Dit betekent dat op 21 posities op het hoofd tegelijkertijd de hersenactiviteit gemeten wordt. Er bestaan echter ook meetsystemen met 128 en zelfs met 256 elektrodes. De vraag is of de extra gegevens, die je met deze systemen meet ook klinisch relevant zijn. Het werken met meer electrodes betekent echter ook meer voorbereidingstijd, mogelijk duurdere apparatuur en een extra belasting voor de patiënt. Er moet dus afgewogen worden of de baten opwegen tegen de extra kosten, belasting en tijd.
Daarnaast zullen er nieuwe methodes moeten worden ontwikkeld om in de grote hoeveelheid gegevens, bij gebruik van multikanaals (>64 elektrodes) EEG registraties, de juiste informatie te halen. Een registratie van 1 minuut kan namelijk al meer dan 7.000.000 meetwaarden opleveren, oftewel een computerbestand van 7 MB.
In dit proefschrift is onderzocht of meten met 128 elektrodes ook daadwerkelijk een meerwaarde heeft voor de klinische praktijk. Om dit uit te zoeken zijn enkele nieuwe analysemethodes ontwikkeld.
In dit onderzoek hebben we ons gericht op evoked potentials (EPs) en event-related potentials (ERPs). Een E(R)P is de elektrische hersenactiviteit die ontstaat door een prikkel (stimulus), bijvoorbeeld een geluid of lichtflits (EP), of het uitvoeren van een taak (ERP). EPs worden tegenwoordig voornamelijk gebruikt voor het beoordelen van de geleiding van zenuwen met behulp van de latentie. De latentie is de tijd tussen het geven van de stimulus en het moment waarop een specifieke stimulus-gerelateerde piek zichtbaar is in de hersenactiviteit. Ook wordt er soms naar de hoogte (amplitude) van een piek gekeken. Een lange latentie en lage amplitude kunnen duiden op zenuwschade.
Er bestaan echter ook andere methodes om relevante informatie uit de meting te extraheren. In hoofdstuk 2 en 3 wordt een overzicht gegeven van andere analysemethodes, die in de literatuur worden beschreven. Deze methodes worden tot dusver voornamelijk gebruikt voor wetenschappelijk onderzoek en niet voor patiëntenzorg. Toch zouden deze methodes mogelijk ook een klinische waarde kunnen hebben, zeker wanneer deze worden toegepast op multikanaals EEG data.

Somatosensorische evoked potentials

Somatosensorische EPs (SEP) zijn evoked potentials waarbij de stimulus een elektrische schok is. SEP onderzoek wordt met name klinisch gebruikt voor het bepalen van de geleiding van gevoelszenuwbanen. Bij dit onderzoek worden normaal gesproken minder dan 10 elektrodes op het hoofd gebruikt. Er wordt vooral naar de latentie gekeken en niet naar de amplitude. De amplitude leek namelijk tot dusver minder bruikbaar, omdat deze veel varieert tussen gezonde personen en omdat er een grote overlap is in amplitude tussen gezonde personen en patiënten met een neurologische aandoening. Door deze overlap is het onmogelijk om de amplitude te gebruiken om onderscheid te maken tussen gezonde en afwijkende pathologische waarden. Mogelijk wordt de grote amplitude variatie en overlap veroorzaakt door het feit dat er maar met een beperkt aantal elektrodes gemeten wordt. Nu wordt er bij iedere persoon op dezelfde positie op het hoofd gemeten. De elektrode posities worden bepaald met behulp van vaste punten op het hoofd, zoals het nasion bij de neusbrug. De amplitude verschilt echter per positie op het hoofd en de positie waar de amplitude maximaal is zou wel eens kunnen verschillen per persoon. Ieder brein is immers weer anders en het hersengebied wat geactiveerd wordt door de stimulus kan bij iedere persoon net weer iets anders liggen.
In hoofdstuk 4 hebben we onderzocht of de amplitude nauwkeuriger gemeten kan worden met 128 elektrodes in plaats van slechts enkele elektrodes. Voor het analyseren van de 128-kanaals registratie hebben we een methode geïntroduceerd die de maximale amplitude op het hoofd bepaalt. Deze methode hebben we toegepast op 50 gezonde proefpersonen en vergeleken met een standaard methode met slechts enkele elektrodes. Er is getest of de variatie in amplitude tussen gezonde personen afneemt bij het gebruik van meer elektrodes. De amplitude variatie tussen personen bleek bij de 128-kanaals methode niet te zijn verminderd. De positie van de maximale amplitude bleek echter wel sterk te variëren tussen personen. Door de hogere amplitude en de vergelijkbare variatie zou de 128-kanaals registratie toch gevoeliger kunnen zijn voor pathologische veranderingen. De 128-kanaals amplitude bepaling zou dus mogelijk een bijdrage kunnen leveren bij het diagnosticeren van neurologische ziektes. Tevens hebben we in dit hoofdstuk leeftijdsgerelateerde normaalwaarden bepaald, zodat we in een later stadium de SEPs van patiënten hiermee kunnen vergelijken.
De variatie in SEP amplitude tussen personen is dus groot, maar de verschillen in SEP amplitude tussen de linker en rechter hersenhelft zijn relatief klein. Voor de diagnostiek van neurologische ziektes die slechts één kant van de hersenen beschadigen, kan het interessant zijn om beide hersenhelften te vergelijken. Nu worden er alleen amplitudes en latenties vergeleken, maar het kan ook interessant zijn om het hele verloop van hersenactiviteit in de tijd, ten gevolge van stimulatie van de linker en rechter lichaamshelft, in beide hersenhelften te vergelijken. In hoofdstuk 5 hebben we een nieuwe methode geïntroduceerd om SEPs over een bepaalde periode

met elkaar te vergelijken en de mate van gelijkenis te kwantificeren. We hebben dit vervolgens toegepast op de SEP data, waarvan we in hoofdstuk 4 de amplitude hebben bepaald. We hebben laten zien dat onze methode geschikt is voor het kwantificeren van SEP symmetrie (gelijkenis tussen linker en rechter SEP). Tevens vonden we tegen de verwachting in bij enkele gezonde proefpersonen grote verschillen tussen linker en rechter SEP. Een minder symmetrische SEP betekent dus niet automatisch dat de betreffende persoon aan een ziekte lijdt.
Vervolgens hebben we de methodes, die we in hoofdstuk 4 en 5 hebben geïntroduceerd, toegepast op patiënten met de ziekte van Parkinson (ZvP) en patiënten met verwante ziektes, zoals progressieve supranucleaire paralyse (PSP) en corticobasale degeneratie (CBGD). Deze ziektes worden gekarakteriseerd door gedeeltelijk vergelijkbare symptomen, zoals stijfheid en traagheid van beweging. Daardoor zijn deze ziektes voor de arts in sommige gevallen moeilijk te onderscheiden. Multikanaals SEP zou mogelijk een bijdrage kunnen leveren bij de diagnostiek van deze ziektes. Dit baseren we op het feit dat bij SEP studies met een beperkt aantal elektrodes al afwijkingen zijn gevonden bij patiënten met deze ziektes. De afwijkingen waren echter te klein of waren slechts bij een beperkt aantal patiënten aanwezig om van klinische betekenis te kunnen zijn. Daarnaast wordt CBGD gekarakteriseerd door afwijkingen in de hersengebieden die de SEP genereren. Deze afwijkingen bevinden zich meestal slechts in één hersenhelft, terwijl bij PSP en PD meestal in beide hersenhelften afwijkingen worden gevonden. We zouden dus verwachten dat patiënten met CBGD een groter verschil hebben tussen linker en rechter SEP dan de andere patiënten. In dit onderzoek bleek dit echter niet het geval te zijn. Bij slechts drie van de dertien CBGD patiënten vonden we een groot verschil tussen linker en rechter SEP. Vergelijkbare verschillen vonden we in enkele andere patiënten met PSP of ZvP. Ook wanneer we keken naar de amplitude vonden we geen significante verschillen tussen de verschillende patiëntengroepen. De methodes die we hebben toegepast blijken dus niet geschikt voor het onderscheiden van ZvP, PSP en CBGD. Er zijn echter nog andere ziektes, waarbij deze methodes van klinisch belang kunnen zijn. In dit proefschrift hebben we hier niet verder naar gekeken.
In voorgaande hoofdstukken hebben we de SEP bestudeerd, waarbij steeds een zenuw bij de pols, de nervus medianus, werd gestimuleerd. Dit is een veel gebruikte EP in de klinische praktijk. Een andere positie, die vaak gebruikt wordt voor stimulatie is de binnenkant van de enkel bij de nervus tibialis. Stimulatie van deze zenuw activeert andere hersengebieden dan stimulatie van de nervus medianus. In hoofdstuk 7 hebben we onderzocht of ook bij stimulatie van deze zenuw de 128-kanaals registratie zorgt voor nauwkeurigere amplitude bepaling en een vermindering van de amplitude variatie tussen gezonde proefpersonen. Inderdaad vonden we ook voor de SEP tibialis dat de positie van maximale amplitudes verschilt per persoon. De 128-kanaals registratie resulteerde niet in een verlaging van de amplitude variatie tussen gezonde proefpersonen, maar zorgde wel voor een nauwkeurigere amplitude

bepaling.

Event-related potentials

In tegenstelling tot EPs, worden ERPs tot dusver nauwelijks gebruikt in de klinische praktijk. Een nadeel van ERPs ten opzichte van EPs is dat deze sterk worden beïnvloed door de uitvoering en concentratie van de patiënt. Er wordt namelijk meestal een reactie van de patiënt gevraagd, bijvoorbeeld om een bepaalde beweging te maken of om specifieke aangeboden stimuli te tellen. In eerdere studies met jonge proefpersonen werd ontdekt dat bij het voorbereiden van een beweging en het richten van aandacht vergelijkbare ERPs ontstaan. Er lijken dus hersengebieden te zijn die bij beide activiteiten betrokken zijn. Om meer inzicht te krijgen in de ZvP is het interessant om een vergelijkbaar onderzoek ook bij deze patiënten groep uit te voeren. Bij de ZvP komen immers niet alleen bewegingsproblemen voor, maar ook problemen met het vasthouden van aandacht. Dit zou kunnen komen doordat bij de ZvP hersengebieden zijn aangedaan, die bij beide activiteiten een rol spelen. De eerste vraag bij dit onderzoek was of patiënten met de ZvP ook de taken goed konden uitvoeren, die deze ERPs opwekken. In eerdere studies was namelijk al beschreven dat enkele jonge gezonde proefpersonen ook moeite hadden met het uitvoeren van de taak. In hoofdstuk 8 hebben we laten zien dat veel patiënten inderdaad moeite hebben met het uitvoeren van de taken. In één van de taken moet men de ogen fixeren op een specifiek punt op een beeldscherm, terwijl men de aandacht naar links of rechts moet verplaatsen. Voor de meeste gezonde jonge mensen is dit geen probleem en ook de oudere mensen in onze studie hadden hier weinig problemen mee, maar de meeste patiënten in onze studie konden niet hun aandacht verplaatsen zonder de ogen te bewegen. De oogbewegingen van deze patiënten kunnen zorgen voor verstoring van het EEG. Tevens is dan de vraag of de ERPs die je dan waarneemt worden veroorzaakt door het richten van de aandacht of door het bewegen van de ogen. Daarom zal in de toekomst gekeken moeten worden naar andere of vereenvoudigde taken om aandachtsgerelateerde ERPs te onderzoeken bij patiënten met de ZvP.

Conclusie

In dit proefschrift zijn nieuwe analysemethodes geïntroduceerd voor multikanaals EPs. Ten eerste is een methode ontwikkeld om de SEP amplitude te bepalen bij 128-kanaals registraties. We hebben aangetoond dat SEP amplitude nauwkeuriger kan worden bepaald met deze nieuwe techniek. Daarnaast is een nieuwe methode ontwikkeld voor het kwantificeren van SEP symmetrie. Beide methodes bleken niet geschikt als diagnostisch hulpmiddel voor het differentiëren van ZvP, PSP en CBGD. Toekomstig onderzoek moet uitwijzen of kleine aanpassingen aan het SEP

protocol en/of de analysetechnieken leiden tot verbetering van de diagnostische waarde van deze methodes en of deze methodes van klinische betekenis kunnen zijn voor andere neurologische aandoeningen.
Tenslotte hebben we laten zien dat patiënten met de ZvP meer moeite hebben met het onderdrukken van oogbewegingen bij het richten van de aandacht in vergelijking met gezonde proefpersonen. Dit kan problemen geven bij de studie naar aandachtsgerelateerde ERPs, omdat oogbewegingen het EEG kunnen verstoren en zelf ook ERPs kunnen genereren. In de toekomst zal bij studies naar aandachtsgerelateerde ERPs bij patiënten met de ZvP hier duidelijk rekening mee moeten worden gehouden.

Dankwoord

Een promotieonderzoek doe je niet alleen. Goede begeleiding en ondersteuning, een aangename werksfeer en prettige privéomstandigheden zijn essentieel om een promotieonderzoek binnen de 4 jaar die daar voor staan af te ronden. Daarom is het is nu tijd om een aantal mensen te bedanken, die hieraan een bijdrage hebben geleverd.

Allereerst, wil ik natuurlijk mijn 1e promotor en dagelijkse begeleidster, Natasha Maurits, bedanken. Natasha, was iedere aio begeleider maar zoals jij, dan zouden er heel wat minder problemen en frustraties zijn onder aio's. Ik kon altijd bij je binnen lopen en je kon me altijd weer op de goede weg helpen. Tevens was je altijd razend snel in het corrigeren van teksten, wat je ook nog eens uiterst kritisch deed. Hier kan menig aio begeleider nog een voorbeeld aan nemen. Ik heb veel van je geleerd en vond de samenwerking uiterst prettig.
Vervolgens wil ik Nico Leenders, mijn tweede promotor en Han van der Hoeven, mijn copromotor, bedanken voor de hulp bij het includeren van patiënten, het beoordelen van de data, het interpreteren van de resultaten en het corrigeren van de manuscripten.
Alle leden van de beoordelingscommissie wil ik bedanken voor het doorlezen en beoordelen van dit proefschrift.
Wendy Kruizinga, ook jij bedankt! Als student onderzoeker heb je een belangrijke bijdrage geleverd aan hoofdstuk 7.
Dit onderzoek was niet mogelijk geweest zonder de deelname van proefpersonen en patiënten. Velen van jullie hebben duizenden elektrische schokjes moeten doorstaan en dat alles voor de wetenschap. Ik wil dan ook alle proefpersonen en patiënten, die meegedaan hebben aan dit onderzoek, bedanken.
De metingen die zijn verricht bij proefpersonen en patiënten kon ik niet alleen uitvoeren. Gelukkig kon ik telkens rekenen op de hulp van de laboranten van de KNF afdeling. Bedankt voor jullie hulp tijdens alle metingen. Het meten werd een gezellige bezigheid met jullie erbij!

Naast de mensen, die mij direct hebben geholpen bij mijn onderzoek, wil ik ook een aantal mensen bedanken die hebben bijgedragen aan een prettige werksfeer.
Allereerst wil ik hiervoor mijn kamergenoten in het UMCG bedanken die de afgelopen vier jaar bij mij op de kamer hebben gezeten voor korte of langere tijd;

Renate, Petra, Marcus, Jop, Iris, Suzan, Zwany en Maarten. Ten tweede wil ik graag de collega's van de GNIP kamer bedanken voor de gezellige lunches en binnenloop sessies. Paulien, Anne-Marthe, Janneke en Carolien, jammer dat onze wegen nu een andere kant op gaan!
De onderzoeksschool BCN wil ik bedanken voor het organiseren van cursussen en andere activiteiten. Daarnaast ben ik hen erg dankbaar voor het financieel mogelijk maken van mijn onderzoek aan de Universiteit van Birmingham.
Michael, Jantien, Rick en Tita het was erg prettig met jullie samen te werken voor de BCN aio-raad en samen de BCN enquête te organiseren.

Tenslotte zijn prettige privéomstandigheden, die zorgen voor voldoende afleiding, noodzakelijk om goed onderzoek te kunnen doen.
Vier jaar geleden vertrok ik als Brabantse naar Noord-Nederland, veel vrienden en familie achterlatend. Ik heb hier vrij snel het volleyballen weer opgepakt en kwam meteen terecht in een kampioensteam! Kristel, Astrid, Margot en Jannemieke, het was erg gezellig om met jullie in een team te spelen. Ik ben erg blij dat ondanks dat we niet meer met elkaar volleyballen ons contact blijft!
Door de verhuizing naar Eelde, heb ik met veel vrienden niet zo vaak kunnen afspreken als dat ik eigenlijk zou willen. Mirjam, Marcia, Tamara, Kristie, Silvia, Rachel, Noortje, Saskia, Anne-Cathrien, Sjoerd en Nicole, gelukkig is het elke keer als ik met jullie afspreek, carnaval vier of op wintersport ga, weer gezellig zoals vanouds!
Kristel en Mirjam, fijn dat jullie mijn paranimfen willen zijn en aan mijn zijde de Aula willen binnentreden op 8 december.
Graag wil ik ook mijn familie bedanken voor de interesse die jullie altijd tonen in mijn onderzoek en de gezellige momenten die we samen beleven.
Pap en mam, jullie wil ik speciaal bedanken voor de vrijheid die jullie mij altijd hebben gegeven in het maken van mijn keuzes. Tevens wil ik jullie bedanken voor alle gezelligheid en verwennerij elke keer als we weer bij jullie zijn!
Dan rest mij nog een zeer speciaal persoon te bedanken. Gerben, bedankt voor alles! Samen met jou ga ik met veel vertrouwen de toekomst tegemoet! Enneh, volgend jaar eindelijk minstens samen 3 weken op zomervakantie?!